arXiv:hep-ph/9702367v2 28 Jan 1998

SAGA-HE-97-97, DOE/ER/40561-255-INT96-19-01 Jan. 15, 1998

Flavor Asymmetry of Antiquark Distributions in the Nucleon

S. Kumano *

Department of Physics, Saga University, Saga 840, Japan
and
Institute for Nuclear Theory, University of Washington
Seattle, WA 98195, U.S.A.

ABSTRACT

Violation of the Gottfried sum rule was suggested by the New Muon Collaboration in measuring proton and deuteron F_2 structure functions. The finding triggered many theoretical studies on physics mechanisms for explaining the antiquark flavor asymmetry $\bar{u}-\bar{d}$ in the nucleon. Various experimental results and proposed theoretical ideas are summarized. Possibility of finding the flavor asymmetry in Drell-Yan experiments is discussed together with other processes, which are sensitive to the $\bar{u}/\bar{d}$ asymmetry.

---

* Email: kumanos@cc.saga-u.ac.jp. Information on his research is available at http://www.cc.saga-u.ac.jp/saga-u/riko/physics/quantum1/structure.html.

submitted to Physics Reports

PREPARED FOR THE U.S. DEPARTMENT OF ENERGY UNDER GRANT DE-FG06-90ER40561

This report was prepared as an account of work sponsored by the United States Government. Neither the United States nor any agency thereof, nor any of their employees, makes any warranty, express or implied, or assumes any legal liability or responsibility for the accuracy, completeness, or usefulness of any information, apparatus, product, or process disclosed, or represents that its use would not infringe privately owned rights. Reference herein to any specific commercial product, process, or service by trade name, mark, manufacturer, or otherwise, does not necessarily constitute or imply its endorsement, recommendation, or favoring by the United States Government or any agency thereof. The views and opinions of authors expressed herein do not necessarily state or reflect those of the United States Government or any agency thereof.

Contents

1 Introduction 1

2 Possible violation of the Gottfried sum rule 6
- 2.1 Gottfried sum rule 6
- 2.2 Early experimental results 9
- 2.3 NMC finding and recent progress 10
- 2.4 Small x contribution 12
- 2.5 Nuclear correction: shadowing in the deuteron 13
- 2.6 Parametrization of antiquark distributions 16

3 Expectations in perturbative QCD 20
- 3.1 Operator product expansion 20
- 3.2 Perturbative correction to the Gottfried sum 23

4 Theoretical ideas for the sum-rule violation 26
- 4.1 Lattice QCD 26
- 4.2 Pauli exclusion principle 28
- 4.3 Mesonic models 29
  - 4.3.1 Meson-cloud contribution 29
  - 4.3.2 Chiral models 36
  - 4.3.3 Anomalous Q^2 evolution 40
- 4.4 Diquark model 43
- 4.5 Isospin symmetry violation 46
- 4.6 Flavor asymmetry $\bar{u} - \bar{d}$ in nuclei 46
- 4.7 Relation to nucleon spin 49
- 4.8 Comment on effects of quark mass and transverse motion 51

5 Finding the flavor asymmetry $\bar{\mathbf{u}} - \bar{\mathbf{d}}$ in various processes 52
- 5.1 Drell-Yan process 52
  - 5.1.1 Fermilab-E866 results 57
- 5.2 W and Z production 58
- 5.3 Quarkonium production at large x_F 61
- 5.4 Charged hadron production 63
- 5.5 Neutrino scattering 65
- 5.6 Experiments to find isospin symmetry violation 68

6 Related topics on antiquark distributions 71

7 Summary and outlook 73

§ **Acknowledgments** **73**

§ **References** **74**

1 Introduction

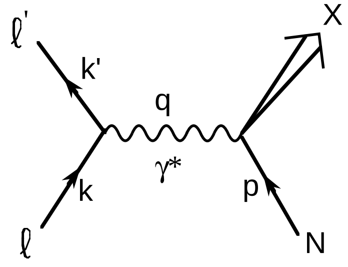

Figure 1.1: Lepton-nucleon scattering.

Nucleon substructure has been investigated through various high-energy experiments. Electron or muon projectile is ideal for probing minute internal structure of the nucleon. The reaction is illustrated in Fig. 1.1, where the virtual photon from the lepton interacts with the target nucleon. Its cross section is related to two structure functions F_1 and F_2 depending on transverse and longitudinal reactions for the photon. They depend in general on two kinematical variables $Q^2 = -q^2$ and $x = Q^2/2p \cdot q$ where q is the virtual photon momentum and p is the nucleon momentum. These structure functions provide important clues to internal structure of the nucleon [1, 2, 3]. It is known that the structure functions are almost independent of Q^2, which is referred to as Bjorken scaling. It indicates that the photon scatters on structureless objects, which are called partons. The partons are now identified with quarks and gluons. The cross section is calculated by the lepton scattering on individual quarks with incoherent impulse approximation, then the structure functions are described by quark distributions in the nucleon: for example $F_2(x, Q^2) = \sum_i e_i^2 x[q_i(x, Q^2) + \bar{q}_i(x, Q^2)]$. Because the variable x is the light-cone momentum fraction carried by the struck quark, the structure function F_2 suggests quark-momentum distributions in the nucleon.

Quark-antiquark pairs are created perturbatively according to Quantum Chromodynamics (QCD) so that there could be infinite number of quarks and antiquarks in the nucleon. A meaningful quantity is, for example, the difference between quark and antiquark numbers. It is certainly restricted by the baryon number and charge of the proton. The valence-quark distribution q_v is defined by $q_v \equiv q - \bar{q}$, then the quark distribution is split into two parts: valence and sea distributions. With the definition of the valence quark, the sea-quark distribution is given by $q_s = q - q_v = \bar{q}$. The valence quarks are the "net" quarks in the nucleon. On the other hand, the sea quarks are thought to be produced mainly in the perturbative process of gluon splitting into a $q\bar{q}$ pair. Because u, d, and s quark masses are fairly small compared with a typical energy scale in the deep inelastic scatting, the splitting processes are expected to occur almost equally for these quarks. Therefore, it was assumed until rather recently that the sea was flavor symmetric ($\bar{u} = \bar{d} = \bar{s}$) [4].

Both the valence and sea contribute to the electron or muon cross section, so that other processes have to be used in addition for studying the details of the sea. Valence-quark distributions are obtained in neutrino interactions. Once the valence distributions are fixed, the antiquark distributions in the nucleon are estimated from electron and muon scattering data or independently from Drell-Yan processes. The flavor-symmetric antiquark distributions in $\bar{u}$, $\bar{d}$, and $\bar{s}$ had been used for a while; however, neutrino induced dimuon events revealed that the strange sea is roughly half of the u-quark or d-quark sea [5, 6]. It had been, however, assumed that antiquark distributions $\bar{u}$ and $\bar{d}$ are same. If they are different, it should appear as a failure of the Gottfried sum rule [7]. The sum rule was obtained by integrating the difference between the proton and neutron F_2 structure functions over x, $I_G \equiv \int dx(F_2^p - F_2^n)/x = 1/3$. There is an important assumption in this sum rule, and it is the light antiquark flavor symmetry $\bar{u} = \bar{d}$. If it is not satisfied, the Gottfried sum rule is violated. However, it should be noted that the sum rule is not an "exact" one, which can be derived by using current algebra without a serious assumption. Therefore, the fundamental theory of strong interaction, QCD, is not in danger even if the sum-rule violation is confirmed.

There is an earlier indication of the sum-rule violation in the data at the Stanford Linear Accelerator Center (SLAC) in the 1970's [I_G=0.200 ± 0.040] [8]. The analysis in 1975 showed a significant deviation from the Gottfried value 1/3. However, no serious discussion could be made on the possible violation because the smallest accessible x point in the experiment was x=0.02 and there could be a significant contribution to the sum from the smaller x region. Nevertheless, it is interesting to conjecture a possible physics mechanism of the sum-rule violation. Because the integral is given by $I_G = \int dx(u + \bar{u} - d - \bar{d}) = 1/3 + (2/3)\int dx(\bar{u} - \bar{d})$, the fact that the measured value I_G=0.200 is smaller than 1/3 suggests a $\bar{d}$ excess over $\bar{u}$ in the nucleon. Proposed ideas for creating the flavor asymmetry in the 1970's are, as far as the author is aware, a diquark model [9] and a Pauli blocking mechanism [10, 11]. The details of these models are discussed in sections 4.2 and 4.4. Other experimental information came from Drell-Yan processes. Fermi National Accelerator Laboratory (Fermilab) E288 Drell-Yan data in 1981 [12] suggested also a flavor asymmetric sea: $\bar{u} = \bar{d}(1-x)^{3.48}$. Later, the sum rule was tested by the European Muon Collaboration (EMC) in 1983 and 1987 [13]. The 1987 analysis indicates that the sum is $0.197 \pm 0.011(stat.) \pm 0.083(syst.)$ in the region $0.02 \le x \le 0.8$, and the extrapolated value is $0.235^{+0.110}_{-0.099}$. Again, the data suggested a significant deficit in the sum rule. It was, however, not strong enough to surprise our community because the measured difference was still within the standard deviation. The another muon group at the European Organization for Nuclear Research (CERN), Bologna-CERN-Dubna-Munich-Saclay (BCDMS) collaboration, also investigated the sum rule in muon scattering on the hydrogen and deuterium [14]. The BCDMS result in 1990 is $0.197 \pm 0.006(stat.) \pm 0.036(syst.)$ in the region $0.06 \le x \le 0.8$ at Q^2=20 GeV^2. Their estimate of the small x contribution is between 0.07 and 0.22, so that the result could be consistent with 1/3.

Although the sum rule was proposed in 1967, there is little progress in 1970's and 1980's. The crucial point was, as it is common in most sum rules, the lack of small x data with good accuracy. The first clear indication of the sum-rule breaking was suggested by the New Muon Collaboration (NMC) in 1991 [15]. They obtained data with x as small as 0.004 by using a CERN muon beam. They fitted $F_2^p(x) - F_2^n(x)$ data by a smooth curve and extrapolated it into the unmeasured small x region. According to the NMC, the integral I_G became 0.240±0.016, which is approximately 28% smaller than the Gottfried sum. Their reanalysis in 1994 indicates a similar value 0.235±0.026. Considering the small errors, we conclude that the light antiquark distributions are not flavor symmetric and we have a $\bar{d}$ excess over $\bar{u}$ in the proton.

Recent measurements of F_2^p/F_2^n by the Fermilab-E665 [16] and the HERMES [17] collaborations agree with the NMC results. Estimate of the Gottfried sum is not reported yet; however, the agreement of F_2^p/F_2^n suggests a violation of the sum. Moreover, the charged-hadron-production data by the HERMES support the NMC flavor asymmetry.

On the other hand, there are existing Drell-Yan data. As it was mentioned, the Fermilab-E288 in 1981 suggested a $\bar{d}$ excess over $\bar{u}$ [12]. However, later Fermilab-E772 collaboration data showed no significant flavor asymmetry [18] in 800 GeV proton-induced Drell-Yan measurements for the deuteron, carbon, and tungsten. Strictly speaking, these nuclear data cannot be compared with the NMC results because nobody knows how large nuclear modification is. A possible nuclear modification of $\bar{u}-\bar{d}$ is discussed in section 4.6. There are data from p-p and p-d Drell-Yan processes by the NA51 collaboration [19] at CERN. The data indicated large flavor asymmetry $\bar{u}/\bar{d}$=0.51±0.04±0.05 at x=0.18. It is again a clear indication of the flavor asymmetry in the light antiquark distributions. In order to get more information for the asymmetry, the E866 experiment is in progress at Fermilab by measuring the Drell-Yan processes [20]. Preliminary data also indicate $\bar{u} < \bar{d}$ which could be consistent with the NMC. The existing E288, E772, and NA51 Drell-Yan results and the details of the Drell-Yan processes are explained in section 5 together with other processes, which are sensitive to the flavor asymmetry $\bar{u} - \bar{d}$.

Next, we discuss a brief outline of theoretical studies. First, there is a conservative view that the Gottfried sum is satisfied without the $\bar{u}/\bar{d}$ asymmetry by including a significant contribution from the small x region ($x \leq 0.004$) [21]. However, this idea is not consistent with the NA51 data. We also note that perturbative corrections to I_G are fairly small and it is of the order of 0.3% at Q^2=4 GeV^2 [22, 23, 24, 25]. The small correction is from the $\bar{q} \rightarrow q$ splitting process which can occur in the next-to-leading-order (NLO) case. If the sum-rule violation or the flavor asymmetry is confirmed, it should be explained by a nonperturbative mechanism.

A reliable way of treating nonperturbative phenomena is to use lattice QCD. Although real lattice calculation of the Gottfried sum is not available at this stage, scalar matrix elements were evaluated in Ref. [26]. The studies of the isoscalar-isovector ratio indicated significant flavor asymmetry when the quarks are light. The difference comes from the process with quarks propagating backward in time. In order to understand the meaning of the sum-rule violation, we should rely on quark-parton models.

Proposed theoretical ideas in the 1970's and 1980's are the diquark model [9] and the Pauli exclusion effect [10, 11, 27] which were originally intended to explain the old SLAC data. In the diquark model, the violation is expected due to the vector-diquark admixture. Even though earlier results [9, 28] seemed to be in agreement with the

SLAC and NMC data, the deviation from the Gottfried sum becomes very small if the virtual-photon interaction with a quark inside the diquark is taken into account with a realistic mixing factor between vector and scalar diquarks [29]. According to the Pauli blocking model, $u\bar{u}$ pair creations are more suppressed than $d\bar{d}$ creations because of the valence u quark excess over valence d in the proton. However, the effect would not be large enough to explain the NMC result because a naive counting estimate is $\bar{u}/\bar{d} = 4/5$. Furthermore, it was found recently [27] that antisymmetrization between quarks could change the situation. If its effects are combined with the Pauli-exclusion ones, the $\bar{u}$ distribution could be larger than the $\bar{u}$.

On the other hand, mesonic models seem to be the most popular idea for explaining the NMC result and the flavor asymmetry, at least by judging from number of publications. Because of the difference between $\bar{u}$ and $\bar{d}$ in virtual pion clouds in the nucleon, we have the flavor asymmetry [30, 31, 32]. For example, the proton decays into $\pi^+ n$ or $\pi^0 p$. Because the π^+ has a valence $\bar{d}$ quark, these processes produce an excess of $\bar{d}$ over $\bar{u}$ in the proton. This model was further developed by including many virtual states [33]. Combined mesonic and nuclear-shadowing effects were studied in Ref. [34]. In the early stage of these models, about a half of the NMC violation was explained by the virtual states. In the Adelaide model [32], the NMC deficit was explained by adding the Pauli exclusion effect. On the other hand, there is a possibility of explaining the whole violation within the mesonic model by considering different πNN and $\pi N\Delta$ form factors [35], or by including many virtual states [33]. Recently, off-shell pion effects were studied in Refs. [36, 37], but they did not change the pionic contribution to $\bar{u} - \bar{d}$ significantly. The mesonic mechanism can be described also in chiral models [38, 39, 40, 41, 42, 43, 44, 45, 46, 47]. In the chiral field theory with quarks, gluons, and Goldstone bosons [40, 43, 46, 47], the flavor asymmetry comes from the virtual photon interaction with the pions. The obtained results also indicated a significant deviation from the Gottfried sum. In the chiral soliton models [38, 39, 44], a fraction of the nucleon isospin is carried by the pions, and the deviation from the sum is given by the ratio of moments of inertia for the nucleon and pion. A possible relation to the σ term was also discussed in the chiral models [41, 42, 48]. The virtual mesons could modify not only the x distribution $\bar{u}(x) - \bar{d}(x)$ but also Q^2 evolution of I_G at relatively small Q^2 [49].

Although it is usually thought to be very small, isospin-symmetry violation, e.g. $u_p \neq d_n$, was studied in Ref. [50, 51]. In order to distinguish the isospin-symmetry violation from the flavor asymmetry, we should investigate neutrino reactions, the Drell-Yan p-n asymmetry, and charged-hadron production. On the other hand, shadowing effects in the deuteron were investigated [52, 53, 54, 55, 56, 57, 58] to find nuclear corrections in extracting the neutron F_2 from the deuteron data. Although there are uncertain factors in nuclear potential, the obtained correction to the sum is about $\delta I_G = -0.02$. We should mention that it varies depending on the shadowing model. However, the correction is a small negative number (except for the pion excess model). If it is taken into account, the NMC deficit is magnified! There are also papers on parton-transverse-motion corrections [59, 60]. It became possible to make flavor decomposition in parametrization of antiquark distributions. With the NMC and NA51 data, new parametrizations of parton distributions were studied [61, 62, 63, 64].

The flavor asymmetry in the nucleon could be related to other observables. Nuclear modification of the $\bar{u}-\bar{d}$ was investigated in a parton-recombination model [65]. Because of the difference between u and d quark numbers in neutron-excess nuclei, $u\bar{u}$ and $d\bar{d}$ recombination rates are different. This mechanism produces a finite $\bar{u}-\bar{d}$ distribution in a nucleus even if it vanishes in the nucleon. On the other hand, a relation to spin physics was studied [66, 40, 47]. For example, if the Pauli blocking is the right mechanism for producing the asymmetry, it also affects the spin content problem. Because $u_v^\uparrow$ is larger than $u_v^\downarrow$ in the quark model, a $u_s^\downarrow$ excess over $u_s^\uparrow$ is expected. This could be one of the interpretations of the proton spin problem.

We introduced various theoretical models. In order to distinguish among these models, we need theoretical and experimental efforts, in particular by studying consistency with other observables.

The NMC flavor asymmetry can be checked by other experimental reactions. The best possibility is the aforementioned Drell-Yan process. We have already explained the existing data. Theoretical analyses of the Drell-Yan p-n asymmetry are discussed in Refs. [67, 68, 69, 70, 71, 72, 73]. The asymmetry should become much clearer by the Fermilab-E866 experiment. Charged-hadron-production data in muon scattering by the EMC [74, 75] were analyzed for finding the $\bar{u}-\bar{d}$ [76]. At that time, experimental errors were not small enough to judge whether or not the flavor distributions are symmetric. However, the recent HERMES measurements show more clearly the NMC type flavor asymmetry [17]. On the other hand, $W^\pm$ and Z^0 production can also be used [21, 77, 78, 79]. Even though the W production is not very sensitive to the $\bar{u}/\bar{d}$ asymmetry in the $p+\bar{p}$ reaction, the $\bar{u}/\bar{d}$ ratio can be measured in the $p+p$ [79]. Quarkonium production is usually dominated by the gluon-gluon fusion process; however, the $\bar{u}/\bar{d}$ could be measured in the large $|x_F|$ region [80] if experimental data are accurate enough. Neutrino scattering is another possibility. Combining neutral-current and charged-current structure functions, or combining different ones F_1, F_2, and F_3 for a practical purpose, we could obtain the $\bar{u}-\bar{d}$ distribution [22, 31].

In the following sections, we summarize theoretical and experimental studies on the Gottfried sum rule and on the antiquark flavor asymmetry $\bar{u}-\bar{d}$ in the nucleon. Future experimental possibilities are also discussed.

2 Possible violation of the Gottfried sum rule

First, the Gottfried sum rule is derived in a naive parton model. Earlier experimental results by the SLAC, EMC, and BCDMS are explained. Then NMC experimental results are discussed. We also comment on recent HERMES data. As an independent experimental test of the NMC flavor asymmetry, existing Drell-Yan data are shown.

2.1 Gottfried sum rule

The Gottfried sum rule is associated with the difference between the proton and neutron F_2 structure functions measured in unpolarized electron or muon scattering. Because there is no fixed neutron target, the deuteron is usually used for obtaining the neutron F_2 by subtracting out the proton part with nuclear corrections.

The cross section of unpolarized electron or muon deep inelastic scattering is calculated by assuming the one-photon exchange process in Fig. 1.1 [1, 2, 3]:

$$d\sigma = \frac{1}{4\sqrt{(k\cdot p)^2 - m^2 M^2}} \overline{\sum_{pol}} \sum_{X} (2\pi)^4 \, \delta^4(k + p - k' - p_{_X}) \times \; |\mathcal{M}(ep \to e'X)|^2 \, \frac{d^3k'}{(2\pi)^3 2E'} \quad , \tag{2.1}$$

where the matrix element is

$$\mathcal{M}(ep \to e'X) \;=\; \bar{u}(k',\lambda') e\gamma_\mu u(k,\lambda) \, \frac{g^{\mu\nu}}{(k-k')^2} \; < X \,|\, eJ_\nu(0) \,|\, p,\sigma > \quad . \tag{2.2}$$

M and m are the proton and lepton masses, k and k' (λ and λ') are initial and final lepton momenta (helicities), and J_ν is the electromagnetic current. The proton momentum and spin are denoted by p and σ, and $p_{_X}$ is the momentum of the hadron final state X. The notation $\overline{\sum}_{pol}$ indicates that spin average and summation are taken for the initial and final states respectively. From these equations, the cross section is expressed by a leptonic current part $L^{\mu\nu}$ and a hadronic one $W_{\mu\nu}$:

$$d\sigma = \frac{2M}{s - M^2} \, \frac{\alpha^2}{Q^4} \, L^{\mu\nu} \, W_{\mu\nu} \, \frac{d^3k'}{E'} \quad , \tag{2.3}$$

where α is the fine structure constant, s is given by $s = (p+k)^2$, E' is the scattered lepton energy, and Q^2 is defined by $Q^2 = -q^2$. Throughout this paper, the convention $-g_{00} = g_{11} = g_{22} = g_{33} = +1$ is used so as to have $p^2 = p_0^2 - \vec{p}^{\,2} = M^2$. The lepton tensor can be calculated as

$$\begin{aligned} L^{\mu\nu} &= \overline{\sum_{\lambda,\lambda'}} \, [\bar{u}(k',\lambda')\gamma^\mu u(k,\lambda)]^* \; [\bar{u}(k',\lambda')\gamma^\nu u(k,\lambda)] \\ &= 2\,(k^\mu k'^\nu + k'^\mu k^\nu - k\cdot k' g^{\mu\nu}) \quad , \end{aligned} \tag{2.4}$$

in the unpolarized case. The hadronic part is given by

$$W_{\mu\nu} = \frac{1}{4\pi M} \sum_X (2\pi)^4 \, \delta^4(p + q - p_{_X}) \overline{\sum_\sigma} < p, \sigma | J_\mu(0) | X >< X | J_\nu(0) | p, \sigma >$$
$$= \frac{1}{4\pi M} \overline{\sum_\sigma} \int d^4\xi \, e^{iq\cdot\xi} < p, \sigma | \, [J_\mu(\xi), J_\nu(0)] \, | p, \sigma > \quad . \tag{2.5}$$

Using light-cone variables $q^\pm = (q^0 \pm q^3)/\sqrt{2}$ with $q = (\nu, 0, 0, -\sqrt{\nu^2 + Q^2})$ and $\nu = E - E'$, we have $q^+ = -Mx/\sqrt{2}$ =finite and $q^- = \sqrt{2}\nu \to \infty$ in the Bjorken scaling limit, $Q^2 \to \infty$ with finite x. The exponential factor becomes $e^{iq\cdot\xi} = e^{iq^+\xi^-} e^{iq^-\xi^+}$. Because the q^- part is a rapidly oscillating term, the integral vanishes except for the singular region of the integrand according to the Riemann-Lebesque theorem. Therefore, the integral is dominated by the light-cone region $\xi^+ \approx 0$. In the deep inelastic lepton scattering, we can probe light-cone momentum distributions of internal charged constituents in the proton. The formal approach for analyzing the hadron tensor is to use operator product expansion. It is discussed in section 3 in explaining QCD corrections to the sum rule. Here, we do not step into the details and simply discuss general properties. Using parity conservation, time-reversal invariance, symmetry under the exchange of the Lorentz indices μ and ν, and current conservation, we can express the hadron tensor in term of two structure functions W_1 and W_2:

$$W_{\mu\nu} = -W_1 \left(g_{\mu\nu} - \frac{q_\mu q_\nu}{q^2} \right) + W_2 \frac{1}{M^2} \left(p_\mu - \frac{p\cdot q}{q^2} q_\mu \right) \left(p_\nu - \frac{p\cdot q}{q^2} q_\nu \right) \quad . \tag{2.6}$$

From Eqs. (2.3), (2.4), (2.6), the cross section becomes

$$\frac{d\sigma}{d\Omega dE'} = \frac{\alpha^2}{4E^2 \sin^4 \frac{\theta}{2}} \left[2W_1(\nu, Q^2) \sin^2 \frac{\theta}{2} + W_2(\nu, Q^2) \cos^2 \frac{\theta}{2} \right] \quad . \tag{2.7}$$

Scaling structure functions F_1 and F_2 are defined in terms of W_1 and W_2:

$$F_1 \equiv M\, W_1 \quad , \quad F_2 \equiv \nu \, W_2 \quad . \tag{2.8}$$

The F_1 is associated with the transverse cross section, and the F_2 is with the transverse and longitudinal ones. In the Bjorken limit, two structure functions are related by the Callan-Gross relation $2xF_1 = F_2$. In the parton picture, the deep inelastic process can be described by virtual photon interactions with individual quarks with incoherent impulse approximation. It is supposed to be valid at large Q^2 in the sense that virtual-photon-interaction time with a quark is fairly small compared with the interaction time among quarks. Then, the leading-order (LO) or DIS-scheme structure function F_2 is given by quark-momentum distributions in the nucleon:

$$F_2(x, Q^2) = \sum_i e_i^2 \, x \, [\, q_i(x, Q^2) \, + \, \bar{q}_i(x, Q^2) \,] \quad , \tag{2.9}$$

where i denotes the quark flavor. In the next-to-leading order (NLO) except for the DIS scheme case, the gluon distribution also contributes to F_2 through the splitting $g \rightarrow q\bar{q}$. With the assumption of isospin symmetry in the nucleon, parton distributions in the neutron could be related to those in the proton. The d-quark distribution in the neutron is equal to the u-quark distribution in the proton $[u_n(x,Q^2) = d_p(x,Q^2)]$ and in the similar way for other partons $[d_n = u_p$, $\bar{u}_n = \bar{d}_p$, $\bar{d}_n = \bar{u}_p$, and etc.]. Hereafter, the parton distributions are assumed as those in the proton except for section 4.5 where possible isospin-symmetry breaking is discussed. Then, the difference between the proton and neutron structure functions is given by

$$F_2^p(x,Q^2) - F_2^n(x,Q^2) = \frac{1}{3}\, x\, [u_v(x,Q^2) - d_v(x,Q^2)] + \frac{2}{3}\, x\, [\bar{u}(x,Q^2) - \bar{d}(x,Q^2)] \ . \tag{2.10}$$

The valence-quark distributions should satisfy

$$\int_0^1 dx\, u_v(x,Q^2) = 2 \ \ , \ \ \int_0^1 dx\, d_v(x,Q^2) = 1 \quad , \tag{2.11}$$

due to the proton and neutron charges, $\int dx(2u_v - d_v)/3 = 1$ and $\int dx(2d_v - u_v)/3 = 0$ where elastic scattering amplitudes are expressed in the parton model by considering an infinite momentum frame. Substituting Eq. (2.11) into Eq. (2.10) and integrating over the variable x, we obtain

$$\int_0^1 \frac{dx}{x}\, [F_2^p(x,Q^2) - F_2^n(x,Q^2)] = \frac{1}{3} + \frac{2}{3} \int_0^1 dx\, [\bar{u}(x,Q^2) - \bar{d}(x,Q^2)] \quad . \tag{2.12}$$

If the sea is flavor symmetric $\bar{u} = \bar{d}$, the second term vanishes and it becomes the Gottfried sum rule [7]:

$$\int_0^1 \frac{dx}{x}\, [F_2^p(x,Q^2) - F_2^n(x,Q^2)] = \frac{1}{3} \quad . \tag{2.13}$$

As it is obvious in the above derivation in a naive parton model, there is a serious assumption of the flavor symmetry in the light antiquark distributions. Therefore, it is not a rigorous one like the Bjorken sum rule. Even if violation of the sum rule is found in experiments, there is virtually no danger in the fundamental theory of strong interactions, quantum chromodynamics. It is nevertheless interesting to test it because its violation could suggest an SU(2)-flavor asymmetric sea in the nucleon as it was found in the neutrino-induced dilepton production in the case of SU(3). Because of small u and d quark masses, large $\bar{u}/\bar{d}$ asymmetry cannot be expected in perturbative QCD. Therefore, a possible sum-rule violation gives an opportunity for learning more details on internal structure of the nucleon.

2.2 Early experimental results

Because the small x region could have a significant contribution to the sum rule, it was not possible to test it until recently. The minimum x is restricted by the lepton-beam energy E as $min(x) = Q^2/2ME$, where Q^2 should not be smaller than a few GeV^2 in order to be deep inelastic scattering. The first test of the sum rule was studied at SLAC in the 1970's. The electron-beam energy is 4.5–20 GeV so that the smallest x is about 0.02. Targets are hydrogen, deuterium, and heavier ones. The data are taken in the x range from 0.02 to 0.82 for the hydrogen and deuterium targets. The Q^2 varies depending on the x region, but it is from 0.1 GeV^2 to 20 GeV^2. In the 1975 analysis [8], the data with $0.02 \le x \le 0.28$ are combined with previous data in the extended range $x \le 0.82$. The neutron structure function is extracted by taking into account Fermi smearing effects: $F_2^n/F_2^p = (SF_2^d - F_2^p)/F_2^p$, where S is the Fermi smearing factor. The difference becomes $F_2^p - F_2^n = 2F_2^p - SF_2^d$. We define a Gottfried integral by

$$\int_{x_{min}}^{x_{max}} \frac{dx}{x} \, [\, F_2^p(x,Q^2) - F_2^n(x,Q^2) \,] \equiv I_G(x_{min}, x_{max}) \quad . \tag{2.14}$$

According to the SLAC data in 1975 [8], it is

$$I_G(0.02, 0.82) = 0.200 \pm 0.040 \qquad (\text{in} \;\; 1975) \quad . \tag{2.15}$$

It should be noted that the integral contains various Q^2 data ranging from small Q^2, where perturbative QCD may not be valid. In any case, it is interesting to find a significantly smaller value than the Gottfried sum 1/3. Therefore, there was earlier indication of the sum-rule violation in the SLAC data. In fact, the Pauli-blocking and diquark models were proposed, just after the SLAC finding, for explaining the possible deficit in the sum. However, it was not conclusive enough to state that the sum rule is violated experimentally due to a possible large contribution from the smaller-x region.

Next experimental data came from EMC measurements at CERN by deep inelastic muon scattering on the hydrogen and deuterium [13]. The muon-beam energy is 280 GeV, and the measured kinematical range is $0.03 \le x \le 0.65$ and $7 \le Q^2 \le 170$ GeV^2. The neutron structure function is extracted from the deuteron data by taking into account the smearing effects due to the nucleon Fermi motion. The Hulthen and Paris wave functions are used in the 1983 and 1987 analyses to estimate the smearing correction. The mean Q^2 in the data depends on x, and it ranges from 10 GeV^2 at x=0.03 to 90 (80 in 1983) GeV^2 at x=0.65. Using the Q^2 averaged data at each x, they obtained

$$I_G(0.03, 0.65) = 0.18 \pm 0.01 \, (stat.) \pm 0.07 \, (syst.) \quad , \tag{2.16}$$

in 1983. The distribution $F_2^p - F_2^n$ is extrapolated into the unmeasured regions by using a function $F_2^p - F_2^n = Ax^{0.5}(1-x)^\alpha(1+\beta x)$, where the constants α and β are obtained from the data. The 1983 EMC result in the whole x is then given by

$$I_G(0,1) = 0.24 \pm 0.02\,(stat.) \pm 0.13\,(syst.) \qquad (\text{in} \;\; 1983) \quad . \tag{2.17}$$

In the 1987 report, these values became

$$I_G(0.02, 0.8) = 0.197 \pm 0.011\,(stat.) \pm 0.083\,(syst.) \quad , \tag{2.18}$$

and

$$I_G(0,1) = 0.235\,^{+0.110}_{-0.099} \qquad (\text{in} \;\; 1987) \quad . \tag{2.19}$$

It should be noted that different Q^2 data are collected to get the integral, whereas the sum rule is valid at certain Q^2. The above result could be consistent with the sum 1/3 within the experimental error; however, it is also smaller as the SLAC data indicated.

Another muon group at CERN, BCDMS, also obtained the sum by analyzing muon scattering on the hydrogen and deuterium [14]. The muon-beam energies are 120, 200, and 280 GeV. The kinematical range is $0.06 \le x \le 0.80$ and $8 \le Q^2 \le 260$ GeV^2. The structure function ratio is obtained with the smearing factor calculated with the Paris wave function for the deuteron. Integrating the distribution $F_2^p - F_2^n$, the BCDMS obtained

$$I_G(0.06, 0.8) = 0.197 \pm 0.006\,(stat.) \pm 0.036\,(syst.) \qquad (\text{in } 1990) \quad , \tag{2.20}$$

at Q^2=20 GeV^2. The larger-x(>0.8) contribution is negligible, and the smaller-x(<0.06) one varies from 0.07 to 0.22 by considering the behavior $F_2^p - F_2^n \propto x^\alpha$ with $0.3 \le \alpha \le 0.7$. Because of the large uncertainty from the small x region, they did not quote the integral value in the whole range of x. Due to the possible small-x contribution, they concluded that it could be consistent with the sum 1/3.

2.3 NMC finding and recent progress

Although the earlier data suggested violation of the Gottfried sum, it was not conclusive enough because of the large errors and a possible large contribution from the small x region. In the NMC experiment, the kinematical range was extended to the small x region. The NMC obtained 90 and 280 GeV muon scattering data on hydrogen and deuterium targets at CERN [15]. The kinematical range is $0.004 \le x \le 0.8$ and $0.4 \le Q^2 \le 190$ GeV^2. The difference of the structure functions is calculated by

$$F_2^p - F_2^n = 2\,F_2^d\,\frac{1 - F_2^n/F_2^p}{1 + F_2^n/F_2^p} \quad , \tag{2.21}$$

where the ratio $F_2^n/F_2^p = 2F_2^d/F_2^p - 1$ is determined by the NMC experiment, and the absolute value of the deuteron structure function F_2^d is given by a fit to various experimental data. Nuclear corrections such as the Fermi motion in section 2.2 are not

Figure 2.2: Experimental history of the Gottfried sum rule. The SLAC and BCDMS integrals are evaluated in the region of 0.02$\leq x \leq$0.82 and 0.06$\leq x \leq$0.8 respectively. Because unmeasured regions are not included, they are shown by the open circles.

The NMC reanalyzed the integral by using a new parametrization for F_2^d including their own data and revised F_2^n/F_2^p ratios. Their result in 1994 is

$$I_G(0.004, 0.8) = 0.221 \pm 0.008\,(stat.) \pm 0.019\,(syst.) \tag{2.25}$$

at Q^2=4 GeV^2. The larger x contribution becomes $I_G(0.8, 1.0) = 0.001 \pm 0.001$. The smaller x one is $I_G(0, 0.004) = 0.013 \pm 0.005$ by the extrapolation $F_2^p - F_2^n = ax^b$ with $a = 0.20 \pm 0.03$ and $b = 0.59 \pm 0.06$. Then, the overall integral is

$$I_G(0, 1) = 0.235 \pm 0.026 \qquad (\text{in} \;\; 1994) \quad . \tag{2.26}$$

The sum is consistent with the previous NMC result; however, the error is slightly larger due to more extensive examination of the systematic uncertainties.

In the HERMES experiment [17], the positron beam energy is 27.5 GeV and hydrogen, deuterium, and ^3He gas targets are used. The ratio F_2^p/F_2^n is extracted from the unpolarized hydrogen and deuterium data. The measured kinematical range is $0.015 \le x \le 0.55$ (averaged in each bin) and $0.4 \le Q^2 \le 11$ GeV^2. Because the obtained ratios agree with the NMC results, the HERMES experiment seems to support the sum-rule violation. However, the sum I_G is not reported yet. On the other hand, a clearer indication of the flavor asymmetry is given in semi-inclusive data. As it is discussed in section 5.4, the charged-hadron production ratio $r(x, z) = (N^{p\pi^-} - N^{n\pi^-})/(N^{p\pi^+} - N^{n\pi^+})$ is also related to the $\bar{u}/\bar{d}$ asymmetry. The data analysis [17] clearly favors the NMC expectation rather than the flavor symmetric one.

Because of the small errors, the NMC 1991 result is the first one which made us realize that the Gottfried sum rule is actually violated. It strongly suggests the flavor asymmetry in the light antiquark distributions, namely a $\bar{d}$ excess over $\bar{u}$ in the proton. After the NMC finding, many theoretical papers are written on this topic and independent Drell-Yan experiments are proposed at CERN and Fermilab. Some Drell-Yan experimental results were already taken at Fermilab and CERN. They indicate also the NMC type flavor asymmetry. These Drell-Yan results are discussed in section 5.1.

2.4 Small x contribution

One of the reasons why the Gottfried sum rule was not investigated in detail in the 1970's and 1980's is the lack of small x data, which may contribute significantly. The smallest x point of the NMC data is 0.004. Their analysis indicates that the small x contribution is $I_G(0, 0.004) = 0.013 \pm 0.005$, which is merely 4% of the sum 1/3. In evaluating the integral, they extrapolate the data by using the fitting $F_2^p - F_2^n = 0.20x^{0.59}$ to the experimental data. However, it is not very obvious whether the small x contribution is so small. Slight variations of the NMC small x data could make a significant change in the integral as it is obvious in Fig. 2.3.

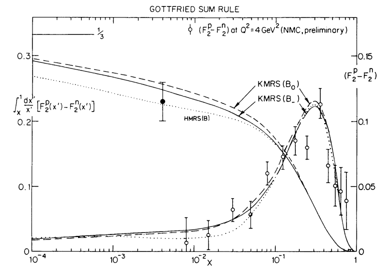

Figure 2.3: Small x contributions (taken from Ref. [21]).

The small x contribution was investigated in Refs. [21] and [31]. Three MRS-group (Martin-Roberts-Stirling) parametrizations, which were available in 1990, were studied [21]. They are HMRS-B, KMRS-B0, and KMRS-B$_-$ which are fit to various experimental data without any small x constraint for the HMRS-B, x^0 type sea-quark and gluon distributions in the limit $x \to 0$ for the KMRS-B0, and $x^{-0.5}$ for the KMRS-B$_-$. Comparison of these parametrizations with the NMC experimental data is shown in Fig. 2.3 [21]. It indicates that the parametrization curves are consistent with the data points, and yet they satisfy the Gottfried sum rule without any flavor asymmetry for the $\bar{u}$ and $\bar{d}$ quarks. The NMC raw data $I_G(0.004, 0.8)$ is shown by the filled circle with an error bar. It is also consistent with the three predictions. The only difference comes from small x behavior of $F_2^p - F_2^n$. According to the KMRS-B0, valence-quark distributions at small x behave like $x(u_v + d_v) \sim x^{0.27}$ and $xd_v \sim x^{0.61}$. The small x fall-off $x^{0.27}$ is much slower than the NMC one $x^{0.59}$, which makes a significant contribution from the small x region. In fact, three parametrizations have $I_G(0, 0.004)$=0.07−0.11 so that the missing 10% strength could come from the smaller-x region. More recent parametrizations are discussed in section 2.6.

Therefore, it is not definite whether the small x contribution is relatively small as suggested by the NMC. In the HMRS-E case, the sum 1/3 can be reached if the integral region is extended to very small $x \approx 10^{-10}$. This is an unrealistic number for experimental measurement. However, as it is obvious from Fig. 2 of the KL paper [31], the small-x contribution should become obvious at $x \approx 10^{-5}$. There is an experimental possibility of measuring F_2^d at such small x by accelerating the deuteron at the Hadron-Electron Ring Accelerator (HERA) in Hamburg. However, it is not clear whether such experiment could be realized at HERA. Therefore, the best way of testing it, at least at this stage, is to use other experimental processes. The NA51 experimental data [19] support the NMC conclusion, a $\bar{d}$ excess over $\bar{u}$ in the nucleon. More complete information will come from the Fermilab-E866 experiment in the near future [20].

2.5 Nuclear correction: shadowing in the deuteron

Because there is no fixed target for the neutron, the deuteron is usually used for measuring the neutron structure function F_2^n. In the NMC analyses, the deuteron and proton structure-function ratios are measured and they are related to the proton-neutron ratio by $F_2^n/F_2^p = 2F_{2D}/F_2^p - 1$. Together with world-averaged deuteron structure functions, the difference $F_2^p - F_2^n$ is calculated by Eq. (2.21). To be precise, the NMC result can be compared with the Gottfried sum only if there is no nuclear

Figure 2.4: Virtual photon interaction with the deuteron (a) in the impulse approximation and (b) in the double scattering case.

The shadowing is traditionally described by the VMD model in particular at small Q^2. Estimates of its effects on the Gottfried sum are found in Refs. [57, 58]. The virtual photon transforms into vector-meson states (v), which then interact with the deuteron. The hadron-deuteron cross section is given by an individual nucleon term in Fig. 2.4(a) and a double scattering term in Fig. 2.4(b) in the Glauber theory: $\sigma_{vD} = 2\sigma_{vN} + \delta\sigma_{vD}$, where

$$\delta\sigma_{vD} = -\frac{\sigma_{vN}^2}{8\pi^2} \int d^2\vec{k}_T \, S_D(\vec{k}^2) \quad . \tag{2.27}$$

The $S_D(\vec{k}^2)$ is the deuteron form factor given by the S and D state wave functions: $S_D(\vec{k}^2) = \int dr[u^2(r) + w^2(r)]j_0(kr)$. Then, the virtual-photon cross section is written as $\delta\sigma_{\gamma^* D} = \sum_v (e^2/f_v^2) \, \delta\sigma_{vD}/(1+Q^2/M_v^2)^2$. This equation is expressed in the F_2 form:

$$\delta F_{2D}(x) = \frac{Q^2}{\pi} \sum_v \frac{\delta\sigma_{vD}}{f_v^2 \, (1+Q^2/M_v^2)^2} \quad . \tag{2.28}$$

The ρ, ω, and ϕ mesons are included as the vector mesons. The most contribution comes from the ρ meson and it is about 80%. With this shadowing correction, the deuteron F_2 becomes $F_{2D} = F_2^p + F_2^n + \delta F_{2D}$. Because no nuclear correction is assumed in the NMC analysis, namely $[F_2^p - F_2^n]_{NMC} = 2F_2^p - F_{2D}$, the Gottfried sum becomes

$$I_G = I_G^{NMC} + \int \frac{dx}{x} \, \delta F_{2D}(x) \quad . \tag{2.29}$$

In Ref. [58], the VMD model is investigated further by including $q\bar{q}$ continuum in addition to the vector mesons, ρ, ω, and ϕ. The model can explain the NMC shadowing data for various nuclei. Applying the same model to the deuteron, they find the shadowing correction from $\delta I_G(0.004, 1)$=-0.039 to -0.017 depending on different nuclear potentials. The results qualitatively agree with those in Ref. [57], where the Pomeron and meson exchange contributions are added to the VMD one.

Because the shadowing effects on I_G are more or less same in all realistic models, other descriptions are not explained in detail. There are other studies in the Pomeron and meson exchange models. We briefly discuss these ideas in the following. For the details of formalism, the reader may read the original papers. Historically, the first estimate of shadowing contribution to I_G is discussed by the Pomeron exchange model [52, 53]. A possible way of describing the high-energy scattering in the diffractive region is in terms of Pomeron exchange. The virtual photon transforms into a $q\bar{q}$ pair which then interacts with the deuteron. In the diffractive case, the target is remain intact and only vacuum quantum number, namely the Pomeron, could be exchanged between the $q\bar{q}$ pair and the nucleons. In the earlier works, the shadowing correction in this model was rather large $\delta I_G \approx -0.08$ [53, 56]. However, the Pomeron contribution is reduced if more realistic deuteron wave functions are used according to Ref. [57]. Next, meson-exchange corrections were investigated in Refs. [54, 57]. The studied mesons are π, ω, and σ in Ref. [54], and ρ is also included in Ref. [57]. The formalism is essentially the same with the one in subsection 4.3.1. If the corrections due to the π, ω, and σ mesons were taken into account, the NMC result became $I_G = 0.29 \pm 0.03$ [54]. Therefore, meson-exchange contributions reduce the discrepancy between the NMC data and the Gottfried sum.

The VMD contributions are compared with the Pomeron and meson exchange results in Fig. 2.5. The Pomeron contribution is of the same order of magnitude with the VMD effect at Q^2=4 GeV^2. Because the meson exchange produces extra sea-quark distributions, its effects show antishadowing. This fairly large antishadowing cancels much of the shadowing produced by the vector-meson dominance and the Pomeron exchange. The shadowing due to the Pomeron is rather small at $x > 0.05$ compared with other contributions, and it becomes comparable only in the small x region, $x < 0.01$. Adding these contributions, we show the total deuteron shadowing in Fig. 2.6. From these results, we obtain the correction to the NMC analysis at Q^2=4 GeV^2: $F_2^p - F_2^n = (F_2^p - F_2^n)_{NMC} + \delta F_{2D}$. The correction to the sum ranges from δI_G=-0.026 to -0.010 depending on the nuclear potential [57]. The description in Ref. [57] is consistent with the Fermilab-E665 data [16] on the deuteron shadowing. This fact suggests the above result of δI_G is a correct estimate.

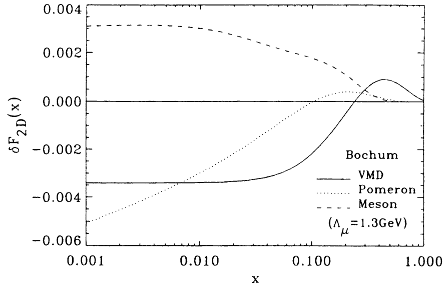

Figure 2.5: Vector-meson-dominance, Pomeron, and meson-exchange contributions at Q^2=4 GeV^2 (taken from Ref. [57]).

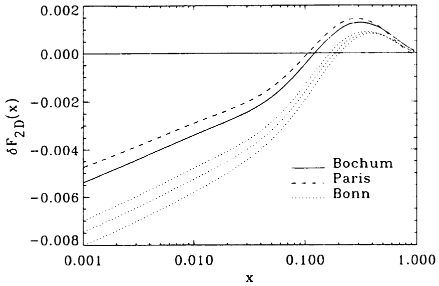

Figure 2.6: Total shadowing in the deuteron. The Bochum, Bonn, and Paris wave functions are used (taken from Ref. [57]).

In the beginning, the estimated shadowing effects on the Gottfried sum were fairly large, $\delta I_G = -0.08$. However, the recent numerical values seem to converge into about $\delta I_G = -0.02$ although there are still uncertain factors due to the nuclear potential. In comparison with the NMC value $I_G = 0.235 \pm 0.026$, it is about 10% effect. The shadowing studies do not alter the NMC conclusion. However, it has to be taken into account carefully because the shadowing magnifies the deviation from the Gottfried sum.

2.6 Parametrization of antiquark distributions

There are various factors which affect the NMC finding. Even the failure of the Gottfried sum is not undoubtedly confirmed. So present parametrizations of the flavor asymmetry $\bar{u} - \bar{d}$ is subject to change depending on future experimental results. We introduce several parametrizations in the following, but these should be considered as preliminary versions. If independent Fermilab Drell-Yan experiments confirm the NMC result and the NA51, they should be taken seriously.

Early version of the parametrization was proposed in Ref. [10] for explaining the SLAC data. The Fermilab-E288 collaboration analyzed its Drell-Yan data and obtained a parametrization in 1981 [12]. After the NMC measurement, several parametrizations have been proposed. The first one is Ref. [61]. They find that the global parametrization MRS-B (1988) overestimates the NMC $F_2^p - F_2^n$ data at small x even though it works for the neutrino structure function xF_3 and the Gross-Llewellyn Smith sum rule. The differences between the MRS-B and the NMC data are used for finding the flavor asymmetric distribution. In the similar way, the difference from the parametrization EHLQ1 is used for finding $\bar{u} - \bar{d}$ in Ref. [67].

New global MRS parametrizations were proposed by including the NMC data. The total sea-quark distribution at Q_0^2 is parametrized as

$$xS = 2x(\bar{u} + \bar{d} + \bar{s} + \bar{c}) = A_S x^{-\lambda} (1-x)^{\eta_S} (1 + \epsilon_S x^{1/2} + \gamma_S x) \quad , \tag{2.30}$$

and each distribution is

$$\begin{aligned} \bar{u} &= 0.2\, S\,(1-\delta) - \Delta/2 \quad , \\ \bar{d} &= 0.2\, S\,(1-\delta) + \Delta/2 \quad , \\ \bar{s} &= 0.1\, S\,(1-\delta) \quad , \\ \bar{c} &= \delta\, S/2 \quad , \end{aligned} \tag{2.31}$$

$$\text{with} \qquad x\Delta = A_\Delta x^{\eta_\Delta} (1-x)^{\eta_S} (1 + \gamma_\Delta x) \quad . \tag{2.32}$$

The parameters are determined by fitting many experimental data.

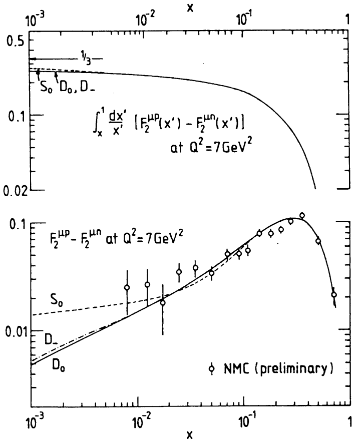

Figure 2.7: MRS-1993 parametrizations are compared with NMC data $F_2^p - F_2^n$ (taken from Ref. [62]).

The 1993 version is a good example in showing flavor symmetric and asymmetric distributions in comparison with the NMC F_2 data [62]. Therefore, we explain them in the following. Three possibilities are studied in the parametrization: (1) S (same), flavor symmetric sea $\bar{u} = \bar{d}$, (2) D_0 (different), asymmetric sea $\bar{u} \neq \bar{d}$, (3) D_-, asymmetric sea $\bar{u} \neq \bar{d}$ with a singular gluon distribution. The parametrizations are compared with the NMC data, and they explain the data fairly well as shown in Fig. 2.7. The flavor symmetric distribution (S_0) deviates from the asymmetric ones (D_0, D_-) only at small $x (< 0.01)$, where the data do not exist. In the NMC kinematical region, it is not possible to detect the differences between these parametrizations. Because the S_0 distribution recovers the Gottfried sum 1/3, there is significant contribution from the very small x region. However, the sum 1/3 can be reached only at very small $x \approx 10^{-10}$. The situation should be clarified by the Fermilab Drell-Yan experiments. The MRS group published new ones after the MRS-1993 version, in particular by including the NA51 asymmetry, HERA data, and the single jet cross sections at the Fermilab $p\bar{p}$ collider. Obtained parameters of the recent 1996 version are listed in Table 2.1 together with those of the 1993 version. The comparison of the recent one with other parametrizations is discussed in the end of this subsection.

Year	1993			1996			
Name	S_0	D_0	D_-	R_1	R_2	R_3	R_4
Q_0^2	4.0	4.0	4.0	1.0	1.0	1.0	1.0
$\Lambda_{\overline{MS}}^{n_f=4}$	215	215	215	241	344	241	344
A_S	1.87	1.93	0.054	0.42	0.37	0.92	0.92
λ	0	0	0.5	0.14	0.15	0.04	0.04
η_S	10.0	10.0	6.5	9.04	8.27	9.38	8.93
ϵ_S	-2.21	-2.68	19.5	1.11	1.13	-1.65	-2.34
γ_S	6.22	7.38	-3.28	15.5	14.4	11.8	12.0
A_Δ	0	0.163	0.144	0.039	0.036	0.040	0.038
η_Δ	/	0.45	0.46	0.3	0.3	0.3	0.3
γ_Δ	/	0	0	64.9	64.9	64.9	64.9
δ	0	0	0	0	0	0	0

Table 2.1: Parameters in the MRS 1993 and 1996 versions. The Q_0^2 and $\Lambda_{\overline{MS}}^{n_f=4}$ are listed in the units of GeV^2 and MeV respectively.

There are other parametrizations, for example by the CTEQ (Coordinated Theoretical/Experimental Project on QCD Phenomenology and Tests of the Standard Model) group [63]. The recent CTEQ parametrizations included the HERA data, which provided information on the small x behavior of the parton distributions. The HERA data and others from the CCFR, the Collider Detector at Fermilab (CDF), the NA51 on $\bar{u}/\bar{d}$ are included in the new parametrization analyses. The functional forms of the parton distributions are similar to the MRS ones, and they are provided at Q^2=2.56 GeV^2. According to the $\overline{MS}$ version of the CTEQ4 parametrization, the light antiquark distributions are obtained as [63]

$$\begin{aligned} x(\bar{d}+\bar{u})/2 &= 0.255x^{-0.143}(1-x)^{8.041}(1+6.112\sqrt{x}+x) \ \ , \\ x(\bar{d}-\bar{u}) &= 0.071x^{0.501}(1-x)^{8.041}(1+30.0x) \ \ , \end{aligned} \tag{2.33}$$

at Q^2=2.56 GeV^2. The scale parameter is $\Lambda_{\overline{MS}}^{n_f=5}$=202 MeV.

In contrast to the above parametrizations, the GRV (Glück, Reya, and Vogt) model supplies input distributions at very small Q^2 ($\approx$0.3 GeV^2). The original motivation was to set $\bar{q}(x) = g(x) = 0$ at certain small Q^2 ($\equiv \mu^2$) by allowing only the valence-quark distributions. Then, the sea-quark and gluon distributions are considered to be produced perturbatively through the evolution from μ^2. This attempt is slightly modified to the form including valence-like sea-quark and gluon distributions even at μ^2

$\overline{MS}$ scheme are plotted in Fig. 2.8. They are the MRS-R1 [62], CTEQ4M [63], and GRV-95 [64] distributions at Q^2=4 GeV^2. Because the GRV-95 was made so as to agree with the older version (MRS-A) of MRS at Q^2=4 GeV^2, the MRS-R1 and GRV-95 distributions are almost the same. Even though the CTEQ4M agrees with the others in the region $x > 0.2$, it is very different in the small x region. The CTEQ4M distribution is much smaller than the others. Because the NA51 Drell-Yan result is taken into account in the parametrizations, these distributions are almost the same at $x = 0.18$. However, we do not have enough constraint in the small x region. The only one is the NMC data on the Gottfried sum. The small x region should be clarified by future experiments, for example by the Fermilab-E866.

Figure 2.8: $x(\bar{u} - \bar{d})$ distributions at Q^2=4 GeV^2 in the MRS-R1, CTEQ4M, and GRV-95 parametrizations.

Updated information on the various parametrizations of the parton distributions is given at http://durpdg.dur.ac.uk/HEPDATA/PDF.

3 Expectations in perturbative QCD

According to the NMC conclusion, the Gottfried sum rule should be violated. In this section, we discuss how much corrections are expected in perturbative QCD. First, a general treatment of operator product expansion is discussed. Then possible perturbative QCD corrections to the sum rule are discussed.

3.1 Operator product expansion

In order to discuss QCD corrections to the Gottfried sum rule, we introduce operator-product expansion which is used in applying perturbative QCD methods to the structure functions. The hadron tensor $W_{\mu\nu}$ is expressed as the current product in Eq. (2.5). It is known in the light-cone limit $\xi^2 \to 0$ that the product is expressed in terms of local operators and their coefficients. For example if the current is given by $J_\mu(\xi) = \bar\psi(\xi)\gamma_\mu \mathcal{Q}\psi(\xi)$ with the charge matrix $\mathcal{Q}$ in the free massless Dirac theory, it becomes [81]

$$\frac{1}{2}\left([J_\mu(\xi/2), J_\nu(-\xi/2)] + [J_\nu(\xi/2), J_\mu(-\xi/2)] \right)$$
$$\xrightarrow[\xi^2\to 0]{} \sum_{odd\ n} \frac{i}{2^n n! \pi}\, \xi^{\mu_1} \cdots \xi^{\mu_n}\, S_{\mu\alpha\nu\beta} \left[\partial_\xi^\alpha\, \delta(\xi^2)\, \varepsilon(\xi^0) \right] O^\beta_{\mu_1 \cdots \mu_n} \quad , \tag{3.1}$$

where $\delta(\xi^2)$ is the δ function, $\varepsilon(\xi^0)$ is a step function: $\varepsilon(\xi^0) = +1$ for $\xi^0 > 0$ and -1 for $\xi^0 < 0$, $S_{\mu\alpha\nu\beta}$ is given by $S_{\mu\alpha\nu\beta} = g_{\mu\alpha}g_{\nu\beta} + g_{\mu\beta}g_{\nu\alpha} - g_{\mu\nu}g_{\alpha\beta}$, and the operator is defined by

$$O^\beta_{\mu_1\cdots\mu_n} = i\bar\psi(0)\mathcal{Q}^2\gamma^\beta\, \overset{\leftrightarrow}{\partial}_{\mu_1} \cdots \overset{\leftrightarrow}{\partial}_{\mu_n}\, \psi(0) \quad . \tag{3.2}$$

Virtual forward Compton amplitude is usually analyzed instead of the hadron tensor $W_{\mu\nu}$, because it is more convenient to use time-ordered product and to treat interference terms. The hadron tensor is related to the imaginary part of the Compton amplitude by the optical theorem $2M\, W_{\mu\nu} = (4/\pi)\, Im T_{\mu\nu}$, where $T_{\mu\nu}$ is given by the time-ordered product of currents:

$$T_{\mu\nu}(q^2,\nu) = \frac{i}{4} \overline{\sum_\sigma} \int d^4\xi\, e^{iq\cdot\xi} < p,\sigma \,|\, T(J_\mu(\xi)J_\nu(0)) \,|\, p,\sigma > \quad . \tag{3.3}$$

Here, only the unpolarized case is considered. The amplitude is decomposed into three invariant ones [82]:

$$T_{\mu\nu}(q^2,\nu) = e_{\mu\nu}T_L(q^2,\nu) + d_{\mu\nu}T_2(q^2,\nu) - i\epsilon_{\mu\nu\alpha\beta}\, \frac{p^\alpha p^\beta}{\nu}\, T_3(q^2,\nu) \quad , \tag{3.4}$$

where the tensors are defined by $e_{\mu\nu} = g_{\mu\nu} - q_\mu q_\nu / q^2$ and $d_{\mu\nu} = -p_\mu p_\nu q^2/\nu^2 + (p_\mu q_\nu + p_\nu q_\mu)/\nu - g_{\mu\nu}$. The amplitude T_L is the longitudinal one, T_2 is the longitudinal plus transverse one, and T_3 appears only in the weak current case.

As it is shown in Eq. (3.1), a product of current operators could be written by local operators and their coefficients. The singular behavior at $\xi^2 \to 0$ can be absorbed into the coefficients. Therefore, the Compton amplitude is expanded in terms of possible operators. However, infinite number of operators contribute to the amplitude in the expansion near the light cone. A convenient way to classify the contributions is to introduce twist τ, which is defined by the mass dimension of the operator minus its spin: $\tau = d_O - n$. For example, the twist for the operator $\bar\psi \gamma^\beta \partial_{\mu_1} \cdots \partial_{\mu_n} \psi$ is two because the mass dimension of ψ is 3/2, the dimension of the derivatives are n, and the spin is n+1. In this way, the current product is expanded near the light cone, and the amplitude becomes [2, 3]

$$i\,T(J(\xi)J(0)) \longrightarrow \sum_{\tau=2}^{\infty} \sum_{n=0}^{\infty} C_n^\tau(\xi^2, \mu^2)\, \xi^{\mu_1} \cdots \xi^{\mu_n}\, O^\tau_{\mu_1 \cdots \mu_n}(\mu^2) \quad , \tag{3.5}$$

where $C_n^\tau(\xi^2, \mu^2)$ are called coefficient functions and $O^\tau_{\mu_1 \cdots \mu_n}(\mu^2)$ are operators. For simplicity, the Lorentz indices μ and ν are dropped in the above equation. In the case of interacting fields, it is necessary to introduce a scale μ^2 in renormalizing the operators. This is the reason why explicit dependence on the renormalization point μ^2 is written in the above equation. In this way, the Compton amplitude is factorized into the long distance part and the light-cone part which could be handled in perturbative QCD. As it is given in Eq. (3.1), the product of the currents has a singular behavior in the limit $\xi^2 \to 0$, so that the coefficients could be written in a singular form $C_n^\tau(\xi^2) \sim (1/\xi^2)^{d_C/2}$. Counting dimensions in Eq. (3.5), we obtain $d_C = n - d_O + 2d_J = -\tau + 2d_J$ where d_O and d_J are mass dimensions of the operator and the current. From the dimensional counting, we find that the lowest-twist contribution, namely the twist-two, is most singular in the operator product expansion. From Eqs. (3.3), (3.4), and (3.5), the Compton amplitude becomes

$$T(q^2, \nu) \longrightarrow \sum_{\tau, n} \overline{C}_n^\tau(Q^2, \mu^2)\, \overline{O}_n^\tau(\mu^2)\, \frac{1}{x^n} \quad , \tag{3.6}$$

where $T(q^2, \nu)$ represents T_L, T_2, or T_3. The above $\overline{C}_n^\tau(Q^2, \mu^2)$ and $\overline{O}_n^\tau(\mu^2)$ are defined by

$$\int d^4\xi\, e^{iq\cdot\xi}\, C_n^\tau(\xi^2, \mu^2)\, \xi^{\mu_1} \cdots \xi^{\mu_n} = \frac{q^{\mu_1} \cdots q^{\mu_n}}{(Q^2/2)^n}\, \overline{C}_n^\tau(Q^2, \mu^2) \quad , \tag{3.7}$$

$$\frac{1}{4} \overline{\sum_\sigma} < p, \sigma \,|\, O^\tau_{\mu_1 \cdots \mu_n}(\mu^2) \,|\, p, \sigma > = \overline{O}_n^\tau(\mu^2)\, p_{\mu_1} \cdots p_{\mu_n} \quad . \tag{3.8}$$

In relating the Compton amplitudes to the structure functions, the following dispersion relation is used:

$$T(q^2,\nu) = \frac{2}{\pi}\int_{-q^2/2M}^{\infty} \frac{\nu' d\nu'}{\nu'^2-\nu^2}\, ImT(q^2,\nu) = \int_{-q^2/2M}^{\infty} \frac{\nu' d\nu'}{\nu'^2-\nu^2}\, M\,W(q^2,\nu)$$
$$= \sum_n \frac{1}{x^n}\int_0^1 dx'\, x'^{n-1}\, M\,W(q^2,x') \ . \quad (3.9)$$

Comparing Eq. (3.6) with Eq. (3.9), we obtain moments of the corresponding structure function. They are then expressed by the scaling functions:

$$\int_0^1 dx x^{n-1} F_1(x,Q^2) = \sum_\tau \overline{C}^{\tau}_{1,n}(Q^2,\mu^2)\,\overline{O}^{\tau}_{1,n}(\mu^2) \quad , \quad n=2,4,6\cdots \quad , \qquad (3.10)$$

and similar equations for F_2 and F_3, except that the moments are given by $\int dx x^{n-2} F_2$ in the F_2 case. Because of the crossing properties of the structure function under $\mu \leftrightarrow \nu$ and $x \leftrightarrow -x$, the only even-spin operators contribute in Eq. (3.10). The moments of the structure functions are thus given by the long-range part, which cannot be calculated without resorting to nonperturbative methods such as lattice QCD, and the light-cone part which can be evaluated in perturbative QCD.

There exist only even twists in the expansion Eq. (3.10) in the massless quark case. Therefore, higher-twist contributions are suppressed by the factor of $1/Q^2$ compared with the twist-two. The Gottfried sum rule is a flavor nonsinglet one. A twist-two nonsinglet operator is given by

$$O^{\tau=2,NS}_{\mu_1\cdots\mu_n} = \frac{i^{n-1}}{n!}\left[\bar\psi\frac{\lambda^a}{2}\gamma_{\mu_1}D_{\mu_2}\cdots D_{\mu_n}\psi + permutations\right] \quad , \qquad (3.11)$$

where D^μ is the covariant derivative $D_\mu = \partial_\mu - igT^a A^a_\mu$ with eight generators T^a of the color SU(3) group.

The renormalization point μ^2 is an arbitrary constant, so that physical observable should not depend on its scale. This fact leads to a renormalization group equation. It can be applied to the coefficients $C^\tau_{k,n}(Q^2,\mu^2)$ by comparing a renormalization group equation for a Green's function with the one for the local operator. In the nonsinglet case, it is given by

$$\left[\mu\frac{\partial}{\partial\mu} + \beta(g)\frac{\partial}{\partial g} - \gamma^{n,NS}(g)\right]\overline{C}^{NS}_{k,n}\left(\frac{Q^2}{\mu^2},g^2\right) = 0 \quad , \qquad (3.12)$$

where k indicates the structure-function type (k=1, 2, or 3) and τ is omitted for simplicity. The $\gamma^{n,NS}$ is anomalous dimension of the operator which is related to the renormalization factor of the operator ($Z^{NS}_n = O^{0,NS}_n/O^{NS}_n$) by $\gamma^{n,NS}(g) = \mu(\partial/\partial\mu)\ln Z^{NS}_n$. The β function is given by $\beta(g) = \mu(\partial/\partial\mu)g(\mu)$. The solution of Eq. (3.12) is

$$\overline{C}^{NS}_{k,n}\left(\frac{Q^2}{\mu^2},g^2\right) = \overline{C}^{NS}_{k,n}\left(1,\bar g^2\right) exp\left[-\int_{\bar g(\mu^2)}^{\bar g(Q^2)} dg' \frac{\gamma^{n,NS}(g')}{\beta(g')}\right] \quad . \qquad (3.13)$$

The anomalous dimension, coefficient function, and β function are expanded in α_s: $\gamma^{n,NS}(g) = \gamma_0^{n,NS}(g^2/16\pi^2)+\gamma_1^{n,NS}(g^2/16\pi^2)^2+\cdots$, $\overline{C}_{k,n}^{NS}(1,\bar{g}^2) = 1+B_{k,n}^{NS}(\bar{g}^2/16\pi^2)+\cdots$, and $\beta(g) = -g[\beta_0(g^2/16\pi^2) + \beta_1(g^2/16\pi^2)^2 + \cdots]$. Then the moments of the structure function become

$$M_{k,n}^{NS}(Q^2) = M_{k,n}^{NS}(Q_0^2)\left[\frac{\alpha_s(Q^2)}{\alpha_s(Q_0^2)}\right]^{d_n}\left[1 + C_{k,n}^{NS}\left(\frac{\alpha_s(Q^2)-\alpha_s(Q_0^2)}{4\pi}\right)\right] \quad , \tag{3.14}$$

where

$$d_n = \frac{\gamma_0^{n,NS}}{2\beta_0} \quad , \quad C_{k,n}^{NS} = B_{k,n}^{NS} + \frac{\gamma_1^{n,NS}}{2\beta_0} - \frac{\beta_1\,\gamma_0^{n,NS}}{2\beta_0^2} \quad . \tag{3.15}$$

Because Q_0^2 is an arbitrary scale, it is often convenient to express the above equation without Q_0^2:

$$M_{k,n}^{NS}(Q^2) = A_{k,n}^{NS}\left[\alpha_s(Q^2)\right]^{d_n}\left[1 + C_{k,n}^{NS}\frac{\alpha_s(Q^2)}{4\pi}\right] \quad , \tag{3.16}$$

where $A_{k,n}^{NS}$ is a constant given by $M_{k,n}^{NS}(Q_0^2) = A_{k,n}^{NS}[1+C_{k,n}^{NS}\alpha_s(Q_0^2)/(4\pi)][\alpha_s(Q_0^2)]^{d_n}$. In getting various sum rules, $A_{k,n=1}^{NS}$ may be evaluated in the parton model. Then LO and NLO anomalous dimensions $\gamma_0^{1,NS}$ and $\gamma_1^{1,NS}$ are calculated by studying renormalization of the nonsinglet operator. In order to obtain $B_{k,n=1}^{NS}$, we calculate first perturbative correction to the Compton amplitude and then $O_{k,n}^{\tau=2,NS}(p^2/\mu^2, g^2)$ by considering a matrix element of the nonsinglet operator between quark states. From these results, the NLO correction to the coefficient function $B_{k,1}^{NS}$ is obtained [82]. Combining these anomalous dimensions and the coefficient, we obtain the NLO correction $C_{k,n=1}^{NS}$ in Eq. (3.16).

3.2 Perturbative correction to the Gottfried sum

In the previous subsection, it is derived how the moments of a structure function at certain Q^2 can be calculated with given moments at Q_0^2 by using the prescriptions of the operator product expansion and the renormalization-group equation. Before discussing the Gottfried sum rule, we first check NLO corrections to another nonsinglet quantity, for example the Gross-Llewellyn Smith sum rule. It is related to the F_3 structure functions in neutrino scattering: $\int dx(F_3^{\nu N}+F_3^{\bar{\nu}N})/2$, where $F_3^N = (F_3^p+F_3^n)/2$. In the parton model without NLO effects, $(F_3^{\nu N}+F_3^{\bar{\nu}N})/2$ is given by $u_v(x,Q^2)+d_v(x,Q^2)$ so that it's integration over x is three ($A_1^{NS} = 3$). Because the first LO nonsinglet anomalous dimension vanishes ($\gamma_0^{n=1,\,NS}$=0), the coefficient d_1 becomes d_1=0. The NLO corrections are given by $B_{3,1}^{NS} = -4$ and $\gamma_1^{n=1,\,NS(-)}$=0 [83], so that we obtain $C_{3,1}^{NS(-)} = -4$. The notation $NS(-)$ indicates a $q-\bar{q}$ type nonsinglet distribution.

Figure 3.1: NLO contribution to the splitting $\bar{q} \to q$.

The NLO correction to the Gross-Llewellyn Smith sum rule is about 11%; however, the correction to the Gottfried sum is very different. Because the NLO term in the coefficient function vanishes ($B_{2,1}^{NS} = 0$) for the nonsinglet structure function F_2^{NS}, the only contribution is from the NLO anomalous dimension $\gamma_1^{NS(+)}$. Because the structure-function combination in Eq. (3.17) is given by $F_3^{\nu N} + F_3^{\bar{\nu} N} = (u - \bar{u}) + (d - \bar{d})$ in the leading order, it is a $q - \bar{q}$ type distribution. On the other hand, the Gottfried integrand is given in the parton model by $(F_2^p - F_2^n)/x = (1/3)[(u + \bar{u}) - (d + \bar{d})]$, which is a $q + \bar{q}$ type. This difference makes the anomalous dimension $\gamma_1^{n=1,\,NS(+)}$ finite. Even though the LO anomalous dimension vanishes in both cases, there is a finite contribution from the NLO process in Fig. 3.1. Namely, the $\bar{q} \to q$ splitting becomes possible. Because evolution of the $q \pm \bar{q}$ distributions is controlled by the splitting functions $P_{qq} \pm P_{q\bar{q}}$, the $q + \bar{q}$ evolution is different from the $q - \bar{q}$ one [84]. Because of baryon number conservation, the first anomalous dimension in the $NS(-)$ case has to vanish. However, there is an extra contribution from the $P_{q\bar{q}}$ (note: $P_{qq} + P_{q\bar{q}} = [P_{qq} - P_{q\bar{q}}] + 2P_{q\bar{q}}$) in the $NS(+)$ case. The anomalous dimension is calculated as [85]

$$\begin{aligned} \gamma_1^{n=1,\,NS(+)} &= -8\, P_{NS(+)}^{(1)}(n=1) \\ &= -16\,(C_F^2 - C_F C_A/2) P_A(n=1) \\ &= -4\,(C_F^2 - C_F C_A/2)\,[13 + 8\zeta(3) - 2\pi^2] \quad . \end{aligned} \tag{3.18}$$

With the numerical values $\zeta(3)$=1.2020569..., $C_F = (N_c^2 - 1)/2N_c$, $C_A = N_c$, and N_c=3, we obtain $\gamma_1^{n=1,\,NS(+)}$=+2.5576. In this way, the NLO term becomes $C_1^{NS(+)} = \gamma_1^{n=1,NS(+)}/(2\beta_0) = -6(C_F^2 - C_F C_A/2)[13 + 8\zeta(3) - 2\pi^2]/(33 - 2n_f)$. Including the NLO correction, we obtain the Gottfried sum [22, 23]:

$$
\begin{aligned}
I_G &= \frac{1}{3}\left[1+\frac{3(C_F C_A/2-C_F^2)}{2(33-2n_f)}\,(13+8\zeta(3)-2\pi^2)\,\frac{\alpha_s(Q^2)}{\pi}\right] \\
&= \frac{1}{3}\left[1+\begin{pmatrix}0.03552\,(n_f=3)\\ 0.03836\,(n_f=4)\end{pmatrix}\frac{\alpha_s(Q^2)}{\pi}\right] \quad . \qquad (3.19)
\end{aligned}
$$

The NLO contribution is merely 0.3% at Q^2=4 GeV^2. It obviously cannot explain the large violation found by the NMC. The NNLO α_s correction is estimated recently in Ref. [24]:

$$
I_G = \frac{1}{3}\left[1+\begin{pmatrix}0.036\,(n_f=3)\\ 0.038\,(n_f=4)\end{pmatrix}\frac{\alpha_s(Q^2)}{\pi}+\begin{pmatrix}0.72\,(n_f=3)\\ 0.55\,(n_f=4)\end{pmatrix}\left\{\frac{\alpha_s(Q^2)}{\pi}\right\}^2\right] \quad . \qquad (3.20)
$$

The NNLO correction is about 0.4% at Q^2=4 GeV^2. We find from these higher-order analyses that the perturbative corrections are too small to account the NMC deficit.

The tiny scaling violation is understood in the following way. The Q^2 dependence comes from the difference between the flavor-diagonal and nondiagonal splitting processes. Because there are two identical particles in the flavor-diagonal case, they should be antisymmetrized. If it could be neglected, the Q^2 evolution is flavor symmetric and there is no scaling violation in the Gottfried sum. However, the above-mentioned antisymmetrization provides the very small scaling violation [49].

We comment on experimental information about possible Q^2 dependence in Ref. [25]. The neutron $F_2(x,Q^2)$ is obtained from various proton and deuteron measurements with nuclear corrections. With the F_2^p parametrization for explaining the NMC, H1, or ZEUS data, the Q^2 variation

$$
I_G(Q^2) = S_0\,\left[\,1+c_1\,(\alpha_s/\pi)+c_2\,(\alpha_s/\pi)^2\,\right] \qquad (3.21)
$$

is investigated. The obtained parameters averaged over the NMC92, NMC95, and H1 are $S_0 = 0.242 \pm 0.21$, $c_1 = -6.00 \pm 0.74$, and $c_2 = 40.4 \pm 11.1$. The result indicates large Q^2 dependence which cannot be accounted by the perturbative QCD. However, the analysis with the ZUES F_2^p shows rather different values: $S_0 = 0.383$, $c_1 = -12.9$, and $c_2 = 76.2$. Therefore, accurate information cannot be obtained at this stage. Future HERA measurement of F_2^D at small x is necessary to find the precise Q^2 variation.

The perturbative QCD studies show that perturbative mechanisms cannot account for the large violation of the Gottfried sum rule. If the violation is confirmed by further experiments, the deficit should come from another source, namely a nonperturbative mechanism.

4 Theoretical ideas for the sum-rule violation

The NMC results in 1991 and in 1994 indicate a significant deviation from the Gottfried sum. We showed that the perturbative mechanisms cannot account for the possible violation of the sum rule. It is even not clear whether or not the sum rule is in fact violated by considering the small x part. A possible way to answer these problems theoretically is to use a nonperturbative approach. Various theoretical ideas have been proposed for explaining the deficit in terms of explicit flavor asymmetry $\bar{u} - \bar{d} \neq 0$. These ideas are discussed in the following.

4.1 Lattice QCD

The most fundamental way to treat nonperturbative physics is to use lattice QCD. The following discussions are based on Ref. [26]. The forward Compton amplitude Eq. (3.3) could be computed by taking the ratio of a four-point function and a two-point function:

$$\widetilde{W}_{\mu\nu}(\vec{q}^{\,2},\tau) = \left. \frac{\frac{1}{2M_N} < O_N(t) \int \frac{d^3\xi}{2\pi} e^{-i\vec{q}\cdot\vec{\xi}} J_\mu(\vec{\xi},t_1) J_\nu(0,t_2) O_N(0) >}{< O_N(t-\tau) O_N(0) >} \right|_{t-t_1,t_2>>1/\Delta M_N} , \tag{4.1}$$

where τ is given by $\tau = t_1 - t_2$, ΔM_N is the mass difference between the nucleon and the first excitation state, and $O_N(t)$ is the interpolation field for the nucleon. The hadron tensor $W_{\mu\nu}$ is then calculated by the inverse Laplace transformation.

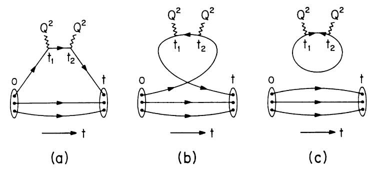

Figure 4.1: Twist-two contributions (taken from Ref. [26]).

Euclidean path-integral formalism can be used for evaluating the four-point function. The leading-twist contributions come from the diagrams in Fig. 4.1. Quark propagators are involved in the diagrams of Figs. 4.1(a) and (c), and antiquark ones are in Figs. 4.1(b) and (c). Therefore, antiquark contributions come from either the connected insertion in Fig. 4.1(b) or the disconnected one in Fig. 4.1(c). We may call the contribution in Fig. 4.1(b) from "cloud" antiquarks and the one in Fig. 4.1(c) from "sea" antiquarks, so that an antiquark distribution could be written as $\bar{q}_i(x) = \bar{q}_i^c(x) + \bar{q}_i^s(x)$. In the same way, a quark distribution is expressed as $q_i(x) = q_i^V(x) + q_i^c(x) + q_i^s(x)$. If the light-quark masses are equal $m_u = m_d$, there is no contribution to the flavor asymmetry $\bar{u} - \bar{d}$ from the sea graphs in Fig. 4.1(c). Then, the contributions become $I_G = 1/3 + (2/3)\int_0^1 dx[\bar{u}_c(x) - \bar{d}_c(x)]$.

The hadron tensor has not been calculated directly due to a huge numerical task, so that three-point function with one current may be investigated. However, the Gottfried sum cannot be calculated because the first moment of $F_2^p - F_2^n$ cannot be expressed in terms of the matrix element of a twist-two operator. Therefore, real lattice QCD estimate of the Gottfried sum is not available at this stage. Instead, scalar matrix elements were studied in Ref. [26] in order to learn about the cloud contributions to the $\bar{u} - \bar{d}$ number. The scalar charge $\int d^3x \bar{\Psi}\Psi = \int d^3k (m/E) \sum_s [b^\dagger_{k,s} b_{k,s} + d^\dagger_{k,s} d_{k,s}]$ is the sum of quark and antiquark numbers with the weight factor m/E, so that they could be a measure of the difference $\bar{u} - \bar{d}$. Because we are interested in the cloud antiquarks, only the connected insertion (CI) is discussed in the following. In order to reduce the artificial lattice effects, it is better to investigate ratios of matrix elements. The ratio of isoscalar and isovector matrix elements for the CI is then approximated as

$$R_s = \left. \frac{\langle p|\bar{u}u|p\rangle - \langle p|\bar{d}d|p\rangle}{\langle p|\bar{u}u|p\rangle + \langle p|\bar{d}d|p\rangle} \right|_{CI} = \frac{1 + 2\int dx [\bar{u}_c(x) - \bar{d}_c(x)]}{3 + 2\int dx [\bar{u}_c(x) + \bar{d}_c(x)]} \quad . \tag{4.2}$$

Numerical results are obtained by using $16^3 \times 24$ lattices with β=6 and the hopping parameter κ=0.105−0.154. In Fig. 4.2, the obtained ratios R_s are plotted as a function of the quark mass $m_q a$. Because the antiquark number is positive, the ratio has to be smaller than 1/3. The cloud antiquarks are suppressed in the heavy-quark case, so that the ratio agrees with the valence-quark expectation 1/3 in Fig. 4.2. As the quark mass decreases, the ratio becomes smaller than 1/3. This decrease should be interpreted as the cloud effects. In order to verify this interpretation, we consider a valence approximation, which means amputating the backward time hopping. The ratios with this approximation are shown by the filled circles and they are 1/3 as expected. Next, we discuss comparison with the NMC result. The state with the $q\bar{q}$ clouds has higher energy than one of the valence-quark state, which means that the m/E factor is smaller. Therefore, we could estimate the upper bound for the $\bar{u} - \bar{d}$ number by $n_{\bar{u}} - n_{\bar{d}} \le [< N|\bar{u}u - \bar{d}d|N >_{cloud} \; / \; < N|\bar{u}u - \bar{d}d|N >_{valence} -1]/2$. Their result extrapolated to the chiral limit is $n_{\bar{u}} - n_{\bar{d}} \le -0.12 \pm 0.05$. It indicates a $\bar{d}$ number excess over the $\bar{u}$. The obtained result could be used as a measure of the flavor asymmetry although the quantitative comparison with the Gottfried sum is not obvious. It is, however, interesting to find that the obtained value is consistent with the NMC asymmetry in Eq. (2.24).

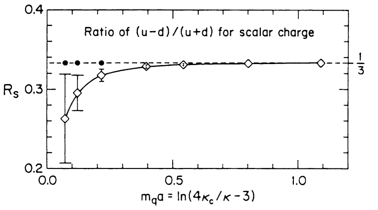

Figure 4.2: Ratio of the isoscalar to isovector scalar charge (taken from Ref. [26]).

Even though there is no direct estimate of the Gottfried sum in the lattice QCD right now, there is an indication of the large light-antiquark flavor asymmetry. It is shown that the difference comes from the connected insertion involving quarks propagating backward in time by studying the isovector-isoscalar charge ratio. Because the flavor asymmetry comes from the cloud antiquarks, physics mechanism behind the above results is considered as the Pauli blocking and/or the mesonic effects.

4.2 Pauli exclusion principle

Pauli exclusion model was investigated in Refs. [10, 11] for explaining the SLAC data. Because the proton has two valence u quarks and one valence d quark, the $u\bar{u}$ pair creation receives more Pauli exclusion effect than the $d\bar{d}$ pair creation does. This results in the difference between $\bar{u}$ and $\bar{d}$ in the nucleon. No qualitative calculation is done in Ref. [10] except for a parametrization based on the above intuition. In order to explain the SLAC data (I_G=0.27 according to the analysis in Ref. [10]) the following parametrization was proposed

$$x\bar{u} = 0.17(1-x)^{10} \quad , \quad x\bar{d} = 0.17(1-x)^{7} \quad . \tag{4.3}$$

First, we explain how the flavor asymmetry can be calculated in a model even though a realistic four dimensional calculation is not available at this stage. A qualitative calculation on the Pauli blocking effects is discussed in Refs. [27] and [32]. A parton distribution in the nucleon is calculated by [86]

$$\begin{aligned} \bar{q}_i(x) &= \frac{\sqrt{2}}{4\pi}\int d\xi^- e^{-ixp^+\xi^-} < p\,|\,\psi_{i,+}(\xi^-)\,\psi^\dagger_{i,+}(0)\,|\,p>_c |_{\xi^+=0} \\ &= \frac{1}{\sqrt{2}}\sum_n \int \frac{dp'_n}{4\pi p^0_n}\delta(p^+_n-(1-x)p^+)\;|<n\,|\psi^\dagger_{i,+}(0)|\,p>|^2 \quad , \end{aligned} \tag{4.4}$$

where the subscript c indicates a connected matrix element, ψ_+ is defined by $\psi_+ = \gamma^-\gamma^+\psi/2$, and p'_n is the momentum of the intermediate state. It is the probability of removing an antiquark q_i with momentum xp^+, leaving behind a state $|\,n>$. The 1+1 dimensional MIT bag model is used for evaluating the antiquark distribution. However, a realistic 3+1 dimensional calculation has not been done yet. We estimate the effect by a simple counting estimate.

In the 1+1 dimension, there are three color states for each flavor. Two of the three u-quark ground states and one of the three d-quark states are occupied. It is possible to have only one more u-quark in the ground state, but two more d-quarks can be accommodated. Therefore, expected sea-quark asymmetry is fairly large: $\bar{d} = 2\bar{u}$ in the 1+1 dimensional bag picture. In the four dimensional case, there are six states (three-color times two-spin states) in the ground state. There are four available ground states for u-quarks and five states for d-quarks, so that the asymmetry becomes

$$\frac{\bar{d}}{\bar{u}} = \frac{5}{4} \qquad \text{(in a naive counting estimate)} \quad . \tag{4.5}$$

Because there is no valence antiquarks in the bag, Eq. (4.4) indicates that the contribution comes from a quark being inserted, interacting in the bag, and then being removed. Therefore, the $\bar{d}$ excess is related to the distribution associated with a four-quark intermediate state $f_4(x)$

$$\int_0^1 dx[d_{sea}(x) - u_{sea}(x)] = \int_0^1 dx f_4(x) = 1 - P_2 \quad , \tag{4.6}$$

where P_2 is the integral of a distribution associated with a two-quark intermediate state. Because the $\bar{u}$ and $\bar{d}$ distributions are not calculated in the four dimensional model, the Pauli contributions are given by a simple function $x^\alpha(1-x)^\beta$ in Ref. [32]. The constant α is chosen to match the small x behavior of used valence distributions, and β=7 is taken so that it contributes only at small x. The overall normalization is not determined theoretically at this stage. Roughly speaking, we expect to have $1-P_2$ in the 25% range because of the naive counting estimate in Eq. (4.5). The obtained x dependent results are studied together with pionic effects in the following subsection.

It is shown that the Pauli blocking effects could produce the excess of $\bar{d}$ quark over $\bar{u}$. The naive counting in four dimension indicates $\bar{d}/\bar{d}$=5/4. Unfortunately, qualitative x dependence is not calculated except for the 1+1 dimensional model. It is indicated that 10% Pauli effects together with pionic contributions can explain the NMC data $F_2^p - F_2^n$ fairly well [32]. However, it was found recently that the conclusion should be changed drastically if the antisymmetrization between quarks is considered in addition [27]. The same u-valence excess, which suppresses the $u\bar{u}$ pair creation, also produces extra diagrams involved in the $u\bar{u}$ creation because of the antisymmetrization with the extra u. These extra diagrams contribute to a $\bar{u}$ excess over $\bar{d}$. According to Ref. [27], if the Pauli-principle and antisymmetrization effects are combined, the $\bar{u}$ could be larger than $\bar{d}$, which is in contradiction to the NMC conclusion.

4.3 Mesonic models

The Pauli exclusion mechanism produces the flavor asymmetry; however, its effects on the sum rule do not seem to be large enough to explain the NMC result according to the counting estimate. Furthermore, if they are combined with the antisymmetrization contributions, we could have a $\bar{u}$ excess over $\bar{d}$. On the other hand, the meson-cloud mechanism is the most successful one in explaining the major part of the NMC flavor asymmetry. Because a significant amount of papers are written on this idea, we explain the model in detail. We first discuss conventional virtual-meson contributions in section 4.3.1. Second, chiral models in a similar spirit are explained in 4.3.2. Third, possible modification of the Q^2 evolution due to the meson emission is discussed in 4.3.3.

4.3.1 Meson-cloud contribution

It is well known that virtual mesons play a very important dynamical role in nucleon structure, as they have been studied in the context of cloudy bag or other chiral models. The proton decays into π^+ and neutron, π^0 and proton, and other states within the time allowed by the uncertainty principle. The virtual pion state is essential for explaining many dynamical properties, for example the large Δ decay width and negative square charge radius of the neutron. Therefore, it is important to study whether or not the mechanism could produce a flavor asymmetry. It should be noted that perturbative contributions to the antiquark distributions through the gluon splitting into $q\bar{q}$

should be much larger than the mesonic ones at reasonably large Q^2. However, these contributions are supposed to be flavor symmetric, and the asymmetric distributions $(\bar u + \bar d)/2 - \bar s$ and $\bar u - \bar d$ could be used for testing the meson mechanism.

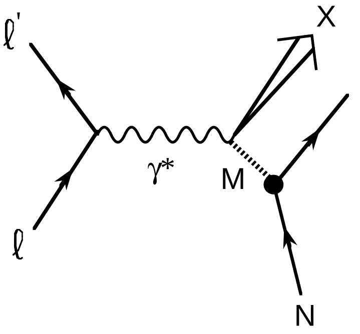

Figure 4.3: Mesonic contribution to $\bar q$.

The original idea stems from Ref. [87] in 1972, so that the process in Fig. 4.3 is sometimes called “Sullivan process”. The proton splits into a pion and a nucleon, and the virtual photon interacts with the pion. Antiquark distributions in the pion contribute to the corresponding antiquark distributions in the proton. Although the idea is interesting, it had not been a very popular topic until recently. It is partly because experimental data are not accurate enough to shed light on the mechanism. After the NMC discovery, it is shown that the pion-cloud mechanism could explain a significant part of the NMC finding [30, 31, 32]. This idea is developed further by including many meson and baryon states [33] and by considering different form factors at the meson-baryon vertices [35] so as to explain the whole NMC asymmetry.

The formalism in Ref. [87] is the following. The cross section of Fig. 4.3 with $M=\pi$ is derived by replacing the $\gamma^* + p \to X$ vertex in the $e+p \to e' + X$ formalism in section 2.1 by

$$\mathcal{M}_\mu = < X|eJ_\mu(0)|\pi > \ \frac{1}{p_\pi^2 - m_\pi^2}\, F_{\pi NN}(t)\, \bar u(p')\, i\, g_{_{\pi NN}}\, \widetilde{\phi}_\pi^* \cdot \widetilde{\tau}\, \gamma_5\, u(p) \quad , \tag{4.7}$$

where $F_{\pi NN}(t)$ is the πNN form factor, $g_{_{\pi NN}}$ is the πNN coupling constant, and $\widetilde{\phi}_\pi^* \cdot \widetilde{\tau}$ is the isospin factor. The W_2 structure function for the pion is defined in the same way with Eq. (2.6) by the replacements $p \to p_\pi$ and $M \to m_\pi$. Then, projecting out the F_2 part, we obtain

$$F_2^{pionic}(x,Q^2) = |\widetilde{\phi}_\pi^* \cdot \widetilde{\tau}|^2\, \frac{g_{_{\pi NN}}^2}{16\pi^2} \int_x^1 dy\, y\, F_2^\pi(x/y, Q^2) \int_{-\infty}^{t_m} dt\, \frac{-t}{(t-m_\pi^2)^2}\, |F_{\pi NN}(t)|^2 \quad , \tag{4.8}$$

where t_m is the maximum energy transfer: $t_m = -m_N^2 y^2/(1-y)$. This equation is understood by the convolution of the pion structure function with a light-cone momentum distribution of the pion. The formalism is used for antiquark distributions in the same manner.

The studies of the pionic mechanism used to be somewhat confusing. The direct interaction of the photon with mesons being present in the cloud of a nucleon does not contribute to the Gottfried sum. This does not mean that the mesons do not contribute to the Gottfried sum and the $\bar{u}-\bar{d}$ distribution as explained in this subsection. In dealing with this issue, there are two types of descriptions. One is to calculate only mesonic contributions to the $\bar{u}-\bar{d}$ distribution [30, 31, 35] and another is to include recoiling baryon interaction with the virtual photon in addition [32, 33]. Both are essentially the same. The details of the compatibility are discussed in the following.

[I. Models with only meson contributions]

First, we discuss the former approach with the only meson contributions. The Seattle [30] and Indiana [31] papers proposed pionic ideas for the sum-rule violation in this description. The only major difference is the inclusion of $p \to \pi\Delta$ processes in Ref. [31] in addition to the πNN ones. Relative magnitude and sign of the πNN and $\pi N\Delta$ contributions can be understood in the following way. We consider the processes $p \to \pi^+ + n$, $\pi^0 + p$, $\pi^+ + \Delta^0$, $\pi^0 + \Delta^+$, and $\pi^- + \Delta^{++}$, where the virtual photon interacts with the pions. Assuming the flavor symmetry in the pion sea, we have the $\bar{u}-\bar{d}$ distributions in the pions:

$$(\bar{u}-\bar{d})_{\pi^+} = -V_\pi \quad , \qquad (\bar{u}-\bar{d})_{\pi^0} = 0 \quad , \qquad (\bar{u}-\bar{d})_{\pi^-} = +V_\pi \quad , \tag{4.9}$$

where V_π is the valence-quark distribution in the pions. The flavor symmetry assumption in the pions does not alter our conclusion unless at very small x with the following reason. For example, let us consider the $\bar{u}-\bar{d}$ distribution at x=0.1. The light-cone momentum distribution of the pion is peaked at y ~0.25; therefore, the most important kinematical region for $(\bar{u}-\bar{d})_\pi$ is at x/y ~0.4. The valence distribution still dominates in this region, so that the sea asymmetry in the pion does not matter. Including isospin coefficients at the πNN and πNΔ vertices,

$$\begin{array}{llll}
|\widetilde{\phi}^*_{\pi^+}\cdot\widetilde{\tau}|^2 = \,2 \;\; , & |\widetilde{\phi}^*_{\pi^0}\cdot\widetilde{\tau}|^2 = \,1 \;\; , & & \\
|\widetilde{\phi}^*_{\pi^+}\cdot\widetilde{T}|^2 = \dfrac{1}{3} \;\; , & |\widetilde{\phi}^*_{\pi^0}\cdot\widetilde{T}|^2 = \dfrac{2}{3} \;\; , & |\widetilde{\phi}^*_{\pi^-}\cdot\widetilde{T}|^2 = \,1 \;\; , &
\end{array} \tag{4.10}$$

we have the isospin times the $(\bar{u}-\bar{d})_\pi$ factors as

$$\begin{aligned}
&\sum_\pi |\widetilde{\phi}^*_\pi\cdot\widetilde{\tau}|^2\,(\bar{u}-\bar{d})_\pi = \,-2\,V_\pi \qquad \text{for the πNN process} \;\; , \\
&\sum_\pi |\widetilde{\phi}^*_\pi\cdot\widetilde{T}|^2\,(\bar{u}-\bar{d})_\pi = \,+\frac{2}{3}\,V_\pi \qquad \text{for the πNΔ} \;\; .
\end{aligned} \tag{4.11}$$

In this way, we find that the πNN contribution to $\bar{u}-\bar{d}$ is negative and is partly canceled by a positive contribution from the πNΔ. The other important factor is the meson-baryon vertex form factor. Because the exact functional form is not known, the following monopole, dipole, and exponential forms are usually used:

$$
\begin{aligned}
F_{MNB}(t) &= \frac{\Lambda_m^2 - m_M^2}{\Lambda_m^2 - t} && \text{monopole} \\
&= \left(\frac{\Lambda_d^2 - m_M^2}{\Lambda_d^2 - t} \right)^2 && \text{dipole} \\
&= e^{(t - m_M^2)/\Lambda_e^2} && \text{exponential}\ , \qquad (4.12)
\end{aligned}
$$

at the MNB vertex. The different parameters could be related, for example, by $\Lambda_m = 0.62\Lambda_d = 0.78\Lambda_e$ [31].

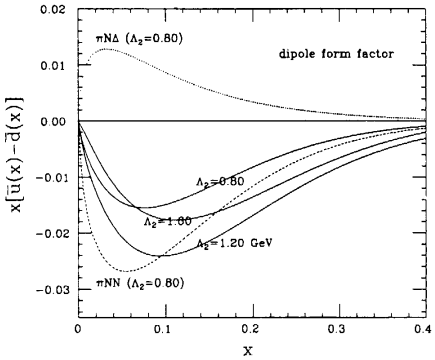

Figure 4.4: πNN and $\pi N\Delta$ contributions to $\bar{u} - \bar{d}$ (taken from Ref. [31])

Detailed numerical results are shown in Fig. 4.4, where pionic contributions from the πNN and $\pi N\Delta$ processes are shown [31]. The dipole cutoff parameter Λ_2=0.8 GeV [$= \Lambda_d$ in Eq. (4.12)] is fixed by fitting the $(\bar{u}+\bar{d})/2-\bar{s}$ experimental data. The dotted curves are πNN and $\pi N\Delta$ contributions. As it is shown in the naive discussion, the πNN effect is negative and it is canceled by the positive $\pi N\Delta$ contribution. The total contribution with Λ_2=0.8 GeV is shown by a solid curve together with those at Λ_2=1.0 and 1.2 GeV. It is noteworthy that the total $\bar{u} - \bar{d}$ curve is not very sensitive to the cutoff although the distribution $(\bar{u} + \bar{d})/2 - \bar{s}$ does depend much on it. Integrating the pionic contribution over x, we obtain $\Delta I_G = 2/3 \int dx(\bar{u} - \bar{d})_\pi = -0.04$, which accounts for about a half the discrepancy found by the NMC. It is encouraging that the mesonic model gives a reasonable value for the magnitude obtained by the NMC. Although we discussed only the πNN and πNΔ processes, other processes should be investigated. For example, kaon, Λ, Σ, and Σ^* are added to π, N, and Δ in Ref. [35]. The first method is well summarized in Ref. [35], so that we quote its results in the following.

Mesonic contributions to an antiquark distribution in the nucleon are given by the convolution of the corresponding antiquark distribution in a meson with the light-cone momentum distribution of the meson. The contributions are given by the equation

$$
x\,\overline{q}_N(x, Q^2) = \sum_{MB} \alpha^q_{MB} \int_x^1 dy\, f_{MB}(y)\, \frac{x}{y}\, \overline{q}_M(x/y, Q^2) \quad , \qquad (4.13)
$$

where the summations are taken over combinations of meson states $M = (\pi,\, K)$ and baryon states $B = (N,\, \Delta,\, \Lambda,\, \Sigma,\, \Sigma^*)$, and α^q_{MB} is the spin-flavor SU(6) Clebsch-Gordan factors. This equation corresponds to Eq. (4.8) in the F_2 case. The light-cone momentum distribution of the virtual meson is

$$f_M(y) = \sum_B f_{MB}(y) \quad , \tag{4.14}$$

with

$$f_{MB}(y) = \frac{g^2_{MNB}}{16\pi^2}\, y \int_{-\infty}^{t_m} dt\, \frac{\mathcal{I}(t, m_N, m_B)}{(-t+m_M^2)^2}\, [F_{MNB}(t)]^2 \quad . \tag{4.15}$$

The integrand factor $\mathcal{I}(t, m_N, m_B)$ is given by

$$\begin{aligned} \mathcal{I}(t, m_N, m_B) &= -\,t + (m_B - m_N)^2 && \text{for } B \in \mathbf{8} \\ &= \frac{\big[\,(m_B+m_N)^2 - t\,\big]^2\,\big[\,(m_B-m_N)^2 - t\,\big]}{12\, m_N^2\, m_B^2} && \text{for } B \in \mathbf{10}\ , \end{aligned} \tag{4.16}$$

depending whether the baryon B is in the baryon octet or in the decuplet. The upper limit of the integral is given by

$$t_m = m_N^2\, y - \frac{m_B^2\, y}{1-y}\ . \tag{4.17}$$

Because the coupling constants are relatively well known, the only factor to be paid attention to is the MNB form factors. There are recent studies on whether the form factor is hard or soft. Instead of stepping into the details, we summarize briefly the historical background and the present situation. A hard form factor with the typical monopole cutoff $1.0 < \Lambda_m < 1.4$ GeV is essential for explaining the deuteron D-state admixture and nucleon-nucleon scattering experiments. On the other hand, softer ones are obtained in quark models: for example $\Lambda_m \approx 0.6$ GeV in the cloudy-bag model [88] $0.7 < \Lambda_m < 1.0$ GeV in a flux-tube model [89]. However, a conflicting result came from the studies of the flavor asymmetric distribution $(\bar{u} + \bar{d})/2 - \bar{s}$. It was originally announced that the cutoff should be much softer, $\Lambda_m < 0.5$ GeV [90], which contradicts awfully to the OBEP one. Later analysis with renewed experimental data show a slightly larger cutoff $\Lambda_m \approx 0.6$ GeV [31], which could be consistent with those in the quark models. In the Jülich approach, which is discussed in the following paragraphs, the obtained cutoff becomes larger $\Lambda_m \approx 0.74$ GeV (note: monopole cutoff is estimated by $\Lambda_m = 0.62\Lambda_d$ with $\Lambda_d = 1.2$ GeV [33]) because more meson and baryons are added to π, N, Δ and because the following normalization factor Z is taken into account. The probability to find the bare nucleon is reduced by the factor Z due to the presence of the meson clouds as explained in detail in the model II. The recent one in Ref. [35] without explicit baryon contributions indicates a similar value $\Lambda_m \approx 0.8$ GeV. Furthermore, it is discussed that kinematical regions, which contribute to the low-energy NN scattering and deep inelastic processes, are very different in the form factor. The discrepancy between the hard OBEP form factor and the soft one should not be taken seriously. Whatever the outcome may be, it does not change our $\bar{u}-\bar{d}$ studies significantly if the parameter is fixed so as to explain the $(\bar{u}+\bar{d})/2-\bar{s}$ distribution.

[II. Models with meson and baryon contributions]

Next, we discuss the second approach, which includes recoil-baryon interactions with the virtual photon in addition to the meson interactions as shown in Fig. 4.5. This type of description is studied in the Adelaide paper, [32], the Jülich [33], and Ref. [34]. In particular, the Jülich group developed this model by including many meson and baryon states. So far πN, ρN, ωN, σN, ηN, $\pi\Delta$, $\rho\Delta$, $K\Lambda$, $K^*\Lambda$, $K\Sigma$, $K^*\Sigma$, KY^*, and K^*Y^* states are included. The pions do not contribute to $F_2^p - F_2^n$, so that the πNN and $\pi N\Delta$ contributions are given by [32]

$$F_2^p(x)-F_2^n(x) = Z\left\{\frac{x}{3}[u_v(x)-d_v(x)] - \frac{1}{3}\int_0^{1-x} dy \frac{f_N(y)}{1-y}\frac{x}{3}\left[u_v\left(\frac{x}{1-y}\right) - d_v\left(\frac{x}{1-y}\right)\right]\right.$$
$$\left. + \frac{1}{6}\int_0^{1-x} dy \frac{f_\Delta(y)}{1-y}\frac{10x}{3} d_v\left(\frac{x}{1-y}\right)\right\} \quad . \qquad (4.18)$$

The functions $f_N(y)$ and $f_\Delta(y)$ are pion light-cone momentum distributions, and Z is the valence normalization factor $Z = 1/(1+N_\pi+\Delta_\pi)$ with probability of finding a pion $N(\Delta)_\pi = \int_0^1 dy f_{N(\Delta)}(y)$. From these equations, the sum becomes $I_G = (Z/3)(1 - N_\pi/3 + 5\Delta_\pi/3)$. According to this equation, the failure of the sum rule is not due to the photon interaction with the virtual pion but it is due to the interaction with the recoil baryons. This may seem contradictory to the conclusion in the first approach. However, it is not a paradox as explained in Refs. [33, 35].

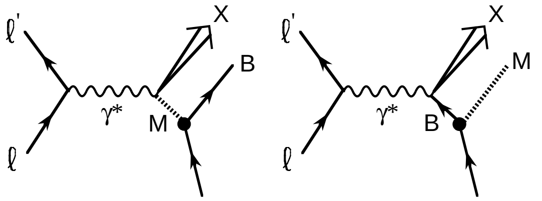

Figure 4.5: Baryon terms in (b) are included in addition to the meson contributions in (a).

Process	A_i^M	A_i^B	B_i^M	B_i^B
πN	0	−1/3	−2/3	0
ρN	0	−1/3	−2/3	0
ωN	0	1	0	0
σN	0	1	0	0
ηN	0	1	0	0
$\pi\Delta$	0	5/3	1/3	0
$\rho\Delta$	0	5/3	1/3	0
$K\Lambda$	1	0	0	0
$K^*\Lambda$	1	0	0	0
$K\Sigma$	−1/3	4/3	0	0
$K^*\Sigma$	−1/3	4/3	0	0
KY^*	−1/3	4/3	0	0
K^*Y^*	−1/3	4/3	0	0

Table 4.1: Coefficient A_i and B_i in two different descriptions [33].

Adding other contributions from light meson and baryon states, we write the previous equation as

$$I_G = \frac{1}{3}\,(Z + \sum_i A_i)\ , \quad \text{with}\ \ A_i = \int_0^1 dx\,(u_i + \bar{u}_i - d_i - \bar{d}_i)_{Sull} \tag{4.19}$$

where the meson and baryon contributions A_i are given in Table 4.1. It should be noted that all the coefficients in the table should be multiplied by the probabilities of finding the meson-baryon states in the nucleon. The nucleon "core" satisfies the valence sum $\int dx(u_v - d_v)_{core} = 1/3$ but its probability is reduced by the normalization factor Z due to the virtual MB states. On the other hand, the sum could be written in a different form. Whatever the normalization mechanism is, the valence sum should be exactly satisfied. Therefore, a part of the meson and baryon contributions can be included into the valence sum 1/3. Then, the deviation from 1/3 is identified with the flavor asymmetry due to the Sullivan processes $\int dx(\bar{u} - \bar{d}) = \int dx(\bar{u} - \bar{d})_{Sull}$ [31, 33, 35]:

$$I_G = \frac{1}{3}\,(1 + \sum_i B_i)\ , \quad \text{with}\ \ B_i = \int_0^1 dx\,(u_i - \bar{d}_i)_{Sull}\ \ . \tag{4.20}$$

Equation (4.20) corresponds to the first approach without the baryon contributions and Eq. (4.19) to the second method by the Adelaide and Jülich. As the coefficients are listed in Table 4.1, there is no contribution from the pion and rho mesons to the sum in the second approach. Therefore, the violation comes from the normalization factor Z and the baryon contributions. Because the distribution $u + \bar{u} - d - \bar{d}$ vanishes for example in the pion, this is a natural consequence. However, the virtual πB contributes to the renormalization of the valence-quark distributions. Therefore, we may take out the pionic renormalization contributions and put them into the obvious valence-sum factor 1/3 in Eq. (4.20) [31]. Then, it becomes apparent that the pion contributes to the deviation from the Gottfried sum as indicated in Eq. (4.20). Because of the flavor symmetry assumption in the MB, the pion and rho are the only light hadrons which contribute to the violation. In this way, the two different mesonic descriptions are equivalent, and both numerical results have to be the same.

In the beginning, it was shown that a significant part, approximately a half, of the NMC deficit could be explained by the virtual pions. The Adelaide group tried to interpret the whole deficit by adding the Pauli exclusion effects. In the Jülich model, it is explained only by the meson model with the additional meson and baryon states [33]. The other possibility for explaining the whole result is to consider different form factors in the πNN and $\pi N\Delta$ vertices [35]. It is also discussed in Ref. [35] that the normalization factor does not affect the meson part because the bare coupling g^0_{MNB} has to be used in the wave function of a physical particle in terms of its constituents. Although there are slight differences among the above models, the meson-cloud approach is successful in explaining at least the major part of the NMC flavor asymmetry.

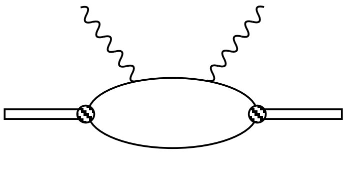

Figure 4.6: Off-shell pion structure function in the NJL model.

According to the above conclusion, we should have the antiquark distributions at least in the virtual pion and rho for a realistic evaluation of the violation. So far, we have been using the distributions in the pion measured in the Drell-Yan processes, namely those in the on-shell pion. If the distributions in the off-shell pion are significantly modified, numerical results in this subsection should be reanalyzed. There is an experimental proposal for measuring virtual pion structure functions by detecting a recoil nucleon at HERA [91]. Here, we discuss model estimates of the off-shell effects [36, 37]. Tokyo-Metropolitan-University (TMU) [36] and Brooklyn [37] groups studied this topic within the Nambu-Jona-Lasinio (NJL) model. While the TMU group calculated distributions at a hadronic scale (Q^2=0.25 GeV^2) and they were evolved to larger Q^2, the Brooklyn group calculated them at large Q^2 directly. The Compton amplitude in Fig. 4.6 is calculated with the πqq vertex given by the NJL model. Then the pion structure function is projected out from the amplitude, and the sea-quark distributions in the proton are calculated in the pion model. Although the πNN cutoff depends much on the off-shell nature of the pion, the obtained contribution to I_G is not very significant. According to Ref. [36], the deviation $\Delta I_G = -0.0557$ with the on-shell pion becomes $\Delta I_G = -0.0586$ with the NJL off-shell pion structure function. The difference is merely 5 % effect (0.9% in the Gottfried sum) because of the cancellation between the πNN and $\pi N\Delta$ in Eq. (4.11). In any case, if model parameters are fixed by fitting other distributions such as $(\bar{u}+\bar{d})/2-\bar{s}$, present mesonic contributions are not significantly changed because of the off-shell nature.

4.3.2 Chiral models

In the previous subsection, we find that the mesonic contributions could explain the major part of the Gottfried-sum-rule violation. The difference between π^+ and π^- production in the process $p \rightarrow B\pi$ gives rise to the antiquark flavor asymmetry. The pion production ratio π^+:π^0:π^- is 2:1:0 in the processes $p \rightarrow N\pi$ [Eq. (4.10)]. However, as it is obvious from Eq. (4.11), the contribution is partly canceled by the $p \rightarrow \Delta\pi$ process. In order to have a better estimate, other resonances have to be included. Their contributions could be included in a more microscopic approach with effective chiral models. In such models, the pion ratio π^+:π^0:π^- becomes 4:3:2 if they are produced in the process $q \rightarrow q\pi$. We explain this kind of approaches in this subsection. Although chiral quark-meson models were studied slightly earlier [38, 39, 44], we discuss first a chiral-field-theory approach in Ref. [40, 43, 46, 47] because of similarity in its formalism to those in the previous subsection. Later, the chiral-meson models are discussed.

In describing hadron properties at low energies, it is important to explain spontaneous chiral symmetry breaking. As an effective model for describing such a property, we have the chiral field theory. This model is used for evaluating the Gottfried-sum deficit [40]. Appropriate degrees of freedom in describing low-energy hadron structure are quarks, gluons, and Goldstone bosons. The effective interaction Lagrangian is

$$\mathcal{L} = \overline{\psi}(iD_\mu + V_\mu)\gamma^\mu\psi + ig_{_A}\overline{\psi}A_\mu\gamma^\mu\gamma_5\psi + \cdots \quad , \tag{4.21}$$

where ψ is the quark field and D_μ is the covariant derivative. The vector and axial-vector currents are expressed by Goldstone-boson fields

$$\begin{pmatrix} V_\mu \\ A_\mu \end{pmatrix} = \frac{1}{2}(\xi^\dagger\partial_\mu\xi \pm \xi\,\partial_\mu\xi^\dagger) \quad , \tag{4.22}$$

$$\xi = exp(i\Pi/f) \quad , \quad \Pi = \frac{1}{\sqrt{2}}\begin{pmatrix} \pi^0/\sqrt{2}+\eta/\sqrt{6} & \pi^+ & K^+ \\ \pi^- & -\pi^0/\sqrt{2}+\eta/\sqrt{6} & K^0 \\ K^- & \overline{K}^0 & -2\eta/\sqrt{6} \end{pmatrix} \quad . \tag{4.23}$$

Expanding the currents in power of Π/f, we have $V_\mu = O(\Pi/f)^2$ and $A_\mu = i\partial_\mu\Pi/f + O(\Pi/f)^2$. Then the quark-boson interaction becomes $\mathcal{L}_{\Pi q} = -(g_{_A}/f)\overline{\psi}\partial_\mu\Pi\gamma^\mu\gamma_5\psi$.

We give an idea how the deficit arises in this model by considering the splitting processes in Fig. 4.7. A valence u quark splits into π^+ and d, and subsequently into d, u, and $\bar{d}$ in the left figure. It also splits into π^0 and u, then into u, u, and $\bar{u}$ or into u, d, and $\bar{d}$. Noting isospin factors and assigning the factor a for the splitting probability $u \to d\pi^+$, we have the final state

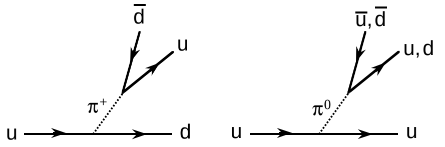

Figure 4.7: Valence u quark splitting.

$$u \to a\pi^+ + ad + \frac{a}{2}\pi^0 + \frac{a}{2}u = \frac{7a}{4}u + \frac{5a}{4}d + \frac{a}{4}\bar{u} + \frac{5a}{4}\bar{d} \quad . \tag{4.24}$$

In the same way, the d quark splitting becomes

$$d \to a\pi^- + au + \frac{a}{2}\pi^0 + \frac{a}{2}d = \frac{5a}{4}u + \frac{7a}{4}d + \frac{5a}{4}\bar{u} + \frac{a}{4}\bar{d} \quad . \tag{4.25}$$

In this simple picture, the sum deficit is estimated by taking the difference between $\bar{u}$ and $\bar{d}$ in the above equations:

$$\Delta I_G = \frac{2}{3}(\bar{u} - \bar{d}) = -\frac{2a}{3} \quad . \tag{4.26}$$

The probability a is calculated in the chiral field theory. With the interaction Lagrangian $\mathcal{L}_{\Pi q}$, the splitting function is given by

$$P_{\Pi q' \leftarrow q}(z) = \frac{g_{_A}^2}{f^2}\,\frac{(m_q + m_{q'})^2}{32\pi^2}\,z\int_{-\Lambda^2}^{t_m} dt\,\frac{(m_q - m_{q'})^2 - t}{(t - M_\Pi^2)^2} \quad , \tag{4.27}$$

where $t_m = m_q^2 z - m_{q'}^2 z/(1-z)$ and the ultraviolet cutoff is taken a chiral-symmetry-breaking scale: $\Lambda \approx$1169 MeV. This equation is analogous to Eq. (4.15) in the previous meson model. Integrating the function over z, we obtain the probability a for the $u \to \pi^+ d$ process:

$$a = \frac{g_A^2\, m_u^2}{8\pi^2 f^2} \int_0^1 dz\, \theta(\Lambda^2 - \tau(z))\, z \left\{ \ln\left[\frac{\Lambda^2 + M_\pi^2}{\tau(z) + M_\pi^2}\right] + M_\pi^2 \left[\frac{1}{\Lambda^2 + M_\pi^2} - \frac{1}{\tau(z) + M_\pi^2}\right]\right\} , \tag{4.28}$$

where $\tau(z) = m_u^2 z^2/(1-z)$ and $\theta(x)$ is a cutoff function defined by $\theta(x) = 1$ for $x > 0$ and 0 for $x < 0$. With the cutoff Λ =1169 MeV, the probability becomes $a = 0.083$ which leads to $I_G = (1-2a)/3 = 0.278$. If a larger cutoff is taken, for example Λ =1800 MeV, the sum becomes smaller (I_G=0.252). The obtained deficit is qualitatively in agreement with the meson-cloud models in the previous subsection. The x distribution is calculated by the convolution [40, 43]

$$\bar{q}_i(x) = \sum_{j=u,d} \sum_{k,l} \left(\delta_{jl}\delta_{ik} - \frac{1}{n_f}\delta_{jk}\delta_{il} \right)^2 \int_x^1 \frac{dy}{y} \int_{x/y}^1 \frac{dz}{z}\, \bar{q}_i^{(\Pi)}(x/(yz))\, P_{\Pi k \leftarrow j}(z)\, q_{v\,j}^{(N)}(y) , \tag{4.29}$$

where the flavor summation is taken for the indices k and l. However, the calculated $\bar{u} - \bar{d}$ distribution is concentrated in the small x region at the NA51 scale $Q^2 = 27$ GeV^2, so that the model only with the pion has difficulty in explaining the large NA51 flavor asymmetry at $x = 0.18$ [43]. The model is compared with the meson-cloud results and it is extended to study the strange quark distribution [46]. On the other hand, model consistency is studied among different quantities: the asymmetry $\bar{u} - \bar{d}$, the $\bar{s}$ distribution, and quark polarizations [47].

As another effective model to describe low-energy properties of hadrons, a chiral quark-meson model was proposed. This is an extension of the linear-sigma model with replacement of the nucleon field by the quark field. The Lagrangian density is given by

$$\begin{aligned} \mathcal{L}(x) = {} & \bar{\psi}(x)\{i\gamma\cdot\partial + g[\sigma(x) + i\tilde{\tau}\cdot\tilde{\phi}(x)\gamma_5]\}\psi(x) \\ & + \frac{1}{2}\partial_\mu\sigma(x)\partial^\mu\sigma(x) + \frac{1}{2}\partial_\mu\tilde{\phi}(x)\cdot\partial^\mu\tilde{\phi}(x) \\ & - \frac{\lambda^2}{4}[\sigma(x)^2 + \tilde{\phi}(x)^2 - \nu^2]^2 - F_\pi m_\pi^2 \sigma(x) \quad . \end{aligned} \tag{4.30}$$

The meson fields are treated as classical mean fields, in which the quarks form bound states. In this model, the nucleon consists of valence quarks and a coherent superposition of mesons, and it is generated from mean-field hedgehog solution. However, it is known that the hedgehog states are not eigenstates of spin nor isospin. The nucleon with definite spin and isospin should be obtained by a semi-classical cranking method.

For slow rotations, cranked meson spin and isospin are linear in the angular velocity. The moment of inertia is given by valence-quark and pion contributions: $\mathcal{I} = \mathcal{I}_q + \mathcal{I}_\pi$. For discussing the flavor asymmetry in the pion model, an important factor is the number difference between π^+ and π^- in the proton. The difference is equal to the fraction of the proton electric charge carried by the pions: $N_{\pi^+} - N_{\pi^-} = \frac{\mathcal{I}_\pi}{\mathcal{I}} \langle I_3 \rangle_p$. Then, the Gottfried sum becomes [38]

$$I_G = \frac{1}{3}\left(1 - \frac{\mathcal{I}_\pi}{\mathcal{I}}\right) \quad . \tag{4.31}$$

The deviation from 1/3 is related to the fact that a fraction of the nucleon isospin is carried by the pions. The fraction is expressed by the moments of inertia for the nucleon and pion.

More rigorous derivation of the sum-rule violation, which is similar to Eq. (4.31), is given in Ref. [39] where a similar chiral-quark-soliton model is used. The model consists of quark and pion fields with the following functional

$$Z = \int \mathcal{D}\pi\, \mathcal{D}\psi\, \mathcal{D}\psi^\dagger exp \left[i \int d^4x\, \bar{\psi}\, (i\partial\!\!\!/ - MU^{\gamma_5} - m)\, \psi \right] \quad , \tag{4.32}$$

with $U^{\gamma_5}(x) = e^{i\gamma_5 \vec{\tau}\cdot\vec{\pi}(x)/f_\pi}$. The nucleon is treated in the same way with the previous chiral quark-meson model. However, the matrix element $I_G = (1/3) < p\,|\,\hat{O}\,|\,p >$ is calculated with a plausible operator $\hat{O} = \int d^3x [\psi_+^\dagger(x)\tau_3\psi_+(x) - \psi_-^\dagger(x)\tau_3\psi_-(x)]$, where ψ_+ and ψ_- are positive and negative energy parts of ψ. As a result, the integral becomes a similar equation to Eq. (4.31):

$$I_G = \frac{1}{3}\left(1 - \frac{\mathcal{I}_{val} + \mathcal{I}_{vp}}{\mathcal{I}}\right) \quad , \tag{4.33}$$

with the moments of inertia

$$\begin{aligned} \mathcal{I}_{val} &= \frac{N_c}{2} \sum_{m\neq 0} \frac{< 0\,|\tau_3|\, m >< m\,|\{\tau_3, P_-\}_+|\, 0 >}{E_m - E_0} \quad , \\ \mathcal{I}_{vp} &= \frac{N_c}{8} \sum_{m,n} f(E_m, E_n; \Lambda) < n\,|\tau_3|\, m >< m\,|\{\tau_3, P_-\}_+|\, n > \quad . \end{aligned} \tag{4.34}$$

The state $|\, m >$ is an eigenstate of the single-quark Dirac equation and $f(E_m, E_n; \Lambda)$ is a cutoff function. The $\mathcal{I}_{val}$ and $\mathcal{I}_{vp}$ are valence quark and vacuum polarization parts respectively, and the P_- is the projection operator of the negative-energy eigenstates. Numerical results depend on the choice of the dynamical quark mass M; the sum ranges from I_G=0.235 for M=450 MeV to I_G=0.288 for M=350 MeV. Similar calculation is discussed in Ref. [44] by using the NJL model. From these results, we find that the chiral models give similar qualitative results to those of the mesonic models in section

4.3.1. However, we have to be careful in comparing the effective-model results with the NMC value. The effective models are considered to be valid at small Q^2, typically $Q^2 \sim \Lambda^2_{QCD}$. On the other hand, the NMC sum is given at Q^2=4 GeV^2 where the perturbative QCD is usually applied. It is not obvious whether these different Q^2 results could be compared directly.

We also comment on other studies in the chiral models. In Ref. [41], the Gottfried sum is assumed to be related to the matrix element: $I_G = (1/3) < p|u\bar{u} - d\bar{d}|p >$. Then it is estimated in a soliton model. The obtained result is a simple relation: $I_G \approx (1/3)(M_n - M_p)/(m_d - m_u)$ [41, 48]. In Ref. [42], the $\bar{u} - \bar{d}$ is related to the σ term by $\sigma = 23(m_u + m_d)(1/2 + \bar{u} - \bar{d})$. Choosing the mass $m_u + m_d$ to fit the pion mass and the σ term, we find $\bar{u} - \bar{d} = -0.134$. There is also an attempt to relate the Gottfried sum to kaon-nucleon scattering cross sections [92]. On the other hand, there is an instanton model approach [45]. The instanton induced quark-nucleon interaction is described by a Lagrangian with terms which do not vanish only for different quark flavors. This feature could be related to the observed $\bar{u}/\bar{d}$ asymmetry. Because we do not discuss the details of these works, the interested reader should look at the original papers.

4.3.3 Anomalous Q^2 evolution

We have learned that the scaling violation phenomena in the structure functions are successfully described by the perturbative QCD (pQCD). We believe that the pQCD can be used in the Q^2 region, $Q^2 >$ a few GeV^2. In the recent years, the experimental data improved much and they provide us an opportunity to investigate beyond the pQCD in the small Q^2 region. We explained that the lattice QCD cannot handle the structure functions themselves at this stage. Studies of small Q^2 physics are difficult and they are inevitably model dependent. It is nevertheless important to study such a Q^2 region by some kind of model in order to learn about underlying physics. For this reason, we have discussed the low-energy effective models in the previous subsection. In the following, we discuss possible meson effects on the scaling violation at small Q^2.

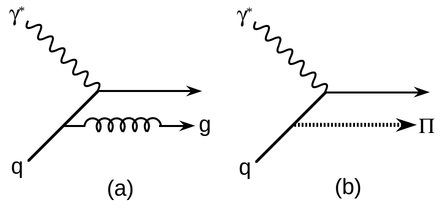

Figure 4.8: Q^2 evolution due to (a) gluon and (b) meson Π emissions.

We found that the mesonic mechanism is a strong candidate in explaining the failure of the Gottfried sum. Because of similarity between the quark splitting $q \to gq$ in Fig. 4.8(a) and the one into a quark and a meson ($q \to \Pi q$) in Fig. 4.8(b), the meson emission is expected to modify the Q^2 evolution. The process (a) together with other splitting processes gives rise to the standard Dokshitzer-Gribov-Lipatov-Altarelli-Parisi (DGLAP) evolution equations. Because the appropriate degrees of freedom at large Q^2 are the quarks and gluons, the evolution has to be described by the interactions among these fundamental particles, namely by the DGLAP equations. However, meson degrees of freedom may become important at relatively small Q^2. If the meson effects are included in the evolution equations, special care should be taken for double counting. We discuss possible mesonic effects on the Q^2 evolution as discussed in Ref. [49].

If the meson interactions are taken into account in addition, the DGLAP evolution equations are modified as

$$\begin{aligned}
\frac{\partial}{\partial t}\, q_i &= \sum_j P_{q_i q_j} \otimes q_j + \sum_j P_{q_i \bar{q}_j} \otimes \bar{q}_j + \sum_a P_{q_i \Pi_a} \otimes \Pi_a \quad , \\
\frac{\partial}{\partial t}\, \bar{q}_i &= \sum_j P_{\bar{q}_i \bar{q}_j} \otimes \bar{q}_j + \sum_j P_{\bar{q}_i q_j} \otimes q_j + \sum_a P_{\bar{q}_i \Pi_a} \otimes \Pi_a \quad , \\
\frac{\partial}{\partial t}\, \Pi_a &= \sum_j P_{\Pi_a q_j} \otimes q_j + \sum_j P_{\Pi_a \bar{q}_j} \otimes \bar{q}_j + \sum_b P_{\Pi_a \Pi_b} \otimes \Pi_b \quad , \qquad (4.35)
\end{aligned}$$

where Π_a is a distribution function of a meson, and t is defined by $t = \ln(Q^2/\mu^2)$. Since the current interest is the nonsinglet evolution, obvious gluon terms are omitted for simplicity. The notation $\otimes$ indicates a convolution integral: $f \otimes g = \int_x^1 dy f(x/y) g(y)$. The function $P_{q\Pi}$ is the splitting probability of the meson Π into a quark and an antiquark, and $P_{\Pi q}$ ($P_{\Pi\Pi}$) represents the Π emission probability from a quark (from another meson Π). Light pseudoscalar mesons are taken into account in the above equations. Isospin and charge-conjugation invariance suggests $P_{u\Pi^0} = P_{d\Pi^0} = P_{\bar{u}\Pi^0} = P_{\bar{d}\Pi^0}$ for neutral pseudoscalar mesons, $P_{u\pi^+} = P_{d\pi^-} = P_{\bar{d}\pi^+} = P_{\bar{u}\pi^-} \equiv P_{q\pi}$ and $P_{d\pi^+} = P_{u\pi^-} = P_{\bar{u}\pi^+} = P_{\bar{d}\pi^-} = 0$ for charged pions. Defining the distribution $q^+ = (u + \bar{u}) - (d + \bar{d})$, we obtain a nonsinglet evolution equation

$$\frac{\partial}{\partial t}\, q^+ = (Q_{qq} + Q_{q\bar{q}}) \otimes q^+ \quad , \qquad (4.36)$$

where Q is defined by the difference between flavor-diagonal and nondiagonal splitting functions $Q = P^D - P^{ND}$. They are given by $P^D_{q_i q_j} = P_{q_i q_j\,(i=j)}$ and $P^{ND}_{q_i q_j} = P_{q_i q_j\,(i \neq j)}$. The meson terms cancel out in Eq. (4.36); however, there are mesonic contributions to the splitting functions.

A contribution of the Π emission to the splitting function $P_{q_i q_j}$ is given by $[P_{q_i q_j}]^{\Pi} = \partial \sigma^{\gamma^* \Pi}_{q_i q_j} / \partial t$. Here, $\sigma^{\gamma^* \Pi}_{q_i q_j}$ is the total cross section integrated over $\vec{k}_\perp$ for absorption of a virtual photon and emission the meson Π. Its anomalous dimension is then calculated by the Mellin transformation: $\gamma^{ud}_{N} = \gamma^{du}_{N} = \partial \sigma^{\gamma^* \pi^+}_{N} / \partial t = \partial \sigma^{\gamma^* \pi^-}_{N} / \partial t$, $\gamma^{uu}_{N} = \gamma^{dd}_{N} = (\partial / \partial t) \left(\sigma^{\gamma^* \pi^0}_{N} / 2 + \sigma^{\gamma^* \eta}_{N} / 6 + \sigma^{\gamma^* \eta'}_{N} / 3 \right)$, where σ_{N} is the Nth moment of the cross section. In discussing the evolution of the Gottfried sum, we calculate the anomalous dimension γ_1^+, which is the first moment of the splitting function for the flavor diagonal minus the one for the nondiagonal. The mesonic contribution is

$$\gamma_{_N}^{+} = \gamma_{_N}^{uu} - \gamma_{_N}^{ud} = \frac{\partial}{\partial t}\left(\frac{1}{2}\sigma_{_N}^{\gamma^*\pi^0} + \frac{1}{6}\sigma_{_N}^{\gamma^*\eta} + \frac{1}{3}\sigma_{_N}^{\gamma^*\eta'} - \sigma_{_N}^{\gamma^*\pi^+}\right)$$

$$\simeq \frac{\partial}{\partial t}\left(\frac{1}{6}\sigma_{_N}^{\gamma^*\eta} + \frac{1}{3}\sigma_{_N}^{\gamma^*\eta'} - \frac{1}{2}\sigma_{_N}^{\gamma^*\pi}\right) \quad . \tag{4.37}$$

In this way, evolution of the Gottfried sum due to the meson emissions becomes

$$I_G(Q^2) = \Delta_1^+(t,t_0)\, I_G(Q_0^2) \ , \quad \Delta_1^+(t,t_0) = exp\left\{\left[\frac{1}{6}\sigma_1^{\gamma^*\eta}(t) + \frac{1}{3}\sigma_1^{\gamma^*\eta'}(t) - \frac{1}{2}\sigma_1^{\gamma^*\pi}(t)\right]\right.$$

$$\left. - \left[\frac{1}{6}\sigma_1^{\gamma^*\eta}(t_0) + \frac{1}{3}\sigma_1^{\gamma^*\eta'}(t_0) - \frac{1}{2}\sigma_1^{\gamma^*\pi}(t_0)\right]\right\} \quad . \tag{4.38}$$

Explicit expressions for the above cross sections are presented in the Appendix of Ref. [49]. In the large mass limit $M \to \infty$, the cross section falls off like $\sigma_1^{\gamma^*\Pi} \sim 1/M^2$, so that massive meson contributions are smaller than those of the light mesons (π, η, and η').

We comment on the consistency with the DGLAP equations at large Q^2 and on double counting. First, the cross section has $\sigma_1^{\gamma^*\Pi} \sim 1/Q^2$ behavior at large Q^2. It means that the anomalous dimension has higher-twist behavior. As Q^2 becomes sufficiently large, the meson contribution becomes eventually smaller than the logarithmic pQCD effect. Therefore, the above formalism is consistent with the DGLAP evolution at large Q^2. Second, the meson contribution to the anomalous dimension should not be added to the pQCD one in order to avoid the double counting. We may just use the meson picture below a certain boundary Q^2 and the pQCD evolution above it.

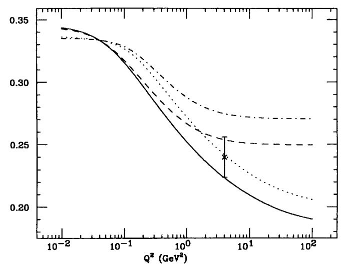

Figure 4.9: Q^2 dependence of the Gottfried sum (taken from Ref. [49])

Numerical results are shown in Fig. 4.9, where the Q^2 dependence of the Gottfried sum is shown. Parameters in the model are dynamical quark mass m_d, derivative and pseudoscalar coupling ratio g_π, and vertex cutoff parameters Λ and $\tilde{\Lambda}$ for two different couplings. The mass m_d is determined by the cutoff Λ (=$\tilde{\Lambda}$) with a normalization condition of the vertex function. In the range of Λ=0.4−0.8 GeV, it is consistent with the constituent quark mass $m_d \approx M_\rho/2 \approx M_p/3$. Therefore, the cutoff is chosen 0.5 GeV. The solid and dashed curves are the results for g_π=0.0 and 1.0 respectively, and the dotted and dot-dashed ones are those for g_π=0.0 and 1.0 including dynamical quark-mass corrections. As it is discussed in section 3, the perturbative QCD predicts a very small Q^2 variation. Therefore, the scaling violation is mostly controlled by the mesonic contributions. Although the results depend much on unknown parameters, it is evident from the figure that the sum rule is violated due to the scaling violation caused by the quark-meson interactions. This is an interesting result, which suggests another possibility of explaining the sum-rule failure. Furthermore, x distribution of $F_2^p - F_2^n$ is calculated at Q^2=4 GeV^2 by using input distributions at small Q^2 without sea-quark distributions [49]. The results agree reasonably well with the NMC $F_2^p - F_2^n$ data. At this stage, these results should be considered as naive ones. We need further refinement of the formalism, including discussions on applicability of the modified evolution equations at small Q^2. In any case, the model predicts very strong Q^2 dependence of the Gottfried sum, so that it can be checked in principle by future experiments.

4.4 Diquark model

Flavor asymmetry $\bar{u} - \bar{d}$ in a diquark model was already noticed in 1976 [9]. Later it was elaborated to compare with the NMC result in Ref. [28, 29]. According to the ordinary quark model, baryons consists of three pointlike quarks with spin-parity $(1/2)^+$ and charges 2/3, $-1/3$, $-1/3$. It is successful in explaining gross properties of hadrons. However, it was rather difficult to understand the small ratio $F_2^n/F_2^p \sim 0.29$ at large x and missing SU(6) baryon multiplets $\underline{20}$ in 1970's, although these problems could be explained within the usual quark-model framework [93]. These difficulties are understood in a diquark model. This model is based on the observation that diquark degrees of freedom are most relevant for some observables.

In the SU(6) model [1], two quarks form twenty-one symmetric states and fifteen antisymmetric ones: $\underline{6} \times \underline{6} = \underline{21} + \underline{15}$. In combination with the remaining quark, the antisymmetric part $\underline{15}$ becomes $\underline{15} \times \underline{6} = \underline{20} + \underline{70}$. If the antisymmetric part $\underline{15}$ does not couple to the quark, it is possible to explain the missing states $\underline{20}$. The SU(3) content of the representation $\underline{21}$ is expressed as $\underline{21} = \{6\} \times 3 + \{\bar{3}\} \times 1$, where the brackets indicate irreducible representation of SU(3) and the factors 3 and 1 are spin degrees of freedom of the diquark. There are SU(3)-sextet axial-vector diquarks and SU(3)-triplet scalar diquarks. We introduce a mixing angle Γ between the vector and scalar diquark states. The usual SU(6) model is recovered in the limit $\Gamma = \pi/4$. The proton state in this diquark model is given by

$$\left| \, p, s_z = \pm\frac{1}{2} \, \right\rangle = \pm\frac{1}{\sqrt{18}} \left\{ \Big[\sqrt{2}\, V_{\pm 1}(ud)\, u_\mp - 2\, V_{\pm 1}(uu)\, d_\mp + \sqrt{2}\, V_0(uu)\, d_\pm \right.$$
$$\left. -V_0(ud)\, u_\pm \Big] \sqrt{2}\, \sin\Gamma \mp S(ud)\, u_\pm \sqrt{2}\, \cos\Gamma \right\} \quad , \qquad (4.39)$$

where $V_m(q_1 q_2)$ and $S(q_1 q_2)$ denote the vector and scalar diquark states consist of q_1 and q_2 quarks, and the subscript m is the spin state.

Quark and diquark contributions to the structure function F_2 are given by [94]

$$\begin{aligned}
F_2^{(q)} &= x \sum_q e_q^2\, q(x) \quad , \\
F_2^{(S)} &= x\, e_{_S}^2\, S(x)\, D_S(Q^2) \quad , \\
F_2^{(V)} &= x \sum_V e_{_V}^2\, \frac{1}{3}\, V(x) \Bigg\{ \Bigg[\left(1 + \frac{\nu}{m_N x}\right) D_1(Q^2) - \frac{\nu}{m_N x}\, D_2(Q^2) \\
&\qquad + 2\, m_N\, \nu\, x \left(1 + \frac{\nu}{2 m_N x}\right) D_3(Q^2) \Bigg]^2 + 2 \left[D_1^2(Q^2) + \frac{\nu}{2 m_N x}\, D_2^2(Q^2) \right] \Bigg\} ,
\end{aligned} \tag{4.40}$$

where $D_S(Q^2)$ and $D_{1,2,3}(Q^2)$ are scalar and vector diquark form factors. The D_1, D_2, and D_3 are defined by tensor structure of the virtual-photon coupling to a spin-one particle:

$$\begin{aligned}
V^\alpha = ie_{_V} \{ &(2k+q)^\alpha g^{\mu\nu} D_1(Q^2) - [(k+q)^\nu g^{\mu\alpha} + k^\mu g^{\nu\alpha}] D_2(Q^2) \\
&+ k^\mu (k+q)^\nu (2k+q)^\alpha D_3(Q^2) \}\, \epsilon_{1,\nu}(\lambda_1) \epsilon^*_{2,\mu}(\lambda_2) \quad ,
\end{aligned} \tag{4.41}$$

where $\epsilon_{1,\nu}(\lambda_1)$ and $\epsilon_{2,\mu}(\lambda_2)$ are the polarization vectors of initial and final diquarks with helicities λ_1 and λ_2. In the limit of pointlike diquarks, the form factors are given by $D_S(0) = 1$, $D_1(0) = 1$, $D_2(0) = 1 + \kappa$, and $D_3(0) = 0$, where κ is the anomalous magnetic moment. Therefore, it is natural to choose $D_S(Q^2) = D_1(Q^2) = D_2(Q^2) = Q_0^2/(Q_0^2 + Q^2) \equiv D(Q^2)$, as expected from a dimensional counting rule, and $D_3 = 0$ for simplicity. From Eqs. (4.39) and (4.40), valence quark and diquark contributions to the proton F_2 are

$$\begin{aligned}
F_2^p = x \Bigg[&\left\{ \frac{4}{9} \frac{1}{3}\, f_u(x) + \frac{1}{9} \frac{2}{3}\, f_d(x) \right\} \sin^2\Gamma + \frac{4}{9}\, f_u(x)\, \cos^2\Gamma + \frac{1}{9}\, f_{_S}(x)\, \cos^2\Gamma\, D^2(Q^2) \\
&+ \left\{ \frac{16}{9} \frac{2}{3}\, f_{V_{uu}}(x) + \frac{1}{9} \frac{1}{3}\, f_{V_{ud}}(x) \right\} \sin^2\Gamma \left(1 + \frac{\nu}{3 m_N x}\right) D^2(Q^2) \Bigg] \quad .
\end{aligned} \tag{4.42}$$

New distribution functions $f_{q,S,V}(x)$ are introduced in the above equation, and they are normalized as $\int_0^1 dx f_{q,S,V}(x) = 1$. In the same way, the neutron F_2 is given by

$$\begin{aligned}
F_2^n = x \Bigg[&\left\{ \frac{4}{9} \frac{2}{3}\, f_d(x) + \frac{1}{9} \frac{1}{3}\, f_u(x) \right\} \sin^2\Gamma + \frac{1}{9}\, f_u(x)\, \cos^2\Gamma + \frac{1}{9}\, f_{_S}(x)\, \cos^2\Gamma\, D^2(Q^2) \\
&+ \left\{ \frac{4}{9} \frac{2}{3}\, f_{V_{uu}}(x) + \frac{1}{9} \frac{1}{3}\, f_{V_{ud}}(x) \right\} \sin^2\Gamma \left(1 + \frac{\nu}{3 m_N x}\right) D^2(Q^2) \Bigg] \quad .
\end{aligned} \tag{4.43}$$

In addition, the virtual-photon scattering off a quark inside the diquark is considered with a diquark-breakup probability $1 - F^2(Q^2)$. From these equations, the Gottfried sum becomes [29]

$$I_G = \frac{1}{3} - \frac{4}{9}\, sin^2\Gamma + \frac{8}{9}\,\sin^2\Gamma \int_0^1 dx\, f_{V_{uu}}(x) \left(1 + \frac{\nu}{3m_N x}\right) D^2(Q^2) \\ + \frac{4}{9}\,[1 - F^2(Q^2)]\, sin^2\Gamma \quad . \qquad (4.44)$$

It should be noted that sea-quark contributions are not taken into account. In other words, the sea-quark distributions are assumed to be flavor symmetric. If the nucleon consists of a scalar diquark and a quark ($\Gamma = 0$), the integral becomes the Gottfried sum 1/3.

In the earlier investigations [9, 28] without the breakup term, the diquark model seemed to account for the deficit of the Gottfried sum. For example, I_G=1/3−0.384 $\sin^2\Gamma$ at Q^2=4 GeV^2 was obtained in Ref. [28]. However, it means that the two quarks in a diquark act as a single extended object, which never breaks apart. This is certainly not realistic. The breakup mechanism plays an important role in the Gottfried sum. With the distribution $f_{V_{uu}}(x) = 12x^2(1-x)$ used in the study of polarized structure function g_1 and with the assumption $F(Q^2) = D(Q^2)$, the sum at Q^2=4 GeV^2 becomes [29]

$$I_G = \frac{1}{3} + \frac{4}{9}\,(0.12)\,\sin^2\Gamma \quad . \qquad (4.45)$$

On the contrary to the previous results, the model produces a positive modification to the sum. The parameter Γ could be taken from other observable such as the ratio of the axial vector to the vector neutron β-decay coupling constant $g_{_A}$. Comparing $g_{_A} = 1 + (2/3)sin(2\Gamma)$ in the diquark model with experimental value $g_{_A}$=1.261±0.004, we obtain $sin^2\Gamma \approx$0.04. Then the sum becomes $I_G = 1/3 + 0.002$, which is a very small positive correction to the sum 1/3.

There are two factors which changed the early result in Ref. [28]. The first one is the addition of the breakup term, and it could result in the positive contribution in Eq. (4.45). The second one is the small mixing angle $sin^2\Gamma \approx 0.04$, which is consistent with $g_{_A}$. It should be noted in Ref. [28] that the NMC result could be explained if the mixing were $sin^2\Gamma \approx 0.27$! Sensitivity of the obtained I_G on the assumed functions is also discussed in Refs. [28, 29]. If the function $F(Q^2)$ is different from $D(Q^2)$, the deviation may become negative instead of the positive one in Eq. (4.45). The results depend, of course, on the assumed functions for $f_{V_{uu}}(x)$, $F(Q^2)$, and $D(Q^2)$; however, the diquark effects are all suppressed by the small factor $sin^2\Gamma$. In this way, the diquark model predicts a very small deviation from the Gottfried sum, so that it cannot explain the NMC results.

4.5 Isospin symmetry violation

Isospin symmetry is usually taken for granted in discussing parton distributions in the proton and neutron. In fact, it is assumed [$u_n = d_p$, $d_n = u_p$, $\bar{u}_n = \bar{d}_p$, $\bar{d}_n = \bar{u}_p$, and etc.] in deriving Eq. (2.10). Electromagnetic interactions are weak compared with strong interactions, so that typical isospin-violation effects are expected to be of the order of the fine structure constant $\alpha = 1/137$. This is in general true, for example, the mass difference of the nucleons is $(m_n - m_p)/m_p$=0.14%. Therefore, we cannot believe that the NMC result is explained only by the isospin-symmetry violation in antiquark distributions. However, it is worth investigating its contributions to the Gottfried sum and to various high-energy processes because isospin-violation effects on the parton distributions are not known. This topic is discussed in Ref. [50].

What would happen to the Gottfried sum if the isospin symmetry cannot be assumed? Without using the isospin symmetry, the sum is expressed as

$$I_G = \frac{1}{3} + \frac{2}{9} \int_0^1 dx \ \Big(\ \big[4\{\bar{u}(x) + \bar{c}(x)\} + \{\bar{d}(x) + \bar{s}(x)\} \big]_p - \big[4\{\bar{u}(x) + \bar{c}(x)\} + \{\bar{d}(x) + \bar{s}(x)\} \big]_n \ \Big) \ . \quad (4.46)$$

If the antiquark distributions are flavor symmetric and if the $\bar{s}$ and $\bar{c}$ terms vanish: $\int dx(s_p - s_n) = 0$ and $\int dx(c_p - c_n) = 0$, it becomes

$$I_G = \frac{1}{3} + \frac{10}{9} \int dx \, [\bar{q}_p(x) - \bar{q}_n(x)] \quad , \quad (4.47)$$

where $\bar{q}_p(x)$ is the light antiquark distribution in the proton [$\bar{q}_p = \bar{u}_p = \bar{d}_p$] and $\bar{q}_n(x)$ is the one in the neutron. If the isospin-symmetry breaking were the only origin of the NMC finding, Eqs. (4.46) and (4.47) could suggest that there are more antiquarks in the neutron than those in the proton. If the NMC 1991 data in Eq. (2.23) is identified with Eq. (4.47), we get $\int dx[\bar{q}_p(x) - \bar{q}_n(x)] = -0.84 \pm 0.014$. Because the Adler sum rule $I_A = \int [F_2^{\bar{\nu}p}(x) - F_2^{\nu p}(x)]dx/2x = 1$ and the Gross-Llewellyn Smith sum rule in Eq. (3.17) are independent of the flavor asymmetry and the isospin symmetry violation, these mechanisms cannot be distinguished. We have to find other observables. Future experimental possibilities are discussed in section 5.6.

4.6 Flavor asymmetry $\bar{u} - \bar{d}$ in nuclei

The NMC finding of the flavor asymmetry can be tested by the Drell-Yan experiments. There exist Drell-Yan data for various nuclear targets, so that some people use, for example, the tungsten data in investigating the flavor asymmetry [18]. However, we have to be careful in comparing the NMC result with the tungsten data because of possible nuclear medium effects. In the analysis of Ref. [18], no nuclear correction is made except for the overall shadowing correction. If the nuclear modification in the

$\bar{u} - \bar{d}$ distribution is very large, the Drell-Yan analysis cannot be compared directly with the NMC result. Therefore, it is worth while estimating the nuclear effect in order to find whether or not such a modification should be taken into account.

In discussing antiquark distributions in a nucleus, it is essential to describe the shadowing phenomena. In the small x region, it is experimentally observed that nuclear structure functions per nucleon are smaller than the deuteron's. There are various models in describing the shadowing as they are discussed in section 2.5. The interesting point is to find whether there is any nuclear mechanism to create extra flavor asymmetry whatever the shadowing model is. It could be possible according to Ref. [65], in which the nuclear modification is calculated in a parton-recombination model. The following discussion is based on this investigation.

First, we discuss the nuclear $\bar{u} - \bar{d}$ distribution without the nuclear modification. If the isospin symmetry could be applied to the parton distributions in the proton and neutron, the distribution per nucleon is given by $[\bar{u}(x) - \bar{d}(x)]_A = -\varepsilon[\bar{u}(x) - \bar{d}(x)]_{proton}$. It is simply the summation of proton and neutron contributions. The neutron-excess parameter ε is defined by $\varepsilon = (N - Z)/(N + Z)$. The above equation indicates that the flavor asymmetry has to vanish if the antiquark distributions are flavor symmetric in the nucleon. However, it is not the case in the recombination model.

In the parton-recombination picture, partons in different nucleons could interact in a nucleus. These interactions become important especially at small x. Parton recombination effects on the antiquark distribution $\bar{q}_i(x)$ are given by

$$\Delta\bar{q}_{i,A}(x) = w_{pp}\,\Delta\bar{q}_{i,pp}(x) + w_{pn}\,\Delta\bar{q}_{i,pn}(x) + w_{np}\,\Delta\bar{q}_{i,np}(x) + w_{nn}\,\Delta\bar{q}_{i,nn}(x)\ , \qquad (4.48)$$

where $w_{n_1 n_2}$ is the combination probabilities of the two nucleons n_1 and n_2. For example, w_{pp} is the probability of the proton-proton combination ($w_{pp} = Z(Z-1)/[A(A-1)]$). The distribution $\Delta\bar{q}_{i,n1\,n2}(x)$ is the modification of the antiquark distribution with flavor i due to a parton interaction in the nucleon $n1$ with a parton in the nucleon $n2$. If the isospin symmetry can be used, the flavor asymmetry becomes

$$\begin{aligned} x[\Delta\bar{u}(x) - \Delta\bar{d}(x)]_A &= -(w_{nn} - w_{pp})\,x\,[\Delta\bar{u}(x) - \Delta\bar{d}(x)]_{pp} \\ &= -\varepsilon\,x\,[\Delta\bar{u}(x) - \Delta\bar{d}(x)]_{pp} \quad , \end{aligned} \qquad (4.49)$$

where $[\Delta\bar{u}(x) - \Delta\bar{d}(x)]_{pp}$ is the asymmetry produced in the proton-proton combination.

Next, we discuss how the flavor asymmetric distribution is created in this model for the simplest situation, $\bar{u} - \bar{d} = 0$ in the nucleon. In this case, many recombinations cancel each other, and the only remaining term is the following:

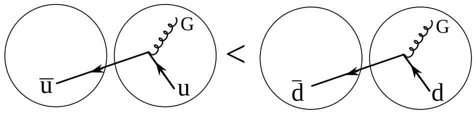

Figure 4.10: Mechanism of creating the flavor asymmetry in a nucleus.

$$x[\Delta\bar{u}(x) - \Delta\bar{d}(x)]_A = \varepsilon\frac{4K_0}{9}x\int_0^1 dx_2\, x\,\bar{u}^*(x)\, x_2[u_v(x_2) - d_v(x_2)]\,\frac{x^2 + x_2^2}{(x + x_2)^4} \quad , \qquad (4.50)$$

Figure 4.11: Created flavor asymmetry in the tungsten nucleus by a recombination model [65].

The recombination contributions are evaluated for the tungsten ${}^{184}_{74}W_{110}$ nucleus by using the input parton distributions MRS-D$_0$ at Q^2=4 GeV^2. The obtained results are shown in Fig. 4.11, where the solid (dashed) curve shows the $x[\Delta\bar{u} - \Delta\bar{d}]_A$ distribution of the tungsten nucleus with the flavor symmetric (asymmetric) sea in the nucleon. In the $(\bar{u} - \bar{d})_N = 0$ case, the positive contribution at small x can be understood by the processes in Fig. 4.10. In the $(\bar{u} - \bar{d})_N \neq 0$ case, the $\bar{q}(x)G \rightarrow \bar{q}$ process is the dominant one kinematically at small x. Its contribution to $\bar{u}(x) - \bar{d}(x)$ becomes negative due to the neutron excess. On the other hand, the $\bar{q}G \rightarrow \bar{q}(x)$ process becomes kinematically favorable in the medium x region. Because it produces $\bar{q}$ with momentum fraction x, its contribution becomes opposite to the one at small x.

The above results are obtained at Q^2=4 GeV^2. Because the factor K_0 is proportional to $\alpha_s(Q^2)/Q^2$, the nuclear flavor asymmetry may seem to be very large at small Q^2. However, the quark distribution $u_v(x) - d_v(x)$ becomes very small in the small x region, so that the overall Q^2 dependence is not so significant according to Eq. (4.50). There are merely factor-of-two differences between the asymmetric distribution at Q^2=4 GeV^2 and the one at $Q^2 \approx 1$ GeV^2. Considering this factor of two, we find that the nuclear modification is of the order of 2%–10% compared with the asymmetry $\bar{u} - \bar{d}$ suggested by the MRS-D0 distribution. Therefore, special care should be taken in comparing flavor asymmetry data of the nucleon with the nuclear ones. On the other hand, because the Drell-Yan experiments on various targets are in progress at Fermilab, the nuclear modification of $\bar{u} - \bar{d}$ could be tested experimentally. The studies could provide important clues in describing nuclear dynamics in the high-energy region.

4.7 Relation to nucleon spin

We explained various mechanisms of creating the flavor asymmetry. It is natural that there is a certain relationship between the light-antiquark flavor asymmetry and the nucleon spin issue. We discuss possible relations in the exclusion principle [66] and in the chiral quark model [40, 47].

One of the ideas in explaining the flavor asymmetry is the Pauli blocking model in section 4.2. This idea could be extended to the proton-spin problem according to Ref. [66]. In a naive quark model, polarized valence-quark distributions are related to the matrix elements of axial charges:

$$u_v^\uparrow = 1 + F \quad , \quad u_v^\downarrow = 1 - F \quad , \quad d_v^\uparrow = \frac{1+F-D}{2} \quad , \quad d_v^\downarrow = \frac{1-F+D}{2} \quad , \tag{4.51}$$

where F and D are axial parameters, and the current values are $F+D$=1.2573±0.0028 F/D=0.575±0.016 experimentally. From these equations, fractions of the proton spin carried by the valence quarks are

$$\Delta u_v = u_v^\uparrow - u_v^\downarrow = 2F \quad , \quad \Delta d_v = d_v^\uparrow - d_v^\downarrow = F - D \quad . \tag{4.52}$$

The Pauli blocking mechanism in the flavor case was the following. Because there is an extra u-valence quark over d-valence, $u\bar{u}$ pair creations suffer more exclusion effects than $d\bar{d}$ creations. Substituting numerical values of F and D into Eq. (4.51), we obtain $u_v^\uparrow$=1.46, $u_v^\downarrow$=0.54, $d_v^\uparrow$=0.33, and $d_v^\downarrow$=0.67. The proton spin is dominated by the $u_v^\uparrow$ distribution. Because $u_v^\uparrow$ is significantly larger than $u_v^\downarrow$, the Pauli blocking could be applied to the spin case in the similar way. As a rough estimate, the fraction of the spin asymmetry created in the exclusion principle is assumed to be the same with the one for the flavor asymmetry

$$\frac{u_s^\downarrow - u_s^\uparrow}{u_v^\uparrow - u_v^\downarrow} = \frac{d_s - u_s}{u_v - d_v} \quad , \tag{4.53}$$

where q_s denotes a sea-quark distribution. The NMC result in 1991 indicates $d_s - u_s$=0.14 for the first moments u_s and d_s. Therefore, the difference becomes

$$u_s^\uparrow - u_s^\downarrow = -0.14\,\Delta u_v = -0.28\,F \quad . \tag{4.54}$$

We also assume that the exclusion mechanism is applied in the same way to the d quark:

$$d_s^\uparrow - d_s^\downarrow = -0.14\,\Delta d_v = -0.14\,(F-D) \quad . \tag{4.55}$$

From these equations, the first moment of $g_1^p(x)$ becomes

$$\int_0^1 g_1^p(x)dx = \frac{1}{18}(9F-D)(1-0.28) = 0.14, \tag{4.56}$$

which is in fair agreement with polarized experimental data. The Pauli blocking interpretation of the proton-spin issue is summarized in the following way. Because of the $u_v^\uparrow$ excess over $u_v^\downarrow$ and the $d_v^\downarrow$ excess over $d_v^\uparrow$, the u-quark (d-quark) sea is negatively (positively) polarized. However, magnitude of the exclusion effect is expected to be larger in the u-quark sea because of $u_v^\uparrow/u_v^\downarrow > d_v^\downarrow/d_v^\uparrow$. In fact, we have $\Delta\bar{u}$=$-0.28F = -0.13$ and $\Delta\bar{d} = -0.14(F-D)$=$+0.05$. The large negative polarization in the u-quark sea could account for the spin deficit.

The relation between the quark flavor and spin can be discussed in the meson models, for example in the chiral quark model [40, 47]. As explained in section 4.3.2, the model produces the $\bar{d}$ excess over $\bar{u}$. In Ref. [47], kaons, eta, and eta prime mesons are included in addition to the pions. Suppression factors are introduced for heavier meson emissions in comparison with the pion case: ϵ for kaons, δ for eta, and ζ for eta prime mesons. Then, after the emission of a meson from the initial proton $(2u+d)$, the $\bar{u}-\bar{d}$ number becomes

$$\bar{u}-\bar{d} = \left[\frac{2\zeta+\delta}{3}-1\right] a \ . \tag{4.57}$$

The proton spin-up state is $|p_+\rangle = (1/\sqrt{6})\,(2\,|u_+u_+d_-\rangle - |u_+u_-d_+\rangle - |u_-u_+d_+\rangle)$. This equation suggests the naive quark model prediction $\Delta u = u_+ - u_- = 4/3$, $\Delta d = d_+ - d_- = -1/3$, and $\Delta s = 0$ with $u_+ = 5/3$, $u_- = 1/3$, $d_+ = 1/3$, and $d_- = 2/3$. Next, we discuss corrections to the quark polarization due to the meson emissions. They are expressed by the probability $P(q_+ \to q_-)$ for the splitting process $q_+ \to q_-$. The probability a is assigned for the process $u_+ \to \pi^+ d_-$. $P\,(d_+ \to s_-) = \epsilon^2 a$ is the probability of a spin-up d quark flipping into a spin-down s quark through the emission of K^+. In this way, the probabilities for the u_+ splitting processes are $P(u_+ \to (u\bar{d})_0 d_-) = a$, $P(u_+ \to (u\bar{s})_0 s_-) = \epsilon^2 a$, $P(u_+ \to (u\bar{u})_0 u_-) = [(\delta{+}2\zeta{+}3)/6]^2 a$, $P(u_+ \to (d\bar{d})_0 u_-) = [(\delta+2\zeta-3)/6]^2 a$, and $P(u_+ \to (s\bar{s})_0 u_-) = [(\delta-\zeta)/3]^2 a$. Substituting these equation and similar ones for other states, we obtain

$$\begin{aligned}
\Delta u =& \frac{4}{3}\,[1-\Sigma P] + \frac{1}{3}P\,(u_- \to u_+) + \frac{2}{3}P\,(d_- \to u_+) - \frac{5}{3}P\,(u_+ \to u_-) - \frac{1}{3}P\,(d_+ \to u_-) \\
=& \frac{4}{3} - \frac{21+4\delta^2+8\zeta^2+12\epsilon^2}{9}a \ , \\
\Delta d =& -\frac{1}{3}\,[1-\Sigma P] + \frac{1}{3}P\,(u_- \to d_+) + \frac{2}{3}P\,(d_- \to d_+) - \frac{5}{3}P\,(u_+ \to d_-) - \frac{1}{3}P\,(d_+ \to d_-) \\
=& -\frac{1}{3} - \frac{6-\delta^2-2\zeta^2-3\epsilon^2}{9}a \ , \\
\Delta s =& \frac{1}{3}P\,(u_- \to s_+) + \frac{2}{3}P\,(d_- \to s_+) - \frac{5}{3}P\,(u_+ \to s_-) - \frac{1}{3}P\,(d_+ \to s_-) \\
=& -\epsilon^2 a \ .
\end{aligned} \tag{4.58}$$

The parameter values, ϵ, δ, and ζ, have to be determined in order to evaluate above quantities numerically. We may simply take the same suppression factors for the K

and η production processes. Because η' is heavier, a smaller value may be taken for ζ. For a rough estimate, we assume $\epsilon = \delta = -2\zeta$. These parameter values are fixed by Eq. (4.57) so as to explain the NMC $\bar{u} - \bar{d}$, and they are $\epsilon = \delta = -2\zeta = 0.6$ and $a = 0.15$. These are substituted into Eq. (4.58) to obtain Δu=0.87, $\Delta d = -0.41$, and $\Delta s = -0.05$. The total quark spin content is $\Delta u + \Delta d + \Delta s$=0.4 which is close to the recent measurements. Comparing these with the naive quark model predictions $\Delta u = 4/3$, $\Delta d = -1/3$, and $\Delta s = 0$, we find that the u quark polarization is significantly reduced due to the meson emission mechanism. Although the above calculation is a very rough one, the results indicate that the chiral quark model could also explain the proton spin problem. In this way, we find that the flavor asymmetry problem is closely connected with the proton spin issue.

4.8 Comment on effects of quark mass and transverse motion

Although the parton model is considered to be valid in the Bjorken scaling limit, there could be some corrections from finite quark masses and transverse motion. Such corrections are estimated in Ref. [59], and the obtained result indicates $\delta I_G = -0.01$ to -0.02 at Q^2=4 GeV^2. Later, a more careful analysis indicates a slightly larger correction $\delta I_G = -0.029$ to -0.051 at Q^2=3 GeV^2 [60]. It is interesting to find that the discrepancy between the NMC result and the sum becomes smaller, but it is not large enough to explain the NMC deficit. Because the correction becomes smaller: $\delta I_G = -0.009$ to -0.017 even at slightly larger Q^2 (=10 GeV^2). This kind of simple interpretation could be tested by future experiments. For the details of this topics, the interested reader may look at the original papers [59, 60].

Figure 5.1: Drell-Yan process.

tion process in hadron-hadron collisions $A + B \rightarrow \ell^+\ell^- X$, where ℓ is for example the muon, as shown in Fig. 5.1. The Drell-Yan experiments have been used in determining quark distributions in a hadron, in particular sea-quark distributions. Therefore, it is ideal for examining the flavor dependence in the light antiquark distributions, even though there is an undetermined K-factor in the experimental analysis. The K-factor is the ratio between the measured cross section and the leading-order prediction. The theoretical studies of α_s and α_s^2 corrections revealed that the K-factor could be rather well explained by the higher-order QCD corrections [95].

Its cross section is given by [2]

$$d\sigma = \frac{1}{4\sqrt{(P_A \cdot P_B)^2 - M_A^2 M_B^2}} \overline{\sum_{pol}} \sum_X (2\pi)^4 \, \delta(P_A + P_B - k_1 - k_2 - P_X)$$

$$\times \ |\mathcal{M}(AB \rightarrow \ell^+\ell^- X)|^2 \, \frac{d^3k_1}{(2\pi)^3 2k_{10}} \, \frac{d^3k_2}{(2\pi)^3 2k_{20}} \quad , \qquad (5.1)$$

where k_1 and k_2 are ℓ^- and ℓ^+ momenta, spin summation is taken for the final state particles, and spin average is taken for the initial hadrons. Because the matrix element is given by

$$\mathcal{M}(AB \rightarrow \ell^+\ell^- X) \ = \ \bar{u}(k_1, \lambda_1) e \gamma_\mu v(k_2, \lambda_2) \, \frac{g^{\mu\nu}}{(k_1 + k_2)^2} \ < X | e J_\nu(0) | AB > \quad , \qquad (5.2)$$

the cross section is written in terms of lepton and hadron tensors:

$$d\sigma = \frac{4\pi M \, e^4}{\sqrt{[s - (M_A^2 + M_B^2)]^2 - 4 M_A^2 M_B^2}} \, \frac{L^{\mu\nu} W_{\mu\nu}}{(k_1 + k_2)^4} \, \frac{d^3k_1}{(2\pi)^3 2k_{10}} \, \frac{d^3k_2}{(2\pi)^3 2k_{20}} \quad , \qquad (5.3)$$

described by the quark-antiquark annihilation process $q + \bar{q} \rightarrow \ell^+ + \ell^-$. For example, Fig. 5.2 indicates that a quark with the momentum fraction x_1 in the hadron A annihilates with an antiquark with x_2 in the hadron B. Considering the color factor $3 \cdot (1/3)^2 = 1/3$, we obtain the LO Drell-Yan cross section

Figure 5.2: Dominant contribution to the Drell-Yan cross section.

$$s\frac{d\sigma}{d\sqrt{\tau}dy} = \frac{8\pi\alpha^2}{9\sqrt{\tau}} \sum_i e_i^2 \, [\, q_i^A(x_1, Q^2)\, \bar{q}_i^B(x_2, Q^2) + \bar{q}_i^A(x_1, Q^2)\, q_i^B(x_2, Q^2)\,] \quad , \tag{5.6}$$

where Q^2 is the dimuon mass squared: $Q^2 = m_{\mu\mu}^2$, and τ is given by $\tau = m_{\mu\mu}^2/s = x_1 x_2$. The rapidity y is defined by dimuon longitudinal momentum P_L^* and dimuon energy E^* in the c.m. system: $y = (1/2)ln[(E^* + P_L^*)/(E^* - P_L^*)]$. The momentum fractions x_1 and x_2 can be written by these kinematical variables: $x_1 = \sqrt{\tau}e^y$ and $x_2 = \sqrt{\tau}e^{-y}$.

According to Eq. (5.6), the process can be used for measuring the antiquark distributions if the quark distributions in another hadron are known. For finding the flavor asymmetry $\bar{u} - \bar{d}$, the difference between p-p and p-n (practically p-d) Drell-Yan cross sections is useful. Considering the rapidity point y=0 and retaining only the valence-sea annihilation terms, we have [67]

$$\begin{aligned}
\sigma^{pp} &= \frac{8\pi\alpha^2}{9\sqrt{\tau}} \left[\frac{8}{9} u_v(x)\bar{u}(x) + \frac{2}{9} d_v(x)\bar{d}(x) \right] \quad , \\
\sigma^{pn} &= \frac{8\pi\alpha^2}{9\sqrt{\tau}} \left[\frac{4}{9} \left\{ u_v(x)\bar{d}(x) + d_v(x)\bar{u}(x) \right\} + \frac{1}{9} \left\{ d_v(x)\bar{u}(x) + u_v(x)\bar{d}(x) \right\} \right] \quad \text{at } y=0 \quad ,
\end{aligned} \tag{5.7}$$

for the proton-proton and proton-neutron cross sections. All the above distributions are at $x = \sqrt{\tau}$ because of $y = 0$. From these equations, the p-n asymmetry becomes

$$\begin{aligned}
A_{DY} &= \frac{\sigma^{pp} - \sigma^{pn}}{\sigma^{pp} + \sigma^{pn}} \\
&= \frac{[4u_v(x) - d_v(x)][\bar{u}(x) - \bar{d}(x)] + [u_v(x) - d_v(x)][4\bar{u}(x) - \bar{d}(x)]}{[4u_v(x) + d_v(x)][\bar{u}(x) + \bar{d}(x)] + [u_v(x) + d_v(x)][4\bar{u}(x) + \bar{d}(x)]} \quad \text{at } y=0 \quad .
\end{aligned} \tag{5.8}$$

This quantity is very sensitive to the $\bar{u} - \bar{d}$ distribution. However, antiquark-quark annihilation processes also contribute to the above equation at the rapidity point y=0. In this sense, it is better to take large x_F ($\equiv x_1 - x_2$) data so that the antiquarks in the projectile do not affect the asymmetry [68]:

$$A_{DY} = \frac{[4u(x_1) - d(x_1)][\bar{u}(x_2) - \bar{d}(x_2)]}{[4u(x_1) + d(x_1)][\bar{u}(x_2) + \bar{d}(x_2)]} \quad \text{at large } x_F \quad . \tag{5.9}$$

The above discussions are, of course, based on the LO cross section. On the other hand, the higher-order corrections are rather large as represented by the K-factor. Therefore, it is important to investigate whether the K-factor cancels out in the asymmetry A_{DY}.

The Drell-Yan process has been already used for studying the flavor asymmetry. There are existing data by the Fermilab-E288, the Fermilab-E772, and the CERN-NA51. Furthermore, detailed studies of the Drell-Yan asymmetry are in progress at Fermilab by the E866 collaboration.

The Fermilab-E288 collaboration measured dileptons produced in proton-nucleus collisions. Proton-beam energies are 200, 300 and 400 GeV, and targets are beryllium, copper and platinum. The dimuon data are taken in the mass region $m_{\mu\mu}$=4−17 GeV, and they are analyzed by using Eq. (5.6). The isospin symmetry is assumed for parton distributions in the proton and neutron. No nuclear correction is made except for the Fermi motion correction. We note that the E288 paper was published before the finding of the EMC effect [97]. Q^2 dependent F_2^p data from electron and muon scattering are used together with a fit $F_2^n/F_2^p = 1.0 - 0.8x$ and parametrized antiquark distributions. The antiquark part is assumed to be Q^2 independent, and they are determined by fitting their data: $\bar{d} = 0.548(1-x)^{7.62}$ and $\bar{u} = 0.548(1-x)^{11.1}$. Calculated DY cross sections with these $\bar{u}$ and $\bar{d}$ distributions are shown by the dashed curve in Fig. 5.3, and flavor-symmetric ones are shown by the solid curve. The E288 data favor a $\bar{d}$ excess over $\bar{u}$: $\bar{u} = \bar{d}(1-x)^{3.48}$.

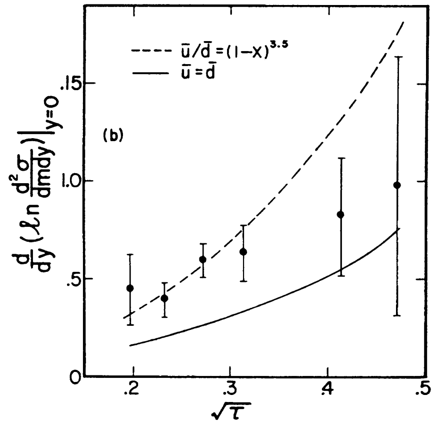

Figure 5.3: Slope of rapidity distribution at y=0 in the E288 experiment (taken from Ref. [12]). Flavor symmetric and asymmetric results are shown by the solid and dashed curves.

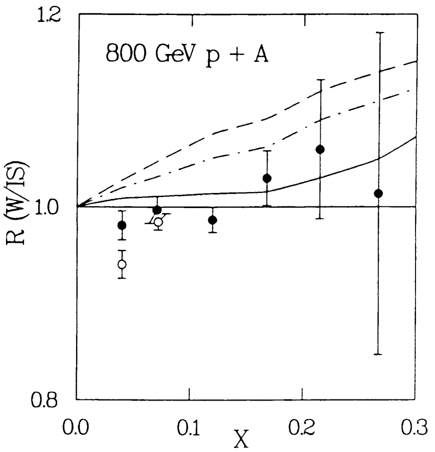

Figure 5.4: Drell-Yan cross section ratio σ_W/σ_{IS} in the E772 experiment (taken from Ref. [18]). Open circles are the data without shadowing correction. Three theoretical asymmetry results are shown by the solid, dashed, and dot-dashed curves.

Next, the Fermilab-E772 collaboration showed their Drell-Yan results on the flavor asymmetry in 1992 [18]. The Drell-Yan experiments are done for isoscalar targets, deuteron and carbon, and for tungsten which has a large neutron excess. The proton beam energy is 800 GeV. Forward production of the dileptons is dominated by beam-quark annihilation with a target antiquark in Eq. (5.9). Therefore, the cross sections in the region $x_F \geq 0.1$ can be used for investigating the antiquark distributions in the target. If sea-quark distributions in a nucleus are just the summation of proton and neutron contributions without nuclear modification, the cross-section ratio for the tungsten (W) and the isoscalar targets (IS) becomes

$$R_A(x) \equiv \frac{\sigma_A(x)}{\sigma_{IS}(x)} \approx 1 + \frac{N-Z}{A}\frac{\bar{d}(x)-\bar{u}(x)}{\bar{d}(x)+\bar{u}(x)} \quad , \tag{5.10}$$

where A, Z, and N are the atomic weight, atomic number, and number of neutrons in the target nucleus. The $d\bar{d}$ annihilation is neglected because the $u\bar{u}$ dominates the cross section. Shadowing correction is applied to the tungsten data at $x < 0.1$ in the following way. First, A-dependent shadowing factor α_{sh} is determined from EMC, NMC, and E665 shadowing data for D, C, and Ca. Then, the tungsten cross sections with $x < 0.1$ are corrected by $\sigma_{_A} = \sigma_{_N} A^{\alpha_{sh}}$. The obtained ratios are shown in Fig. 5.4 together with three theoretical expectations. The solid curve is a pion-model prediction [31, 68] in section 4.3.1. The dashed one is a simple parametrization in section 2.6 for explaining the NMC data: $\bar{d}-\bar{u} = A(1-x)^b$ with $A = 0.15(1+b)$ and b=9.6 [67]. The dot-dashed one is a chiral model result [40, 69] in section 4.3.2. As it is obvious from the figure, the data do not reveal significant flavor asymmetry. Although the E772 data are consistent with the flavor asymmetric model predictions, they could be also explained by the flavor symmetric sea by considering experimental errors. The tungsten is a heavy nucleus, so that there could be a significant nuclear effect on the flavor distribution (see section 4.6). The E772 collaboration also showed the x_F distribution of p+d data in connection with the flavor asymmetry. However, there is also no evidence for the asymmetry. These results are somewhat in conflict with the NMC result and other Drell-Yan data.

There are Drell-Yan data for various nuclear targets; however, the NA51 data point at x=0.18 [19] is the only existing one which is extracted from the p-p and p-d Drell-Yan experiments. Considering the x range of the NA51 measurements, we neglect shadowing correction in the deuteron. Then, the asymmetry can be written as $A_{DY} = 2\sigma^{pp}/\sigma^{pd} - 1$. The NA51 collaboration used 450 GeV primary proton beam from the CERN-SPS. The targets are liquid hydrogen and deuterium. The accepted rapidity range is from -0.5 to 0.6, and the muon mass region $M_{\mu\mu}$ $\geq$4.3 GeV is used for the analysis. The obtained asymmetry is

$$A_{DY} = -0.09 \pm 0.02\,(stat.) \pm 0.025\,(syst.) \quad . \tag{5.11}$$

As the valence-quark value $\lambda_V = u_v/d_v$ at x=0.18, they take λ_V=2.2 averaged over the parton distributions, MRS-S$'_0$, MRS-D$'_0$, and MRS-D$_-'$, GRV-HO, and CTEQ-2M. From Eqs. (5.8) and (5.11), the observed asymmetry becomes

$$\frac{\bar{u}}{\bar{d}} = 0.51 \pm 0.04\,(stat.) \pm 0.05\,(syst.) \qquad at\ x = 0.18 \quad . \tag{5.12}$$

This is a clear indication of the flavor asymmetry in the light antiquark distributions. There is an excess of $\bar{d}$-quarks over $\bar{u}$ in the nucleon, and the NA51 result agrees with the tendency obtained by the NMC. Unfortunately, the only one data point at $x = 0.18$ is available in the NA51. More complete Drell-Yan experiments at the Fermilab (E866) should give a clearer answer to the flavor symmetry problem [20]. At this stage, the preliminary E866 data seem to show the NMC type asymmetry in addition.

The E772 and NA51 data are compared with various model predictions in Refs. [18, 43, 67, 68, 69, 70, 71, 72, 73]. The theoretical works are done mainly to compare the mesonic calculations with the Drell-Yan data. At this stage, the mesonic models could be consistent not only with the NMC result but also with the E772 and NA51 Drell-Yan data.

5.1.1 Fermilab-E866 results

The Fermilab-E866 collaboration reported high statistical experimental results for the ratio of the Drell-Yan cross sections $\sigma_{pd}/2\sigma_{pp}$ [20]. The dimuons are measured in 800 GeV proton scattering on the liquid hydrogen or liquid deuterium target. Six month data were collected until March of 1997, and 350,000 Drell-Yan events were obtained. The goal of the experiment is to measure the cross-section ratios with 1% accuracy in the x range $0.03 < x < 0.15$. The accuracy becomes worse in the larger x region. At large $x_{_F}$, the ratio is approximated as $[\sigma_{pd}/2\sigma_{pp}]_{x_F \gg 0} \approx [1 + \bar{d}(x)/\bar{u}(x)]/2$, so that it is possible to extract the distribution ratio $\bar{d}(x)/\bar{u}(x)$ from the large $x_{_F}$ data of the cross sections. They compared the obtained ratios $\sigma_{pd}/2\sigma_{pp}$ with the flavor symmetric distributions [CTEQ4M($\bar{u} = \bar{d}$) and MRS(S0)] and asymmetric ones [CTEQ4M($\bar{u} \neq \bar{d}$), GRV, and MRS(G)]. The symmetric CTEQ4M($\bar{u} = \bar{d}$) curve is obtained by modifying the distributions as $\bar{u} = \bar{d} = (\bar{u} + \bar{d})/2$. The accurate part of the data in the region $0.03 < x < 0.15$ tends to agree with the asymmetric distributions, in particular with the CTEQ4M($\bar{u} \neq \bar{d}$). However, it is also interesting to find that the data seem to deviate from the present asymmetric parametrizations in the larger x region. Although their results are still preliminary, the accurate E866 data confirm the flavor asymmetry conclusions of the NMC and NA51.

5.2 W and Z production

Instead of the virtual photon production in the Drell-Yan case, weak boson production could also have information on the antiquark distributions [77, 78, 79]. There are existing CDF data for the charged lepton asymmetry (or W charge asymmetry) in the $p + \bar{p}$ reaction: $p\bar{p} \rightarrow W^{\pm}X \rightarrow (\ell^{\pm}\nu_{\ell})X$ [98]. They are first analyzed in Ref. [21] in connection with the $\bar{u} - \bar{d}$ distribution. Although the CDF data constrain the u/d ratio in the region of $x = M_W/\sqrt{s} = 0.045$, they are consistent with the symmetric sea $\bar{u} = \bar{d}$. However, the $p+\bar{p}$ reaction is not very sensitive to the sea-quark distributions as we discuss in this section. Therefore, future $p + p$ colliders such as Relativistic Heavy Ion Collider (RHIC), rather than the $p + \bar{p}$, are crucial for investigating the flavor asymmetry in W and Z production processes. We discuss the sensitivity of $W^{\pm}$ and Z^0 production cross sections on the $\bar{u}/\bar{d}$ asymmetry based on Ref. [79] in the following.

We show how the W production processes in the $p + p$ collider could be used for probing the flavor asymmetry. The W^+ production cross section is given by parton-subprocess ones together with parton distributions in the colliding hadrons [99]:

$$\sigma(p+p \rightarrow W^+X) = \frac{1}{3}\int_0^1 dx_1 \int_0^1 dx_2 \sum_{q,\bar{q}'} q(x_1, M_W^2)\, \bar{q}'(x_2, M_W^2)\, \hat{\sigma}(q\bar{q}' \rightarrow W^+) \quad , \tag{5.13}$$

where 1/3 is the color factor $3 \cdot (1/3)^2 = 1/3$. The subprocess cross section is given by

$$d\hat{\sigma}(q\,\bar{q}' \rightarrow W^+) = \left(\frac{1}{2}\right)^2 \frac{1}{2\hat{s}} \sum_{pol} \left|\mathcal{M}(q\,\bar{q}' \rightarrow W^+)\right|^2 \,(2\pi)^4\, \delta^4(p_1 + p_2 - p)\, \frac{d^3p}{2E_p(2\pi)^3} \ , \tag{5.14}$$

where p_1, p_2, and p are $\bar{q}'$, q, and W^+ momenta respectively, and $\hat{s}$ is given by $\hat{s} = (p_1 + p_2)^2$. The matrix element is

$$\mathcal{M}(q\,\bar{q}' \rightarrow W^+) = -i\, V_{qq'}\, \frac{g}{\sqrt{2}}\, \varepsilon_{\alpha}^{\lambda\,*}(p)\, \bar{v}(p_1)\, \frac{1}{2}\, \gamma^{\alpha}(1-\gamma_5)\, u(p_2) \quad , \tag{5.15}$$

and the Cabibbo mixing is used in our calculation: $V_{ud} = \cos\theta_c$, $V_{us} = \sin\theta_c$, $V_{cd} = -\sin\theta_c$, and $V_{cs} = \cos\theta_c$. Taking the spin summation, we obtain

$$\sum_{pol} \left|\mathcal{M}\left(q\,\bar{q}' \rightarrow W^+\right)\right|^2 = \frac{8}{\sqrt{2}}\, G_F\, M_W^4\, |V_{qq'}|^2 \quad , \tag{5.16}$$

with the Fermi coupling constant $G_F/\sqrt{2} = g^2/(8M_W^2)$. Noting $\delta^4(p_1 + p_2 - p)d^3p/(2E_p) = \delta(\hat{s} - M_W^2)$ and $dx_1dx_2 = d\hat{s}\, dx_F/[(x_1 + x_2)s]$, we have the W^+ production cross section in the $p + p$ reaction in terms of the parton distributions:

$$\frac{d\sigma_{p+p\to W^+}}{dx_F} = \frac{\sqrt{2}\pi}{3} G_F \left(\frac{x_1 x_2}{x_1+x_2}\right) \Big\{ \cos^2\theta_c \, [u(x_1)\bar{d}(x_2) + \bar{d}(x_1)u(x_2)] \\ + \sin^2\theta_c \, [u(x_1)\bar{s}(x_2) + \bar{s}(x_1)u(x_2)] \Big\} \quad . \tag{5.17}$$

The dominant processes of producing W^+ are $u(x_1)+\bar{d}(x_2) \to W^+$ and $u(x_2)+\bar{d}(x_1) \to W^+$; however, the first one becomes much larger than the second at large x_F. Therefore, the cross section is sensitive to the $\bar{d}$ distribution at large x_F. On the other hand, the cross section for the W^- production is given in the same way:

$$\frac{d\sigma_{p+p\to W^-}}{dx_F} = \frac{\sqrt{2}\pi}{3} G_F \left(\frac{x_1 x_2}{x_1+x_2}\right) \Big\{ \cos^2\theta_c \, [\bar{u}(x_1)d(x_2) + d(x_1)\bar{u}(x_2)] \\ + \sin^2\theta_c \, [\bar{u}(x_1)s(x_2) + s(x_1)\bar{u}(x_2)] \Big\} \quad . \tag{5.18}$$

At large x_F, it is sensitive to the $\bar{u}$ distribution instead of the $\bar{d}$ in the W^+ case. This difference makes it possible to find the difference $\bar{u}-\bar{d}$. Because the Cabbibo angle is small, the $\sin^2\theta_c$ terms are neglected for simplicity in the following discussions. The $W^\pm$ production ratio is then given by

$$R_{p+p}(x_F) \equiv \frac{d\sigma_{p+p\to W^+}/dx_F}{d\sigma_{p+p\to W^-}/dx_F} = \frac{u(x_1)\bar{d}(x_2) + \bar{d}(x_1)u(x_2)}{\bar{u}(x_1)d(x_2) + d(x_1)\bar{u}(x_2)} \quad . \tag{5.19}$$

At large x_F (large x_1), the antiquark distribution $\bar{q}(x_1)$ is very small, so that the above equation becomes

$$R_{p+p}(x_F \gg 0) \approx \frac{u(x_1)}{d(x_1)} \, \frac{\bar{d}(x_2)}{\bar{u}(x_2)} \quad , \tag{5.20}$$

which is directly proportional to the ratio $\bar{d}/\bar{u}$.

The situation is very different in the $p+\bar{p}$ reaction case. Replacing the parton distributions in Eq. (5.19) by $q(x_2) \to \bar{q}(x_2)$ and $\bar{q}(x_2) \to q(x_2)$, we obtain the ratio

$$R_{p+\bar{p}}(x_F) = \frac{u(x_1)d(x_2) + \bar{d}(x_1)\bar{u}(x_2)}{\bar{u}(x_1)\bar{d}(x_2) + d(x_1)u(x_2)} \xrightarrow[x_F \gg 0]{} \frac{u(x_1)}{d(x_1)} \, \frac{d(x_2)}{u(x_2)} \quad . \tag{5.21}$$

In the $p+\bar{p}$ reaction, the ratio is no more sensitive to the $\bar{u}/\bar{d}$ asymmetry. How about the $x_F \approx 0$ region? We find from Eq. (5.21) that the $p+\bar{p}$ ratio is independent: $R_{p+\bar{p}}(x_F=0)=1$, even though the $p+p$ ratio is still sensitive to the flavor asymmetry at $x_F=0$: $R_{p+p}(x_F=0) = [u(x)/d(x)][\bar{d}(x)/\bar{u}(x)]$. From these discussions, it is more appropriate to use a $p+p$ collider in finding the $\bar{u}/\bar{d}$ asymmetry from W production data. This fact is numerically shown in Fig. 5.5.

The ratios in the $p+p$ and $p+\bar{p}$ reactions are evaluated at $\sqrt{s}$=500 GeV in Fig. 5.5 by using various parametrizations for the parton distributions [79]. The distributions are evolved to the scale $Q^2 = M_W^2$. The figures a) and b) show the $p+p$ and $p+\bar{p}$ results respectively. The dashed curve indicates the results of using the flavor symmetric ($\bar{u} = \bar{d}$) DO1.1 distributions. The others are the results for flavor asymmetric distributions (MRSD$_-'$, CTEQ2pM, ES, EHQ). Because the NA51 result ruled out the MRSD$_-'$ distribution, the small difference between the flavor asymmetric MRSD$_-'$ and the symmetric DO1.1 should not be taken seriously. As we expected, the $p+p$ reaction is sensitive to the parton-distribution models, in particular the light antiquark flavor asymmetry, not only in the large $|x_F|$ region but also in the $x_F \approx 0$ region. On the other hand, the $p+\bar{p}$ reaction is almost insensitive to the asymmetry. The model dependence appears only in the very small x_F.

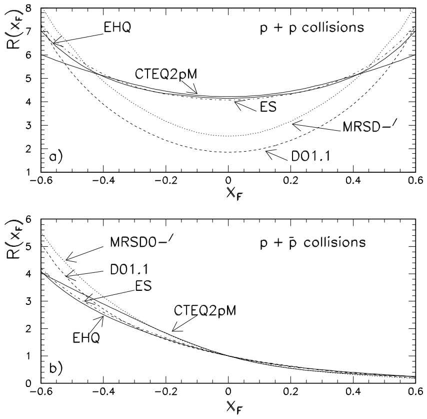

Figure 5.5: $W^{\pm}$ production ratios a) in $p+p$ and b) in $p+\bar{p}$ (taken from Ref. [79]).

The W production processes in the $p+p$ and $p+d$ reactions could also be used for studying the flavor asymmetry. The cross-section ratio is

$$R'(x_F) \equiv 2\,\frac{d\sigma_{p+p\to W^+}/dx_F}{d\sigma_{p+d\to W^+}/dx_F} \approx \frac{u(x_1)\bar{d}(x_2)+\bar{d}(x_1)u(x_2)}{u(x_1)\,[\bar{u}(x_1)+\bar{d}(x_2)]+\bar{d}(x_1)\,[u(x_2)+d(x_2)]} \quad , \quad (5.22)$$

by neglecting nuclear corrections in the deuteron. Although it is independent of the sea distributions at small x_F: $R'(x_F \ll 0) = 1 + [u(x_2)-d(x_2)]/[u(x_2)+d(x_2)]$, large x_F data are useful:

$$R'(x_F) \approx 1 - \frac{\bar{u}(x_2)-\bar{d}(x_2)}{\bar{u}(x_2)+\bar{d}(x_2)} \quad \text{at } x_F \gg 0 \quad . \quad (5.23)$$

In the similar way, Z^0 production data in the $p+p$ and $p+d$ reactions are valuable. The Z^0 production cross section in the $p+p$ is

$$\frac{d\sigma_{p+p\to Z^\circ}}{dx_F} = \frac{\pi}{3\sqrt{2}}\,G_F\left(\frac{x_1x_2}{x_1+x_2}\right)\Bigg\{(1-\frac{8}{3}\chi_w+\frac{32}{9}\chi_w^2)\,[u(x_1)\bar{u}(x_2)+\bar{u}(x_1)u(x_2)]$$
$$+(1-\frac{4}{3}\chi_w+\frac{8}{9}\chi_w^2)\,[d(x_1)\bar{d}(x_2)+\bar{d}(x_1)d(x_2)+s(x_1)\bar{s}(x_2)+\bar{s}(x_1)s(x_2)]\Bigg\} \quad , \quad (5.24)$$

where χ_w is given by the Weinberg angle as $\chi_w = \sin^2\theta_W$. Taking into account the dominant $u\bar{u}$ contribution at large x_F, we obtain the ratio

$$R''(x_F) \equiv 2\,\frac{d\sigma_{p+p\to Z^\circ}/dx_F}{d\sigma_{p+d\to Z^\circ}/dx_F} \approx 1 + \frac{\bar{u}(x_2)-\bar{d}(x_2)}{\bar{u}(x_2)+\bar{d}(x_2)} \quad \text{at } x_F \gg 0 \quad . \quad (5.25)$$

We find that not only the $W^{\pm}$ production but also the Z^0 production could be used in determining the $\bar{u}-\bar{d}$ distribution. Because $p+p$ and $p+d$ reactions are very sensitive to the asymmetry, future colliders such as RHIC should be able to find the antiquark asymmetry by the $W^{\pm}$ and Z^0 production measurements.

5.3 Quarkonium production at large x_F

We discuss the possibility of finding the $\bar{u}-\bar{d}$ distribution in quarkonium production processes. J/ψ production data have been used in extracting gluon distributions in the nucleon and in nuclei. Because the dominant process is the gluon fusion $gg \to c\bar{c} \to J/\psi$, $q\bar{q}$ annihilation is in general a small effect. However, the $q\bar{q}$ process could become important at large $|x_F|$.

The mechanism of producing the quarkonium is a strong interaction, which makes the description more model-dependent than the electromagnetic Drell-Yan case. A popular description is a color-singlet (and recent color-octet) model, which includes gg, gq, $g\bar{q}$, and $q\bar{q}$ fusion up to α_s^3. Instead of stepping into the detailed production mechanism, we discuss general features by selecting a simpler one, the semi-local duality model. The quarkonium production processes are analyzed in this model, and the results are related to the flavor asymmetry in Ref. [80].

The cross section for a $Q\overline{Q}$ pair production is given by parton subprocess cross sections multiplied by the corresponding parton distributions

$$\frac{d\sigma_{Q\overline{Q}}}{dx_F d\tau} = \frac{2\tau}{\sqrt{{x_F}^2+4\tau^2}} \Bigg[G(x_1)G(x_2)\,\sigma(gg\to Q\overline{Q};m^2) + \sum_{\mathrm{i=u,d,s}} \big\{\, q^i(x_1)\bar{q}^i(x_2)+\bar{q}^i(x_1)q^i(x_2)\,\big\}\,\sigma(q\bar{q}\to Q\overline{Q};m^2) \Bigg] \ . \tag{5.26}$$

The only gg and $q\bar{q}$ type subprocesses are taken into account in the above expression, and $\sigma(gg\to Q\overline{Q};m^2)$ and $\sigma(q\bar{q}\to Q\overline{Q};m^2)$ are the corresponding cross sections. The variables x_1 and x_2 are fractional momenta carried by the projectile parton and by the target one, and x_F and τ are given by $x_F = x_1 - x_2$ and $\tau = m/\sqrt{s}$ with the invariant mass of the $Q\bar{Q}$ pair m. The subprocess cross sections are

$$\begin{aligned} \sigma(q\bar{q}\to Q\bar{Q};m^2) &= \frac{8\pi\alpha_s^2}{27m^6}\,(m^2+2m_Q^2)\,\lambda \quad , \\ \sigma(gg\to Q\bar{Q};m^2) &= \frac{\pi\alpha_s^2}{3m^6}\Bigg[(m^4+4m^2m_Q^2+m_Q^4)\,\ln(\frac{m^2+\lambda}{m^2-\lambda}) \\ &\qquad - \frac{1}{4}\,(7m^2+31m_Q^2)\,\lambda \Bigg] \quad , \end{aligned} \tag{5.27}$$

where m_Q is a quark mass and λ is given by $\lambda = \sqrt{m^4 - 4m^2{m_Q}^2}$. According to the semi-local duality model, the quarkonium production cross section is obtained by integrating the subprocesses cross section from the $Q\bar{Q}$ threshold to the open charm (beauty) threshold:

$$\frac{d\sigma_{p+p\to J/\psi(\Upsilon)}}{dx_F} = F \int_{2m_Q/\sqrt{\tau}}^{2m_{D(B)}/\sqrt{\tau}} d\tau \, \frac{d\sigma_{Q\overline{Q}}}{dx_F d\tau} \quad , \tag{5.28}$$

where F is the probability of a J/ψ (Υ) creation from the $Q\overline{Q}$ state.

We hope to find the antiquark flavor asymmetry from these quarkonium production processes. The gluon-gluon fusion process dominates the cross section in general. However, the $q\bar{q}$ processes could become more important in certain kinematical regions. The $q\bar{q}$ fusion contributions in the $p+p$ collision are

$$d\sigma_{p+p} \propto u(x_1)\bar{u}(x_2) + \bar{u}(x_1)u(x_2) + d(x_1)\bar{d}(x_2) + \bar{d}(x_1)d(x_2) \quad . \tag{5.29}$$

In order to find the $\bar{u} - \bar{d}$ distribution, the $p+d$ reaction has to be studied in addition:

$$d\sigma_{p+d} \propto [u(x_1) + d(x_1)][\bar{u}(x_2) + \bar{d}(x_2)] + [\bar{u}(x_1) + \bar{d}(x_1)][u(x_2) + d(x_2)] \quad , \tag{5.30}$$

where the isospin symmetry is assumed. The cross-section ratio

$$R(x_F) = 2\,\frac{d\sigma(p+p \to J/\psi(\Upsilon))/dx_F}{d\sigma(p+d \to J/\psi(\Upsilon))/dx_F} \quad , \tag{5.31}$$

should be sensitive to $\bar{u} - \bar{d}$ particularly at large x_F. From Eqs. (5.29) and (5.30), it is obvious that the ratio is $R(x_F) = 1$ in the flavor symmetric case $\bar{u} = \bar{d}$. Therefore, the deviation from unity is a signature of a finite $\bar{u} - \bar{d}$ distribution.

The ratio $R(x_F)$ is evaluated for the 800 GeV proton beam in Fig. 5.6, where the upper (lower) figure shows the J/ψ (Υ) production results. Input parton distributions are the same in Fig. 5.5. The ratio is unity if the sea is flavor symmetric, and it is shown by the solid lines DO1.1 in Fig. 5.6. As we expected, effects of the flavor asymmetry become conspicuous at large $|x_F|$. This is because the gluon distribution $G(x)$ is much smaller than the quark one $q(x)$ at large x, and the cross section is dominated by the $q\bar{q}$ fusion processes. The parton-distribution dependence is more evident in the Υ production. Because Υ is more massive than J/ψ, we have $(x_1 x_2)_\Upsilon \sim 2m_B/\sqrt{s} > 2m_C/\sqrt{s}$. The Υ process is sensitive to the larger x region, so that the flavor-asymmetry effects become more conspicuous.

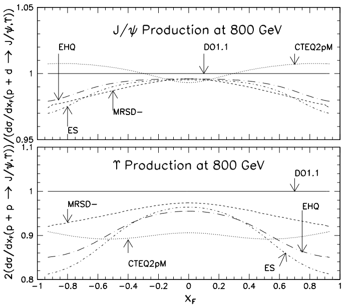

Figure 5.6: J/ψ and Υ production ratios (taken from Ref. [80])

The above results show interesting contributions from the $\bar{u}/\bar{d}$ asymmetry. Therefore, measurements of the J/ψ and Υ production cross sections for the proton and deuteron targets at large x_F should also be able to clarify the $\bar{u}-\bar{d}$ distribution problem. However, the semi-local duality model is probably too simple to explain the quarkonium-production processes. It is now revealed that the prediction of a more sophisticated color-singlet model is inconsistent with the J/ψ and ψ' production data by the CDF. The discrepancy could be understood by the color-octet mechanism. Therefore, a better model analysis is necessary in comparing the theoretical results with future experimental data.

5.4 Charged hadron production

Semi-inclusive reactions in the electron or muon scattering could be used for finding the antiquark distributions. In particular, charged-hadron production could have information on the flavor asymmetry. The hadron-production cross section is written by the lepton and hadron tensors in the same way with the inclusive one in section 2.1. However, in spite of the fact that the semi-inclusive process is dominated by the light-cone region, the operator product expansion cannot be applied [96]. It is because the summation on X in the final state $|\,X; p_h, s_h>$ cannot be taken independently from the hadron state $|\,p_h, s_h>$. Therefore, we discuss the theoretical analysis on a relation between the charged-hadron-production cross section and the distribution $\bar{u}-\bar{d}$ by using a quark-parton model [76].

In the parton picture, the semi-inclusive cross section is given by [1]

$$\frac{1}{\sigma_N(x)}\,\frac{\partial\sigma_N^h(x,z)}{\partial z}=\frac{\sum_i e_i^2\,f_i(x)\,D_i^h(z)}{\sum_i e_i^2\,f_i(x)}\quad , \tag{5.32}$$

where $f_i(x)$ is the quark distribution with flavor i and momentum fraction x, and $D_i^h(z)$ is the i-quark to h-hadron fragmentation function with $z=E_h/\nu$. The numerator for charged hadron production is

$$\begin{aligned} N^{Nh^\pm} &\equiv \sum_i e_i^2\,f_i(x)\,D_i^{h^\pm}(z) \\ &= \frac{4}{9}\,u\,D_u^\pm+\frac{4}{9}\,\bar{u}\,D_{\bar{u}}^\pm+\frac{1}{9}\,d\,D_d^\pm+\frac{1}{9}\,\bar{d}\,D_{\bar{d}}^\pm+\frac{1}{9}\,s\,D_s^\pm+\frac{1}{9}\,\bar{s}\,D_{\bar{s}}^\pm \quad . \end{aligned} \tag{5.33}$$

Assuming the isospin symmetry in the parton distributions, we consider a combination of proton and neutron cross sections:

$$\begin{aligned} R(x,z) &= \frac{(N^{p+}-N^{n+})+(N^{p-}-N^{n-})}{(N^{p+}-N^{n+})-(N^{p-}-N^{n-})} \\ &= \frac{u(x)-d(x)+\bar{u}(x)-\bar{d}(x)}{u(x)-d(x)-\bar{u}(x)+\bar{d}(x)}\cdot\frac{4\,D_u^+(z)+4\,D_{\bar{u}}^+(z)-D_d^+(z)-D_{\bar{d}}^+(z)}{4\,D_u^+(z)-4\,D_{\bar{u}}^+(z)-D_d^+(z)+D_{\bar{d}}^+(z)}\ . \end{aligned} \tag{5.34}$$

Here, N^{p+} (N^{p-}) and N^{n+} (N^{n-}) correspond to the production processes of positively (negatively) charged hadrons from the proton and the neutron respectively. If the denominator and numerator are integrated over x individually, the Gottfried sum is obtained from the numerator integral, and the denominator becomes a sum for the valence quarks:

$$\begin{aligned} Q(z) &= \frac{\int dx \, \{ \, (N^{p+} - N^{n+}) + (N^{p-} - N^{n-}) \, \}}{\int dx \, \{ \, (N^{p+} - N^{n+}) - (N^{p-} - N^{n-}) \, \}} \\ &= 3 \, I_G \, \frac{4 \, D_u^+(z) + 4 \, D_{\bar{u}}^+(z) - D_d^+(z) - D_{\bar{d}}^+(z)}{4 \, D_u^+(z) - 4 \, D_{\bar{u}}^+(z) - D_d^+(z) + D_{\bar{d}}^+(z)} \quad . \end{aligned} \tag{5.35}$$

According to this equation, if the Gottfried sum rule is violated, it should appear in the charged-hadron-production asymmetry. Available EMC data [74] are analyzed by using Eq. (5.35) [76]. Contributions from pion, kaon, and (anti)proton production processes are taken into account in evaluating the fragmentation function, for example

$$D_u^+ = D_u^{\pi^+} + D_u^{K^+} + D_u^p \quad . \tag{5.36}$$

Isospin and charge conjugation invariance reduces the number of fragmentation functions for the pion:

$$\begin{aligned} D &\equiv D_u^{\pi^+} = D_{\bar{d}}^{\pi^+} = D_d^{\pi^-} = D_{\bar{u}}^{\pi^-} \quad , \\ \widetilde{D} &\equiv D_d^{\pi^+} = D_{\bar{u}}^{\pi^+} = D_u^{\pi^-} = D_{\bar{d}}^{\pi^-} \quad . \end{aligned} \tag{5.37}$$

In the kaon case, the reflection symmetry along the V-spin axis ($D_d^{K^+} = D_d^{K^-}$) is used in addition to the isospin and charge conjugation invariance: $D^K \equiv D_{\bar{u}}^{K^-} = D_u^{K^+}$, $\widetilde{D}^K \equiv D_u^{K^-} = D_{\bar{u}}^{K^+}$, $\widetilde{D}'^K \equiv D_d^{K^+} = D_{\bar{d}}^{K^-} = D_{\bar{d}}^{K^+} = D_d^{K^-}$. Furthermore, $\widetilde{D}^K$ and $\widetilde{D}'^K$ are assumed equal. Similar equations are taken for proton and antiproton production: $D^p \equiv D_u^p = D_d^p = D_{\bar{u}}^{\bar{p}} = D_{\bar{d}}^{\bar{p}}$, $\widetilde{D}^p \equiv D_{\bar{u}}^p = D_{\bar{d}}^p = D_u^{\bar{p}} = D_d^{\bar{p}}$. Experimental information is provided for these fragmentation functions. In particular, we use parametrizations fitted to the EMC data [75]:

$$\begin{aligned} &\frac{\widetilde{D}(z)}{D(z)} = \frac{1-z}{1+z} \quad , \\ &\frac{D^K(z)}{D(z)} = 0.35 \, z + 0.15 \quad , \qquad \frac{\widetilde{D}^K(z)}{D(z)} = 0.45 \, z \, \frac{1-z}{1+z} \quad , \\ &\frac{D^p(z)}{D(z)} = 0.20 \quad , \qquad \frac{\widetilde{D}^p(z)}{D(z)} = 0.12 \, \frac{1-z}{1+z} \quad . \end{aligned} \tag{5.38}$$

With these experimental parametrizations for the fragmentation functions, the ratio of the cross sections $Q(z)$ becomes

$$z \, Q^{ch}(z) = 3 \, I_G \, z \, \frac{0.50 \, z^2 + 3.1 \, z + 7.6}{3.2 \, z^2 + 11 \, z + 0.84} \quad . \tag{5.39}$$

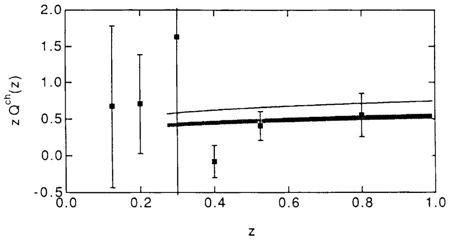

Figure 5.7: Charged-hadron-production ratio $zQ^{ch}(z)$ (taken from Ref. [76]).

Experimental data are given for $(d\sigma_N^h/dz)/\sigma_N$, so that $F_1(x)$ is multiplied in getting N^{Nh}. The experimental data zQ^{ch} obtained in this way are compared with Eq. (5.39) in Fig. 5.7. The upper curve is obtained by assuming the Gottfried sum $I_G = 1/3$ in Eq. (5.39). On the other hand, the hatched area is based on the 1991 NMC result. It is interesting to find the difference between the two results in the semi-inclusive processes. However, as it is obvious from the figure, we cannot judge whether or not the sea is $\bar{u}/\bar{d}$ symmetric from the data.

The recent HERMES preliminary data seem to be accurate enough to find the $\bar{u}/\bar{d}$ asymmetry [17]. The following π^+ and π^- production ratio is related to the function $R(x,z)$ for the pion by

$$r(x,z) = \frac{N^{p\pi^-} - N^{n\pi^-}}{N^{p\pi^+} - N^{n\pi^+}} = \frac{R_\pi(x,z) - 1}{R_\pi(x,z) + 1} \quad . \tag{5.40}$$

The obtained data of $r(x,z)$ in the range $0.1 < x < 0.3$ agree well with the NMC flavor asymmetry, and they are significantly different from the symmetric expectation. The HERMES results will be submitted for publication in the near future.

5.5 Neutrino scattering

Neutrino interactions are useful for determining the valence-quark distributions by taking advantage of parity-violation terms. On the other hand, neutrino-induced dimuon data are used for determining the s and $\bar{s}$ distributions, so that the neutrino interactions could be valuable also for determining the light antiquark distributions $\bar{u}$ and $\bar{d}$. We discuss what kind of cross-section combination is appropriate for finding the $\bar{u} - \bar{d}$ distribution. The neutrino reaction via the charged current is given by the amplitude [3, 99]

$$\mathcal{M}(\nu_\ell p \to \ell X) \;=\; \frac{G_F/\sqrt{2}}{1 + Q^2/M_W^2}\, \bar{u}(k')\gamma^\mu(1-\gamma_5)u(k) < X \,|\, J_\mu^{weak}(0) \,|\, p, \sigma > \quad , \tag{5.41}$$

so that the differential cross section becomes

$$d\sigma = \frac{M}{s - M^2}\, \frac{G_F^2}{(2\pi)^2\,(1 + Q^2/M_W^2)^2}\, \ell^{\mu\nu}\, W_{\mu\nu}\, \frac{d^3k'}{E'} \quad . \tag{5.42}$$

The leptonic tensor is given by

$$\begin{aligned} \ell^{\mu\nu} &= \overline{\sum}_{\lambda,\lambda'} \,[\, \bar{u}(k',\lambda')\gamma^\mu(1-\gamma_5)u(k,\lambda)\,]^*\, [\, \bar{u}(k',\lambda')\gamma^\nu(1-\gamma_5)u(k,\lambda)\,] \\ &= 2\,(\, k^\mu k'^\nu + k'^\mu k^\nu - k\cdot k' g^{\mu\nu} + i\varepsilon^{\mu\nu\rho\sigma} k_\rho k'_\sigma \,) \quad , \end{aligned} \tag{5.43}$$

where $\varepsilon^{\mu\nu\rho\sigma}$ is an antisymmetric tensor with $\varepsilon^{0123} = +1$. The last term does not appear in the electron or muon scattering because it is associated with the parity violation in weak interactions. This term makes it possible to probe new structure in the target hadron. There exists an antisymmetric term under the $\mu \leftrightarrow \nu$ exchange in addition to the hadron tensor in Eq. (2.6):

$$\begin{aligned} W_{\mu\nu} = -W_1 \left(g_{\mu\nu} - \frac{q_\mu q_\nu}{q^2} \right) + \frac{1}{M^2} W_2 \left(p_\mu - \frac{p \cdot q}{q^2} q_\mu \right) \left(p_\nu - \frac{p \cdot q}{q^2} q_\nu \right) \\ - \frac{i}{M} W_3 \, \varepsilon_{\mu\nu\rho\sigma} \, p^\rho q^\sigma \quad . \end{aligned} \tag{5.44}$$

The W_3 structure function is proportional to the difference between left- and right-transverse cross sections for the W boson. With these structure functions, the cross section becomes

$$\frac{d\sigma^\pm}{d\Omega \, dE'} = \frac{G_F^2 \, E'^2}{2\pi^2 \, (1 + Q^2/M_W^2)^2} \left[2 \, W_1 \sin^2 \frac{\theta}{2} + W_2 \cos^2 \frac{\theta}{2} \mp \frac{E + E'}{M} W_3 \sin^2 \frac{\theta}{2} \right] \, , \tag{5.45}$$

where ± indicates $W^\pm$ in the reaction. Structure functions F_1, F_2, and F_3 are defined by $F_1 = M W_1$, $F_2 = \nu W_2$, and $F_3 = \nu W_3$.

On the other hand, the charged-current process is described by neutrino-quark interactions with the current

$$\begin{aligned} J_\mu = \bar{u}(x) \, \gamma_\mu \, (1 - \gamma_5) \, [\, d(x) \, \cos\theta_c + s(x) \, \sin\theta_c \,] \\ + \bar{c}(x) \, \gamma_\mu \, (1 - \gamma_5) \, [\, s(x) \, \cos\theta_c - d(x) \, \sin\theta_c \,] \quad . \end{aligned} \tag{5.46}$$

Comparing a calculated cross section in the parton model with Eq. (5.45), we express the structure functions in terms of quark distributions

$$\begin{aligned} F_1 &= F_2/2x \quad , \\ F_2^{\nu p} &= 2 \, x \, (d + s + \bar{u} + \bar{c}) \quad , \\ F_2^{\bar{\nu} p} &= 2 \, x \, (u + c + \bar{d} + \bar{s}) \quad , \\ x F_3^{\nu p} &= 2 \, x \, (d + s - \bar{u} - \bar{c}) \quad , \\ x F_3^{\bar{\nu} p} &= 2 \, x \, (u + c - \bar{d} - \bar{s}) \quad . \end{aligned} \tag{5.47}$$

For the time being, we discuss only LO contributions without NLO corrections from the coefficient functions. Because the antiquarks have negative parity, there are negative signs in the F_3 structure functions. Combining the ν and $\bar{\nu}$ F_3 structure functions, we obtain the valence quark distribution $(F_3^{\nu p} + F_3^{\bar{\nu} p})/2 = u_v + d_v$ with the assumptions $s = \bar{s}$ and $c = \bar{c}$. Therefore, it is the advantage of neutrino reactions that the valence distribution can be determined. However, they are also used for studying antiquark distributions. In fact, neutrino-induced dimuon data enable us to determine the $\bar{s}$

Figure 5.8: Contributions to the $\bar{u}-\bar{d}$ distribution in Eq. (5.48) or (5.49) (a) from quarks and (b) from antiquarks.

From Eq. (5.47), it is possible to combine the F_2 and F_3 structure functions for the proton and the deuteron in order to get the flavor asymmetry [31]

$$\bar{u}-\bar{d} = \frac{1}{2}\,(F_2^{\nu p}/x - F_3^{\nu p}) - \frac{1}{4}\,(F_2^{\nu d}/x - F_3^{\nu d}) \ , \tag{5.48}$$

by neglecting nuclear effects in the deuteron. It may also be defined in terms of F_1 and F_3 structure functions [22]

$$\bar{u}-\bar{d} = \frac{1}{2}\,(F_1^{\nu p} - F_1^{\bar{\nu} p}) - \frac{1}{4}\,(F_3^{\nu p} - F_3^{\bar{\nu} p}) \quad , \tag{5.49}$$

if the $\bar{s}$ and $\bar{c}$ distributions can be neglected! These expressions are correct only in the LO. However, they are practically convenient because the charged reactions are easier to be measured experimentally. Unfortunately, present data are not accurate enough to be used for finding the $\bar{u}-\bar{d}$ distribution. To be precise, Eqs. (5.48) and (5.49) are not appropriate in defining the $\bar{u}-\bar{d}$ distribution if NLO effects are taken into account. For example, the coefficient functions are different in F_1 and F_3 structure functions, so that $(F_1^{\nu p} - F_1^{\bar{\nu} p})/2 - (F_3^{\nu p} - F_3^{\bar{\nu} p})/4$ has a contribution, already of the order of α_s, from the quark in Fig. 5.8(a) in addition to the antiquark in Fig. 5.8(b). Although it is useful in getting experimental information on $\bar{u}-\bar{d}$ from F_1 and F_3 in the charged reactions, it is not a precise definition if higher-order corrections are taken into account.

A consistent way is to use both the charged and neutral current reactions [22]. The neutrino-quark interaction via the neutral current is described by [3]

$$J_\mu = \sum_i \frac{1}{2}\,\bar{q}_i(x)\,\gamma_\mu\,\left[\, g_{Li}(1-\gamma_5) + g_{Ri}(1+\gamma_5)\,\right]\, q_i(x) \quad , \tag{5.50}$$

where g_{Li} and g_{Ri} are defined by the Weinberg angle θ_W

$$\begin{aligned} g_{Li} &= 1-\frac{4}{3}\sin^2\theta_W \quad , \quad g_{Ri} = -\frac{4}{3}\sin^2\theta_W \qquad \text{for i=u, c} \quad , \\ &= -1+\frac{2}{3}\sin^2\theta_W \quad , \quad\quad\ = +\frac{2}{3}\sin^2\theta_W \qquad \text{for i=d, s} \quad . \end{aligned} \tag{5.51}$$

With the neutral-current observables, the distribution $\bar{u}-\bar{d}$ can be defined by only one type of the structure functions, for example F_1. The neutral-current structure functions F_1 for neutrino and electron reactions become

$$\begin{aligned} F_1^{\nu p \to \nu X} = g^2 \, \sec^2\theta_W \, \Bigg[& \left(\frac{1}{4} - \frac{2}{3}\sin^2\theta_W + \frac{8}{9}\sin^4\theta_W \right) \{u(x) + \bar{u}(x)\} \\ & + \left(\frac{1}{4} - \frac{1}{3}\sin^2\theta_W + \frac{2}{9}\sin^4\theta_W \right) \left\{d(x) + \bar{d}(x)\right\} \Bigg] \quad , \end{aligned} \tag{5.52}$$

$$F_1^{ep \to eX} = g^2 \, \sin^2\theta_W \left[\frac{4}{9} \, \{u(x) + \bar{u}(x)\} + \frac{1}{9} \, \left\{d(x) + \bar{d}(x)\right\} \right] \quad . \tag{5.53}$$

According to the definition of Ref. [22], it is given by combining the charged and neutral current F_1 structure functions as

$$\widehat{F}(x) = \frac{1}{2} \, [\, \widetilde{F}_1(x) - \{F_1(x)_{\bar{\nu}p \to e^+X} - F_1(x)_{\nu p \to e^-X}\} \,] = \bar{u}(x) - \bar{d}(x) \quad , \tag{5.54}$$

where $\widetilde{F}_1(x)$ is defined by the structure functions in the neutral current reactions:

$$\widetilde{F}_1(x) = \frac{5}{\left(\frac{2}{3}\, sin^2\theta_{_W} - \frac{3}{4}\right) sec^2\theta_{_W}} F_1(x)_{\nu p \to \nu X} - \frac{9\left(\frac{1}{2} - sin^2\theta_{_W} + \frac{11}{9}\, sin^4\theta_{_W}\right)}{\left(\frac{2}{3}\, sin^2\theta_{_W} - \frac{3}{4}\right) sin^2\theta_{_W}} F_1(x)_{ep \to eX} \ . \tag{5.55}$$

Because the $\bar{s}$ and $\bar{c}$ distributions are neglected in the above discussion [22] and in Eq. (5.49), it is necessary to subtract out these contributions by combining Eqs. (5.54) and (5.49) with the deuteron F_1 structure functions.

It is impossible to obtain the $\bar{u}/\bar{d}$ asymmetry from present neutrino data. However, we hope that much better data will enable us to extract the flavor asymmetry distribution.

5.6 Experiments to find isospin symmetry violation

We discussed in section 4.5 that the violation of the Gottfried sum rule could be due to the isospin-symmetry violation instead of the flavor asymmetry. These two mechanisms cannot be distinguished at this stage. The isospin-violation effects are believed to be very small in the structure functions. However, it is important to confirm this common sense experimentally. Various processes are discussed in the following for finding the effects of the isospin-symmetry violation in the antiquark distributions [50].

The F_2 structure functions in neutrino interactions are useful in distinguishing between the two mechanisms [50]. The difference between proton and neutron structure functions is

$$\begin{aligned} I_{ISV} &= \int \frac{dx}{x} \frac{1}{2} \, [\, F_2^{\nu p}(x) + F_2^{\bar{\nu} p}(x) - F_2^{\nu n}(x) - F_2^{\bar{\nu} n}(x) \,] \\ &= 2 \int dx \, \left[\{ \, \bar{u}(x) + \bar{d}(x) + \bar{s}(x) + \bar{c}(x) \, \}_p - \{ \, \bar{u}(x) + \bar{d}(x) + \bar{s}(x) + \bar{c}(x) \, \}_n \right] \quad . \end{aligned} \tag{5.56}$$

If the failure of the Gottfried sum is entirely due to the flavor asymmetry, the integral vanishes $I_{ISV} = 0$. On the other hand. if it is entirely due to the isospin violation and if the $\bar{s}$ and $\bar{c}$ terms can be neglected, the integral is $I_{ISV} = -0.336 \pm 0.058$. Because the flavor asymmetry does not contribute, the sum I_{ISV} should give a clue in finding an isospin-violation sign.

Isospin-violation effects on the Drell-Yan processes are also discussed in Ref. [50]. In the pion scattering case $\pi^\pm A \to \ell^+\ell^- X$, we consider the difference of nuclear cross sections at large x_π:

$$R_{sea} = \frac{4\,[\,\sigma(\pi^+A_1) - \sigma(\pi^+A_0)\,] + [\,\sigma(\pi^-A_1) - \sigma(\pi^-A_0)\,]}{\sigma(\pi^+A_0) - \sigma(\pi^-A_0)} \quad . \tag{5.57}$$

The A_0 and A_1 denote different nuclear species, but we may choose A_0 as an isoscalar nucleus and A_1 as a neutron-excess nucleus. With the isospin symmetry assumption, it becomes

$$R_{sea} = \frac{10\,(\epsilon_1 - \epsilon_0)\,(\bar{u} - \bar{d})}{u_V + d_V} \quad , \tag{5.58}$$

where ϵ is a neutron excess parameter $\epsilon = N/A - 1/2$. On the other hand, if the sea is flavor symmetric with the isospin violation, the Drell-Yan ratio becomes

$$R_{sea} = \frac{50\,(\epsilon_1 - \epsilon_0)\,(\bar{q}^{\,p} - \bar{q}^{\,n})}{3\,(u_V + d_V)} \quad , \tag{5.59}$$

where the isospin symmetry is assumed for the valence-quark distributions. Similar equations are obtained for proton Drell-Yan cross sections. The p-n cross section asymmetry is given in the isospin symmetry case as

$$\begin{aligned} A_{DY} &= \frac{\sigma^{pp} - \sigma^{pn}}{\sigma^{pp} + \sigma^{pn}} \\ &= \frac{(4u_V - d_V)(\bar{u} - \bar{d}) + (u_V - d_V)(4\bar{u} - \bar{d})}{(4u_V + d_V)(\bar{u} + \bar{d}) + (u_V + d_V)(4\bar{u} + \bar{d})} \quad . \end{aligned} \tag{5.60}$$

On the other hand, it is given in the isospin-violation case as

$$A_{DY} = \frac{(4u_V - d_V)\,5\,(\bar{q}^p - \bar{q}^n)/3 + (u_V - d_V)(\bar{q}^p + 8\bar{q}^n)/3}{9\,(\sigma^{pp} + \sigma^{pn})} \quad . \tag{5.61}$$

The details of the Drell-Yan cross sections and the asymmetry are discussed in section 5.1. From these equations, we find that the Drell-Yan cross sections could be interpreted in principle either by the flavor asymmetry or by the isospin violation. Both effects are taken into account to explain the NA51 result in Ref. [51]. The obtained result indicates that the ratio $\bar{u}/\bar{d}$ could be larger than the NA51 value at the cost of isospin symmetry violation. However, it is not possible to separate these two contributions clearly.

It is shown in Ref. [76] that the flavor asymmetry could be found in semi-inclusive leptoproduction of charged hadrons. The number of produced h hadrons in the lepton-nucleon scattering at Bjorken x and $z = E_h/\nu$ is given by $N^{Nh}(x,z) = \sum_i e_i^2\, q_i^N(x)\, D_i^h(z)$, where D_i^h is the fragmentation function. The details of the charged-hadron production are discussed in section 5.4. The following equation is obtained for finding the flavor asymmetry:

$$\begin{aligned} Q(z) &= \frac{N^{p+} - N^{n+} + N^{p-} - N^{n-}}{N^{p+} - N^{n+} - N^{p-} + N^{n-}} \\ &= 3\, I_G\, \frac{0.50z^2 + 3.1z + 7.6}{3.2z^2 + 11z + 0.84} \quad , \end{aligned} \tag{5.62}$$

where the notations N^{p+}, N^{n+}, N^{p-}, and N^{n-} are the same as those in Eq. (5.34). The isospin symmetry is assumed in the above equation. If the sea is flavor symmetric and if the isospin symmetry is violated, the above quantity becomes [50]

$$\begin{aligned} Q(z) &= \frac{4\,[\,D_u^+(z) + D_{\bar u}^+(z)\,]\,(1-2\delta\bar q) - [\,D_d^+(z) + D_{\bar d}^+(z)\,]\,(1+2\delta\bar q)}{4\,[\,D_u^+(z) - D_{\bar u}^+(z)\,] - [\,D_d^+(z) - D_{\bar d}^+(z)\,]} \\ &= 3\, I_G\, \frac{0.80z^2 + 3.37z + 7.63}{3.2z^2 + 11z + 0.84} \quad , \end{aligned} \tag{5.63}$$

where $\delta\bar q = \bar q^p - \bar q^n$. Both expressions have different z dependence, so that we should be able to distinguish the mechanisms if experimental data are accurate. At the present stage, charged-hadron production data are not accurate enough for finding the discrepancy.

The experimental studies would be difficult because the isospin effects are considered to be very small theoretically. However, accurate experimental data are desperately needed in order to shed light on the isospin-symmetry violation in the antiquark distributions.

6 Related topics on antiquark distributions

As a topic of flavor asymmetry, we have discussed the light-antiquark-distribution difference in the nucleon. There are other important issues on the antiquark distributions. We briefly comment on related topics.

First, the $\bar{u}/\bar{d}$ asymmetry in hyperons could be studied if charged hyperon beam becomes available in future. For example, a possibility to find the asymmetry in $\Sigma^{\pm}$ is investigated in Ref. [100]. In a naive quark model, they consist of $\Sigma^+(uus)$ and $\Sigma^-(dds)$. The Pauli-blocking and meson-cloud models predict $\bar{d}$ excess over $\bar{u}$ in Σ^+ and $\bar{u}$ excess over $\bar{d}$ in Σ^-. It is an interesting test of the theoretical models in section 4. The Drell-Yan cross section for the $\Sigma^+ p$ reaction at $y=0$ is given by

$$\sigma^{\Sigma^+ p} \approx \frac{8\pi\alpha^2}{9\sqrt{\tau}} \left[\frac{4}{9} \{ \, u_p(x)\bar{u}_\Sigma(x) + u_\Sigma(x)\bar{u}_p(x) \, \} + \frac{1}{9} \{ \, u_p(x)\bar{d}_\Sigma(x) + s_\Sigma(x)\bar{s}_p(x) \, \} \right] \, , \tag{6.1}$$

where only valence-sea annihilation terms are retained, and q_Σ denotes the distribution in Σ^+ ($q_\Sigma \equiv q_{\Sigma^+}$). In calculating cross sections for other reactions $\Sigma^- n$, $\Sigma^+ n$, and $\Sigma^- p$, we assume isospin symmetry, $u_p = d_n$, $\bar{u}_p = \bar{d}_n$, $u_{\Sigma^+} = d_{\Sigma^-}$, $\bar{u}_{\Sigma^+} = \bar{d}_{\Sigma^-}$, together with the assumption $s_{\Sigma^+} = s_{\Sigma^-}$. From the Drell-Yan cross sections with $\Sigma^{\pm}$ beams on the proton and deuteron targets, we take the ratio

$$\begin{aligned} R(x) &\equiv \frac{(\sigma^{\Sigma^+ p} - \sigma^{\Sigma^- n}) + \bar{r}_p(x)\,(\sigma^{\Sigma^- p} - \sigma^{\Sigma^+ n})}{(\sigma^{\Sigma^+ p} - \sigma^{\Sigma^+ n}) + 4\,(\sigma^{\Sigma^- p} - \sigma^{\Sigma^- n})} \\ &= \frac{\bar{r}_\Sigma(x)\,[r_p(x) - \bar{r}_p(x)] - [1 - \bar{r}_p(x) r_p(x)]}{5\,[r_p(x) - 1]} \quad \text{at } y = 0 \quad , \end{aligned} \tag{6.2}$$

where $r_p \equiv u_p/d_p$, $\bar{r}_p \equiv \bar{u}_p/\bar{d}_p$, and $\bar{r}_\Sigma \equiv \bar{u}_\Sigma/\bar{d}_\Sigma$. In this way, if r_p and $\bar{r}_p$ are known from other experiments, $\bar{r}_\Sigma$ could be measured by the hyperon Drell-Yan experiments.

Second, we mentioned the $\bar{s}$-quark distribution difference from the $(\bar{u}+\bar{d})/2$. It has been measured experimentally by the neutrino induced opposite-sign dimuon events. This topic is studied within the meson-cloud models. For example, because the pions do not contain the valence $\bar{s}$ quark, their contributions to $\bar{s}$ and $(\bar{u}+\bar{d})/2$ in the proton are different. It is particularly important in discussing the size of the πNN form factor and its relation to nuclear potentials. This topic is also discussed in the chiral field theory, so that the interested reader may look at the meson-model papers in the reference section.

Third, the difference between s and $\bar{s}$ is also important [101]. Because there is no net strangeness in the proton, the integral of the difference has to vanish: $\int dx(s - \bar{s}) = 0$. However, x dependence of both distributions could be different. In fact, the proton virtually decays into for example $K^+(u\bar{s})\Lambda(uds)$, $K^+(u\bar{s})\Sigma^0(uds)$, and $K^0(d\bar{s})\Sigma^+(uus)$. Within the three decay modes, the valence $\bar{s}$ is contained in the kaons and s is in the hyperons. Because the hyperon masses are larger than those of the kaons, the $\bar{s}$

distribution is distributed in the outer side. It means that the $\bar{s}$ distribution is softer than that of the s-quark one. Of course, the s and $\bar{s}$ distributions should be dominated by the perturbative contributions. However, these could be canceled out by taking the difference $s - \bar{s}$. It is impossible to find this kind of small effect at this stage [6]. We hope to have much accurate data in future.

Fourth, flavor asymmetry in polarized antiquark distributions should become an exciting topic in the near future. As far as the model is concerned, we have explained the flavor dependence in section 4.7. However, because we do not have a variety of polarized data at this stage, it is very difficult to find the difference between $\bar{u}$, $\bar{d}$, and $\bar{s}$ distributions from experimental data. In any case, there is an attempt to study the flavor decomposition by including semi-inclusive data in Ref. [102]. Future experimental programs for the polarized flavor asymmetry are for example the RHIC-SPIN [103] and the Common Muon and Proton Apparatus for Structure and Spectroscopy (COMPASS) [104]. In the similar way with the unpolarized case in section 5.2, the $W^{\pm}$ production measurements by the RHIC-SPIN collaboration should enable us to find $\Delta\bar{u}$ and $\Delta\bar{d}$ distributions. The strange polarization and other polarized valence and sea distributions will be measured in semi-inclusive reactions by the COMPASS collaboration. Much progress is expected on the flavor dependence of the polarized antiquark distributions in the next several years.

Fifth, there is a similar sum rule to the Gottfried in the spin-dependent structure function b_1 for spin-one hadrons. This new structure function is related to quadrupole structure of the spin-one hadrons. Its sum rule was proposed in Ref. [105] as

$$\int dx b_1(x) = \lim_{t\to 0} -\frac{5}{3}\frac{t}{4M^2} F_Q(t) + \delta Q_{sea} \quad , \tag{6.3}$$

where $F_Q(t=0)$ is the quadrupole moment in the unit of e/M^2 for a spin-one hadron with the mass M. The second term δQ_{sea} is the sea-quark tensor polarization defined, for example, $\delta Q^D_{sea} = \int dx[8\delta\bar{u}(x) + 2\delta\bar{d}(x) + \delta s(x) + \delta\bar{s}(x)]^D/9$ for the deuteron. The distribution δq is given by $\delta q = [q^0 - (q^{+1} + q^{-1})/2]/2$, where the superscript indicates the hadron helicity in an infinite momentum frame. The Gottfried sum 1/3 corresponds to the first term $\lim_{t\to 0} -\frac{5}{3}\frac{t}{4M^2} F_Q(t) = 0$. Because the valence-quark number depends on flavor, the finite sum 1/3 is obtained in the Gottfried. However, it does not depend on spin, so that the first term vanishes in the b_1 case. The second term in Eq. (6.3) corresponds to $\int dx(\bar{u} - \bar{d})$ in Eq. (2.12). Therefore, a deviation from the sum $\int dx b_1(x) = 0$ should suggest the sea-quark tensor polarization as the Gottfried sum rule violation suggested the finite $\bar{u} - \bar{d}$ distribution. Recent studies indicate that the diffractive-nuclear-shadowing and pion-excess mechanisms produce a tensor polarization, which leads to violation of the b_1 sum rule [106].

7 Summary and outlook

The light antiquark distributions $\bar{u}$ and $\bar{d}$ had been assumed equal for a long time. The Gottfried sum rule can be derived with this assumption. Even though there were some experimental efforts to test the sum rule and the flavor asymmetry $\bar{u}-\bar{d}$, it was not possible to draw a reliable conclusion. However, recent accurate experimental measurements made it possible to find the difference between the $\bar{u}$ and $\bar{d}$ distributions. The NMC finding of the Gottfried-sum-rule violation and the $\bar{u}/\bar{d}$ asymmetry motivated us to study theoretical mechanisms and different experimental possibilities. The flavor asymmetry is now confirmed by the NA51 Drell-Yan experiment, and it is also suggested by the preliminary HERMES and E866 data. On the other hand, future experimental facilities should be able to pin down the $\bar{u}$ and $\bar{d}$ distributions. For example, Drell-Yan and W-production measurements at RHIC should be very useful. In testing the Gottfried sum itself, we need to accelerate the deuteron at HERA.

On the theoretical side, the perturbative corrections to the sum are very small. Therefore, the violation should be explained by a nonperturbative mechanism. Within the proposed models, the mesonic model is a strong candidate in the sense that it can explain the major part of the violation. The Pauli blocking effect is smaller than that of the mesonic model according to the naive counting estimate. Furthermore, if the antisymmetrization is considered in addition to the Pauli principle, both mechanisms could produce a $\bar{u}$ excess over $\bar{d}$. Because there are other theoretical candidates as explained in this paper, we should investigate more details of these models in order to find a correct explanation. The flavor asymmetry studies provide us an important clue to understand nonperturbative aspects of nucleon substructure. Future experimental and theoretical efforts on this topic are important for understanding internal structure of hadrons.

Acknowledgments

This research was partly supported by the Grant-in-Aid for Scientific Research from the Japanese Ministry of Education, Science, and Culture under the contract number 06640406. S. K. thanks the Institute for Nuclear Theory at the University of Washington for its hospitality and the US Department of Energy for partial support. He thanks the Elsevier Science, A. S. Ito, K. F. Liu, W. Melnitchouk, J. C. Peng, and W. J. Stirling for permitting him to quote some figures directly from their publications. He thanks H.-L. Yu for his hospitality in staying in the Academia Sinica of Taiwan, where this manuscript is partially written.

References

[1] F. E. Close, *An Introduction to Quarks and Partons* (Academic Press, London, 1979).

[2] T. Muta, *Foundations of Quantum Chromodynamics* (World Scientific, Singapore, 1987).

[3] R. G. Roberts, *The Structure of the Proton* (Cambridge University Press, Cambridge, 1990).

[4] For example, A. D. Martin, R. G. Roberts, and W. J. Stirling, Phys. Rev. D37 (1988) 1161.

[5] H. Abramowicz et al. (CDHS collaboration), Z. Phys. C 15 (1982) 19; C 17 (1983) 283.

[6] C. Foudas et al. (CCFR collaboration), Phys. Rev. Lett. 64 (1990) 1207; S. A. Rabinowitz et al., Phys. Rev. Lett. 70 (1993) 134; W. C. Leung et al., Phys. Lett. B 317 (1993) 655; A. O. Bazarko et al., Z. Phys. C 65 (1995) 189.

[7] K. Gottfried, Phys. Rev. 8 (1967) 1174.

[8] S. Stein et al., Phys. Rev. 12 (1975) 1884; A. Bodek et al., Phys. Rev. Lett. 30 (1973) 1087.

[9] M. I. Pavković, Phys. Rev. D 13 (1976) 2128.

[10] R. D. Field and R. P. Feynman, Phys. Rev. D 15 (1977) 2590.

[11] There are other publications on the Pauli-exclusion model in the 1970's: A. Niegawa and K. Sasaki, Prog. Theo. Phys. 54 (1975) 192; J. F. Donoghue and E. Golowich, Phys. Rev. D 15 (1977) 3421; M. H. McCall, J. Phys. G 5 (1979) L117.

[12] A. S. Ito et al. (E288 collaboration), Phys. Rev. D 23 (1981) 604.

[13] J. J. Aubert et al. (EM Collaboration), Phys. Lett. B 123 (1983) 123; Nucl. Phys. B 293 (1987) 740.

[14] A. C. Benvenuti et al. (BCDMS collaboration), Phys. Lett. B 237 (1990) 599 & 592.

[15] P. Amaudruz et al. (NM Collaboration), Phys. Rev. Lett. 66 (1991) 2712; M. Arneodo et al., Phys. Rev. D 50 (1994) R1.

[16] M. R. Adams et al. (E665 collaboration), Phys. Rev. Lett. 75 (1995) 1466; Phys. Rev. D54 (1996) 3006.

[17] K. Ackerstaff (HERMES collaboration), DESY-HERMES-96-01, Ph. D. thesis, Universität Hamburg, 1996.

[18] P. L. McGaughey et al. (E772 collaboration), Phys. Rev. Lett. 69 (1992) 1726.

[19] A. Baldit et al. (NA51 collaboration), Phys. Lett. B 332 (1994) 244.

[20] P.E. Reimer et al. (E866 collaboration), AIP Conference Proceedings 412: Intersections between Particle and Nuclear Physics, T.W. Donnelly, ed., Bigsky, Montana, May 1997 (Woodbury, NY: AIP Press, 1997) p. 643.

[21] A. D. Martin, W. J. Stirling, and R. G. Roberts, Phys. Lett. B 252 (1990) 653.

[22] D. A. Ross and C. T. Sachrajda, Nucl. Phys. B 149 (1979) 497.

[23] I. Hinchliffe and A. Kwiatkowski, Annu. Rev. Nucl. Part. Sci. 46 (1996) 609.

[24] A. L. Kataev, A. V. Kotikov, G. Parente, and A. V. Sidorov, Phys. Lett. B 388 (1996) 179.

[25] M. A. Braun and M. V. Tokarev, Phys. Lett. B 320 (1994) 381; A. V. Sidorov and M. V. Tokarev, hep-ph/9608461.

[26] K. F. Liu and S. J. Dong, Phys. Rev. Lett. 72 (1994) 1790.

[27] A. I. Signal and A. W. Thomas, Phys. Rev. D 40 (1989) 2832; F. M. Steffens and A. W. Thomas, Phys. Rev. C 55 (1997) 900.

[28] M. Anselmino and E. Predazzi, Phys. Lett. B 254 (1991) 203.

[29] M. Anselmino, V. Barone, F. Caruso, and E. Predazzi, Z. Phys. C 55 (1992) 97.

[30] E. M. Henley and G. A. Miller, Phys. Lett. B 251 (1990) 453.

[31] S. Kumano, Phys. Rev. D 43 (1991) 59 & 3067; S. Kumano and J. T. Londergan, Phys. Rev. D 44 (1991) 717.

[32] A. Signal, A. W. Schreiber, and A. W. Thomas, Mod. Phys. Lett. A 6 (1991) 271; W. Melnitchouk, A. W. Thomas, and A. I. Signal, Z. Phys. A 340 (1991) 85; A. W. Schreiber, P. J. Mulders, A. I. Signal, and A. W. Thomas, Phys. Rev. D 45 (1992) 3069; Brief comments are given also in earlier publications, A. W. Thomas, Phys. Lett. B 126 (1983) 97; M. Ericson and A. W. Thomas, Phys. Lett. B 148 (1984) 191.

[33] W.-Y. P. Hwang, J. Speth, and G. E. Brown, Z. Phys. A 339 (1991) 383. W.-Y. P. Hwang and J. Speth, Phys. Rev. D 46 (1992) 1198; A. Szczurek and J. Speth, Nucl. Phys. A 555 (1993) 249; B. C. Pearce, J. Speth, and A. Szczurek, Phys. Rep. 242 (1994) 193; H. Holtmann, A. Szczurek, and J. Speth, Nucl. Phys. A 569 (1996) 631.

[34] V. R. Zoller, Z. Phys. C 53 (1992) 443.

[35] W. Koepf, L. L. Frankfurt, and M. Strikman, Phys. Rev. D 53 (1996) 2586.

[36] T. Shigetani, K. Suzuki, and H. Toki, Phys. Lett. B 308 (1993) 383; Nucl. Phys. A 579 (1994) 413; hep-ph/9512305.

[37] C. M. Shakin and W.-D. Sun, Phys. Rev. C 50 (1994) 2553.

[38] J. Stern and G. Clément, Phys. Lett. B 264 (1991) 426.

[39] M. Wakamatsu, Phys. Rev. D 44 (1991) R2631; D 46 (1992) 3762.

[40] E. J. Eichten, I. Hinchliffe, and C. Quigg, Phys. Rev. D 45 (1992) 2269.

[41] H. Walliser and G. Holzwarth, Phys. Lett. B 302 (1993) 377.

[42] B. A. Li, Nuo. Cim. A 107 (1994) 59.

[43] S. Kretzer, Phys. Rev. D 52 (1995) 2701.

[44] A. Blotz, M. Praszalowicz, and K. Goeke, Phys. Rev. D 53 (1995) 551.

[45] N. I. Kochelev, hep-ph/9511299.

[46] A. Szczurek, A. J. Buchmann, and A. Faessler, J. Phys. G 22 (1996) 1741.

[47] T. P. Cheng and L.-F. Li, hep-ph/9701248.

[48] S. Forte, Phys. Rev. D 47 (1993) 1842.

[49] R. D. Ball and S. Forte, Nucl. Phys. B 425 (1994) 516; R. D. Ball, V. Barone, S. Forte, and M. Genovese, Phys. Lett. B 329 (1994) 505.

[50] B.-Q. Ma, Phys. Lett. B 274 (1992) 111; B.-Q. Ma, A. Schäfer, and W. Greiner, Phys. Rev. D 47 (1993) 51.

[51] F. M. Steffens and A. W. Thomas, Phys. Lett. B 389 (1996) 217.

[52] B. Badelek and J. Kwieciński, Nucl. Phys. B 370 (1992) 278.

[53] V. R. Zoller, Z. Phys. C 54 (1992) 425; Phys. Lett. B 279 (1992) 145; N. N. Nikolaev and V. R. Zoller, Z. Phys. C 56 (1992) 623.

[54] L. P. Kaptari and A. Y. Umnikov, Phys. Lett. B 272 (1991) 359.

[55] L. N. Epele, H. Fanchiotti, C. A. Garcia Canal, and R. Sassot, Phys. Lett. B 275 (1992) 155; L. N. Epele, H. Fanchiotti, C. A. Garcia Canal, E. Leader, and R. Sassot, Z. Phys. C 64 (1994) 285.

[56] V. Barone, M. Genovese, N. N. Nikolaev, E. Predazzi, and B. G. Zakharov, Z. Phys. C 58 (1993) 541; Phys. Lett. B 321 (1994) 137.

[57] W. Melnitchouk and A. W. Thomas, Phys. Rev. D 47 (1993) 3783 & 3794; W. Melnitchouk, A. W. Schreiber, and A. W. Thomas, Phys. Lett. B 335 (1994) 11.

[58] G. Piller, W. Ratzka, and W. Weise, Z. Phys. A 352 (1995) 427.

[59] M. Sawicki and J. P. Vary, Phys. Rev. Lett. 71 (1993) 1320.

[60] B.-Q. Ma and A. Schäfer, Phys. Lett. B 378 (1996) 307; B 380 (1996) 495 (Erratum).

[61] G. Preparata, P. G. Ratcliffe, and J. Soffer, Phys. Rev. Lett. 66 (1991) 687.

[62] A. D. Martin, W. J. Stirling, and R. G. Roberts, Phys. Rev. D 47 (1993) 867; Phys. Lett. B 387 (1996) 419.

[63] H. L. Lai et al. (CTEQ collaboration), Phys. Rev. D 55 (1997) 1280.

[64] M. Glück, E. Reya, and A. Vogt, Z. Phys. C 67 (1995) 433.

[65] S. Kumano, Phys. Lett. B 342 (1995) 339.

[66] F. Buccella and J. Soffer, Mod. Phys. Lett. A 8 (1993) 225; Europhys. Lett. 24 (1993) 165; C. Bourrely and J. Soffer, Phys. Rev. D 51 (1995) 2108; F. Buccella, G. Miele, and N. Tancredi, Prog. Theo. Phys. 96 (1996) 749.

[67] S. D. Ellis and W. J. Stirling, Phys. Lett. B 256 (1991) 258.

[68] S. Kumano and J. T. Londergan, Phys. Rev. D 46 (1992) 457.

[69] E. J. Eichten, I. Hinchliffe, and C. Quigg, Phys. Rev. D 47 (1993) R747.

[70] W.-Y. P. Hwang, G. T. Garvey, J. M. Moss, and J.-C. Peng, Phys. Rev. D 47 (1993) 2649.

[71] A. D. Martin, W. J. Stirling, and R. G. Roberts, Phys. Lett. B 308 (1993) 377.

[72] A. Szczurek, J. Speth, and G. T. Garvey, Nucl. Phys. A 570 (1994) 765; A. Szczurek, M. Ericson, H. Holtmann, and J. Speth, Nucl. Phys. A 596 (1996) 397.

[73] B.-Q. Ma, A. Schäfer, and W. Greiner, J. Phys. G 20 (1994) 719.

[74] J. Ashman et al. (EMC), Z. Phys. C 52 (1991) 361.

[75] J. J. Aubert et al. (EMC), Phys. Lett. B 160 (1985) 417; M. Arneodo et al., Nucl. Phys. B 321 (1989) 541.

[76] J. Levelt, P. J. Mulders, and A. W. Schreiber, Phys. Lett. B 263 (1991) 498.

[77] C. Bourrely and J. Soffer, Phys. Lett. B314 (1993) 132.

[78] M. A. Doncheski, F. Halzen, C. S. Kim, and M. L. Stong, Phys. Rev. D49 (1994) 3261.

[79] J. C. Peng and D. M. Jansen, Phys. Lett. B 354 (1995) 460.

[80] J. C. Peng, D. M. Jansen, and Y. C. Chen, Phys. Lett. B 344 (1995) 1.

[81] C. Itzykson and J. Zuber, *Quantum Field Theory* (McGraw-Hill, New York, 1980).

[82] W. M. Bardeen, A. J. Buras, D. W. Duke, and T. Muta, Phys. Rev. D 18 (1978) 3998.

[83] A. J. Buras, Rev. Mod. Phys. 52 (1980) 199.

[84] R. Kobayashi, M. Konuma, and S. Kumano, Comput. Phys. Commun. 86 (1995) 264; M. Miyama and S. Kumano, Comput. Phys. Commun. 94 (1996) 185.

[85] G. Curci, W. Furmanski, and R. Petronzio, Nucl. Phys. B 175 (1980) 27.

[86] R. L. Jaffe, in *Relativistic Dynamics and Quark-Nuclear Physics*, proceedings edited by M. B. Johnson and A. Picklesimer (Wiley-Interscience, New York, 1986).

[87] J. D. Sullivan, Phys. Rev. D 5 (1972) 1732.

[88] S. Théberge and A. W. Thomas, Nucl. Phys. A 393 (1983) 252.

[89] G. A. Miller, Phys. Rev. C 39 (1989) 1563; S. Kumano, Phys. Rev. D 41 (1990) 195.

[90] L. L. Frankfurt, L. Mankiewicz, and M. I. Strikman, Z. Phys. A 334 (1989) 343.

[91] G. van der Steenhoven, NIKHEF-96-026; see also theoretical works in G. D. Bosveld, A. E. L. Dieperink, and O. Scholten, Phys. Lett. B 264 (1991) 11; Phys. Rev. C 45 (1992) 2616; W. Melnitchouk, A. W. Thomas, and N. N. Nikolaev, Z. Phys. A 342 (1992) 215. For later works, see A. Szczurek, G. D. Bosveld, A. E. L. Dieperink, Nucl. Phys. A 595 (1995) 307.

[92] S. Koretune, Prog. Theo. Phys. 88 (1992) 63; Phys. Rev. D 47 (1993) 2690.

[93] For example, see F. E. Close and A. W. Thomas, Phys. Lett. B 212 (1988) 227; W. Melnitchouk and A. W. Thomas, Phys. Lett. B 377 (1996) 11; page 101 of Particle Data Group, Phys. Rev. D 54 (1996) 1.

[94] M. Anselmino, F. Caruso, E. Leader, and J. Soares, Z. Phys. C 48 (1990) 689.

[95] For example, see R. Hamberg, W. L. van Neerven, and T. Matsuura, Nucl. Phys. B 359 (1991) 343.

[96] R. L. Jaffe, hep-ph/9602236, Lectures at the International School of Nucleon Structure, The Spin Structure of the Nucleon, Erice, Aug. 3-10, 1995.

[97] J. J. Aubert et al. (EM Collaboration), Phys. Lett. B 123 (1983) 275.

[98] F. Abe et al. (CDF collaboration), Phys. Rev. Lett. 74 (1995) 850; S. Kretzer, E. Reya, and M. Stratmann, Phys. Lett. B 348 (1995) 628.

[99] V. Barger and R. Phillips, *Collider Physics* (Addison-Wesley, Redwood City CA, 1987).

[100] M. Alberg and E. M. Henley, hep-ph/9603405; M. Alberg, E. M. Henley, X. Ji, and A. W. Thomas, Phys. Lett. B 389 (1996) 367.

[101] A. I. Signal and A. W. Thomas, Phys. Lett. B 191 (1987) 205; M. Burkardt and B. J. Warr, Phys. Rev. D 45 (1992) 958; X. Ji and J. Tang, Phys. Lett. B 362 (1995) 182; S. J. Brodsky and B.-Q. Ma, Phys. Lett. B 381 (1996) 317.

[102] J. Bartelski and S. Tatur, Z. Phys. C 75 (1997) 477.

[103] Proposal on Spin Physics Using the RHIC Polarized Collider (RHIC-SPIN collaboration), August 1992; update, Sept. 2, 1993.

[104] Proposal "Common Muon and Proton Apparatus for Structure and Spectroscopy" (COMPASS collaboration), CERN/SPSLC 96-14, March 1, 1996.

[105] F. E. Close and S. Kumano, Phys. Rev. D 42 (1990) 2377.

[106] N. N. Nikolaev and W. Schäfer, Phys. Lett. B 398 (1997) 245; J. Edelmann, G. Piller, and W. Weise, Z. Phys. A 357 (1997) 129.